Kundan Chauhan

PLANNING AND ROCK ENGINEERING DESIGN OF THE UNDERGROUND STRUCTURES OF THE TAMAKOSHI V HYDROELECTRIC PROJECT

Master's thesis in Hydropower Development

Supervisor: Krishna Kanta Panthi

June 2020

Master's thesis

NTNU
Norwegian University of Science and Technology
Faculty of Engineering
Department of Geoscience and Petroleum

NTNU
Norwegian University of
Science and Technology

Kundan Chauhan

PLANNING AND ROCK ENGINEERING DESIGN OF THE UNDERGROUND STRUCTURES OF THE TAMAKOSHI V HYDROELECTRIC PROJECT

NTNU
Norwegian University of
Science and Technology

NTNU
Norwegian University of
Science and Technology

Department of Geoscience and Petroleum

Your ref.: MS/I20T56/IGP/KCKP

Date: 06.01.2020

<div align="center">

TGB4910 Rock Engineering - MSc thesis
for
Kundan Chauhan

</div>

<div align="center">

**PLANNING AND ROCK ENGINEERING DESIGN OF THE UNDERGROUND
STRUCTURES OF THE TAMAKOSHI V HYDROELECTRIC PROJECT**

</div>

Background

Correct placement of the underground structures is the key for cost effective and timely completion of hydropower projects. Failure in locating underground structures at the right place brings additional cost and substantial time delays. Especially is the case while planning and design of the underground structure passing through the Himalayan rock mass conditions where extensive earthquakes occur due to tectonic movement. Planned underground structures of Tamakoshi V Hydroelectric Project is located very near to the Main Central Thrust (MCT) of the Himalaya. The rock mass at the area are therefore highly influenced by persistent tectonic movement.

MSc thesis task

This MSc thesis is to focus on the planning and design aspects of major underground elements of the project, with a focus on the following issues:

- Review existing theory on the stability aspects of underground excavation and aspects of planning & design of hydropower structures.
- Briefly describe Tamakoshi V Hydroelectric Project. Present the extent of engineering geological investigations carried out at the project.
- Critically evaluate existing lay-out design and placement of all underground elements of the project. Assess the potential applicability of shotcrete lined headrace tunnel at the project.
- Carry out extensive assessment on the type of stability challenges that different underground elements may experience during excavation. Evaluate each of the challenges using prevailing rock engineering theory discussed in the theory review chapter.
- Carry out stability assessment of the selected segments of headrace and tailrace tunnels using numerical modelling.

- Carry out stability assessment of underground powerhouse cavern using numerical modelling, include earthquake load while carrying out the assessment.
- Discuss the analysis results and conclude the work.

Relevant computer software packages

Candidate shall use *rocscience package* and other relevant computer software for the master study.

Background information for the study

- Relevant information about the project such as reports, maps, information and data given by the supervising professor.
- Scientific papers, reports and books related to the Himalayan geology and tunnelling.
- Scientific papers and books related to international tunnelling cases.
- Literatures in rock engineering, rock support principles, rock mechanics and tunnelling.

Mr. Bibek Neupane will be the co-supervisor of this MSc thesis.

The thesis work is to start on January 15, 2020 and to be completed by June 10, 2020.

The Norwegian University of Science and Technology (NTNU)
Department of Geoscience and Petroleum (IGP)

January 06, 2020

Dr. Krishna Kanta Panthi
Professor of rock and tunnel engineering, main supervisor

Abstract

The Tamakoshi V Hydroelectric Project is a cascade scheme of the under construction 456 MW Upper Tamakoshi Hydroelectric Project. It has an installed capacity of 99.8 MW and will be located in the right bank of Tamakoshi river in Dolakha District, Nepal (NEA 2019).

Evaluation of the existing layout of Tamakoshi V shows that Headrace Tunnel (HRT) and Tailrace Tunnel (TRT) are safe with respect to the major joint sets including foliation joints. However, due to unfavorable orientation of one of the discontinuities in Powerhouse cavern, alternative alignment for Powerhouse has been proposed considering major joint sets and tectonic stress direction. The potentiality of exploiting HRT of Tamakoshi V as shotcrete lined pressure tunnel has been assessed based on Rock engineering assessment, Norwegian Confinement Criteria (NCC), Modified NCC, In-situ stress state assessment and Leakage assessment. It has been found that HRT downstream (d/s) of chainage 5+000m is vulnerable to hydraulic jacking and the leakages compared to HRT upstream of it. However, after implementing pre-injection grouting at the vulnerable sections and assuring long term stability, HRT of Tamakoshi V can be designed as shotcrete lined pressure tunnel.

Due to variation in stresses and rock types along the alignment, different potential stability problems have been assessed using empirical, semi-analytical and numerical modelling methods (RS2). Potential block fall at chainage 5+025m can be avoided using spot or sparsely spaced pattern bolting. Brittle failure analysis shows spalling potential in the Banded gneiss section, which can be controlled by the application fiber reinforced shotcrete (Sfr) and bolt (B). In deformation analysis, squeezing problem ranging from few support problems to extreme squeezing has been assessed in the rock masses d/s of chainage 1+769m. At chainage 3+769m in Tatopani weakness/shear zone, total tunnel strain of 26.6% has been evaluated. This can be controlled by providing early confinement or pre-reinforcement in tunnel periphery and near face prior to excavation, and with application of support systems consisting of Reinforced Ribs of Shotcrete, bolts and invert concrete. Likewise, deformation on the remaining sections along the HRT and TRT can be maintained within 5% strain with support system of fiber reinforced shotcrete, bolts and invert concrete. With these measures, long-term stability problem along the HRT can be assured, which is one of the important requirements for the implementation of shotcrete lined pressure tunnel. Also, Powerhouse cavern has been assessed both statically and dynamically with earthquake load, which shows insignificant problems in the suggested support (cable bolt, fiber reinforced shotcrete and bolt), rock mass and in-situ stress.

Preface

This Master thesis titled '**Planning and Rock Engineering Design of the Underground Structures of the Tamakoshi V Hydroelectric Project'** is submitted to the Department of Geoscience and Petroleum at the Norwegian University of Science and Technology (NTNU). This thesis work has been carried out for the requirement to the partial fulfillment of Master in Hydropower Development (2018-2020).

The thesis mainly focuses on evaluating the existing layout of underground structures of Tamakoshi V Hydroelectric Project and assessing the potentiality of exploiting Headrace Tunnel of Tamakoshi V as Shotcrete lined pressure tunnel. The thesis also focuses on evaluating stability challenges that the different underground elements (including the Powerhouse Cavern along with earthquake load) may experience during excavation, using prevailing rock engineering theory and numerical modelling. The thesis work started in 15th of January 2020 and completed within 10th of June 2020.

Professor Dr. Krishna Kanta Panthi has been the main supervisor of the thesis and PhD fellow Mr. Bibek Neupane has been the co-supervisor. The information about Tamakoshi V Hydroelectric Project has been obtained through the main supervisor, provided to him by Tamakoshi Jal Vidhyut Company Limited.

Kundan Chauhan

NTNU, Trondheim, Norway

June, 2020

Acknowledgement

I would like to express my sincere gratitude towards Professor Dr. Krishna Kanta Panthi, the main supervisor of the thesis, for his valuable guidance, encouragement, suggestions and discussions throughout the entire journey of my thesis, from topic selection to thesis submission. Without his constant guidance, knowledge and suggestions, this thesis would not have been possible, so I am very grateful to have been presented with the opportunity of having him as my main supervisor.

Also, I would to thank my co-supervisor, Mr. Bibek Neupane, PhD candidate in Department of Geoscience and Petroleum, for his valuable guidance regarding the subject matter and constant support throughout the thesis process.

I would like to thank the Department of Civil and Environmental Engineering for accepting me into the Master in Hydropower Development Program and providing me with an opportunity to pursue my Master degree in a subject that I have my deep interest in. My deep gratitude also goes to the Norwegian Agency for Development Cooperation (NORAD) for providing me with the scholarship covering living expenses in Norway and travel expenses among others.

Also, I would like to thank Mr. Nasib Man Pradhan, Chief Executive Officer of Tamakoshi Jal Vidhyut Company Limited for providing me with the Project information required for the thesis.

I am also very thankful to my friends who motivated me throughout the process and helped me through various discussions regarding different topics related to the thesis. Lastly, I would like to thank my family for their constant support and encouragement for the completion of my thesis and my studies.

List of Abbreviations

Ch.	Chainage
ESR	Excavation Span Ratio
FoS	Factor of safety
GWh	Giga Watt Hour
HM	Hoek and Marinos (2000)
HP	Hydroelectric Project
HRT	Headrace Tunnel
Masl	Meters Above Sea level
MCT	Main Central Thrust
MPa	Mega Pascal
MW	Mega Watt
NCC	Norwegian Confinement Criteria
PS	Panthi and Shrestha (2018)
RRS	Reinforced Ribs of Shotcrete
Sfr	Fiber Reinforced Shotcrete
TRT	Tailrace Tunnel
UCS	Uniaxial Compressive Strength
UTHP	Upper Tamakoshi Hydroelectric Project

Table of Contents

Table of Contents

Chapter 1: Introduction

1.1 Background of study

Nepal is blessed with perennial rivers with steep topographic gradient, which provides ideal conditions for the development of Hydropower. Utilizing nature's bountiful gift, the country can boost up its economic development and can be a regional player in fulfilling the energy demand in South Asia. However, its proper utilization is lagging for the well-being of its growing population due to the geographical, economic and techno political situation. With the present installed capacity of around 1400 MW, Nepal has planned to increase its installed capacity to 3000MW by the year 2021 (Gorkhapatra 2020).

As per the Policies and Programmes for Nepal's fiscal year 2077/78 B.S (2020/2021 AD), the government has proposed to start the construction of the Tamakoshi V Hydroelectric project with installed capacity of 99.8 MW (Gorkhapatra 2020). The project is the cascade scheme of the under construction Upper Tamakoshi Hydroelectric Project with all structures underground.

Due to the active tectonic compressional regime in the Himalaya, rock mass has suffered from severe deformation making the rock mass highly folded, faulted, sheared and deeply weathered. As a result of this complex geological and geotectonic environment, severe stability problems have been occurred, creating a challenge for successful tunneling (Panthi 2006). Amidst this, correct placement or alignment of underground structure based on proper understanding of prevailing geology and geotectonic environment is the key for the cost effective and timely completion of underground Hydropower projects. It is an important and fundamental step to know about the possible failure mechanism and to evaluate potential stability problems as early as possible so that the decision regarding realignment, excavation method and support system can be made at an early stage. Despite this, it is always beneficial to explore innovative solution reducing the use of concrete lining, which is a costly solution. This can be achieved by exploiting the rock mass along the waterway to act as natural concrete and to adopt unlined/shotcrete lined pressure tunnel to an extent that existing rock mass permits (Panthi and Basnet 2017).

Taking all of this into consideration, the focus of this thesis is to evaluate the existing layout and placement of underground structures, conduct stability analysis along the alignment and powerhouse cavern using prevailing theories and numerical modelling and explore the possibility of implementing unlined/shotcrete lined low to medium pressure headrace tunnel in Tamakoshi V Hydroelectric Project.

1.2 Project task

The main task assigned in this master thesis is to focus on the planning and design aspects of major underground elements of the project, with a focus on following issues:

➢ Review existing theory on the stability aspects of underground excavation and aspects of planning and design of hydropower structures.

➢ Briefly describe Tamakoshi V Hydroelectric Project. Present the extent of engineering geological investigations carried out at the project.

➢ Critically evaluate the existing lay-out design and placement of all underground elements of the project. Assess the potential applicability of shotcrete lined headrace tunnel at the project.

➢ Carry out extensive assessment on the type of stability challenges that different underground elements may experience during excavation. Evaluate each of the challenges using prevailing rock engineering theory discussed in the theory review chapter.

➢ Carryout stability assessment of the selected segments of headrace and tailrace tunnels using numerical modelling.

➢ Carryout stability assessment of underground powerhouse cavern using numerical modelling, include earthquake load while carrying out the assessment.

➢ Discuss the analysis results and conclude the work.

1.3 Methodology

Following methodology has been applied during the thesis:

1.3.1 Literature review

For literature review, literature related to rockmass properties, planning and design of underground tunnels and caverns and its stability issues and unlined/shotcrete lined pressure tunnel has been considered. For this, different reports, scientific papers, doctoral thesis, lecture notes and books related to Himalayan geology, especially weak rockmass and international cases has been studied using different search engines such as Oria, Google Scholar, among others.

1.3.2 Study of Tamakoshi V Hydroelectric Project

All the information related to the project was obtained from Detail geological and geotechnical report of Tamakoshi V Hydroelectric Project conducted by Tractebel Engineering GmbH. In case of unavailability of any information for analysis, various scientific papers and reports

related to nearby projects such as Upper Tamakoshi hydroelectric project and Khimti I hydroelectric project are referred in discussion with the Supervisor.

1.3.3 Unlined/shotcrete lined tunnel assessment

Potentiality of exploiting Headrace tunnel of Tamakoshi V hydroelectric Project as shotcrete lined pressure tunnel has been assessed based on prevailing theories, which include Norwegian Confinement Criteria, Modified Norwegian Confinement Criteria by Panthi and Basnet (2018b) and In-situ stress state assessment. In addition to this, Rock engineering assessment and Leakage assessment has been evaluated.

1.3.4 Stability analysis of tunnels and powerhouse cavern

Different stability issues that can probably occur along both headrace and tailrace tunnel and in Powerhouse cavern have been determined using existing empirical, semi-analytical and numerical modelling methods (RS2). Results obtained from various methods are then compared with each other on the basis of which support measures are determined.

1.4 Limitations

The main challenge for this thesis has been in obtaining reliable input parameter for analysis. As no any excavation has been carried out in the Project, except for the Test Tunnel at Powerhouse area, various kind of analysis have been conducted based on available data from the project and the assumption of possible situation considering the issues at nearby projects and existing rockmass conditions. In this thesis, there is no involvement of the authorities/employees linked with the project, which has created certain limitations during the analysis. All the information and understanding of the project complexity are based on desk study of available report that were made available by the Supervisor. Likewise, due to the unavailability of in-situ stress data, tectonic stress has been evaluated from Upper Tamakoshi Hydroelectric Project for the uppermost section of HRT and for the remaining sections downstream, tectonic stress has been evaluated from the nearby projects which have almost similar geology and geotectonic environment. Due to time constraint, structurally controlled failure at tunnel and cavern has not been carried out in detail.

Chapter 2: Stability assessment of Underground Openings

Due to excavation of an underground opening, disturbances in the surrounding rock structure occur, which in turn affect the stability. It is very important to understand the behavior of rock mass during and after excavation in order to select the right construction method and optimal support measures (Palmström and Stille 2010). As per Panthi (2012), there are three key engineering geological factors which directly affect the stability of tunnels and caverns, namely Rock mechanical properties, In-situ stress conditions and Groundwater inflow through fractures and weakness/fault zones. In addition, as described by Nilsen and Palmström (2000), the geological factors, size, geometry and orientation of the excavation affect the stability of underground excavation.

2.1   Rock mass properties

Characterization of rock masses is very important in an underground engineering project (Hencher 2016). For rock mass, its intact strength, nature of discontinuities, weathering and rock mass classification are the key issues. Rock mass is an in-situ material which comprises of intact rock, all joints and other discontinuities (Nilsen and Thidemann 1993).

As per Panthi (2006), rock mass is a heterogeneous medium and is characterized by two main features: Rock mass quality and Mechanical process subjected to rock mass as shown in Figure 2-1 which are closely linked. These features along with project's particular features like size, shape, location and its orientation govern the stability of underground openings. Depending
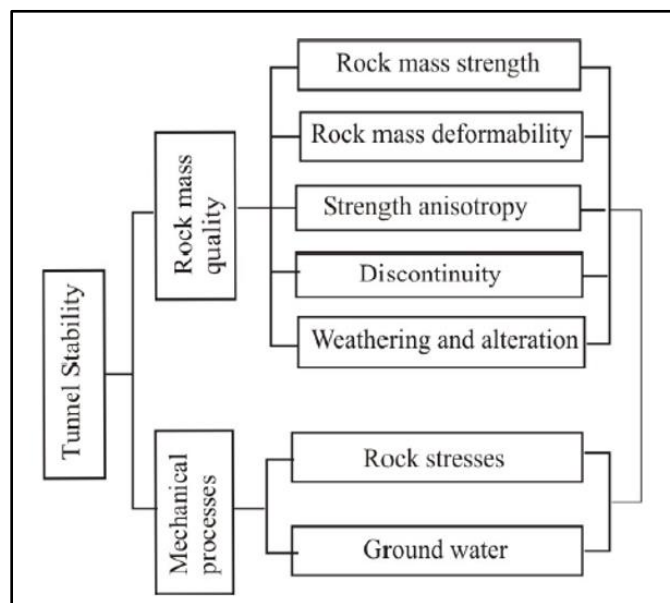
Figure 2-1 Factors influencing on tunnel stability (Panthi 2006)

upon the mineral composition of rock mass, its physical and mechanical properties vary considerably (Nilsen and Thidemann 1993). The most important physical properties of intact rock are density, porosity, wave velocity, heat transfer and expansion.

2.1.1 Discontinuities in the rock mass

Discontinuity is a collective term for different type of joints, weak bedding planes, weak schistosity planes and faults or weakness zone, which are mechanical fractures altering the homogeneity of rock mass. Depending upon its characteristics like roughness, weathering and nature of contacts, among others, its effect on rock mass varies considerably. Thus, they are of significant importance to rock engineering (Nilsen and Palmström 2000). Two major groups of discontinuities are Joints and Weakness zones.

2.1.1.1 Jointing

Joint is a regularly recurring fracture, in which no relative displacement has taken place on either side which cuts the rock with constant orientation and mean spacing ranging from few centimeters to several meters (Goodman 1993). As per ISRM (1978) in Panthi (2006), ten parameters that describe characteristics of discontinuity in rock mass are shown in Figure 2-2. These characteristics are identified during field mapping and joint orientation are presented using joint rosette and stereographic projection.
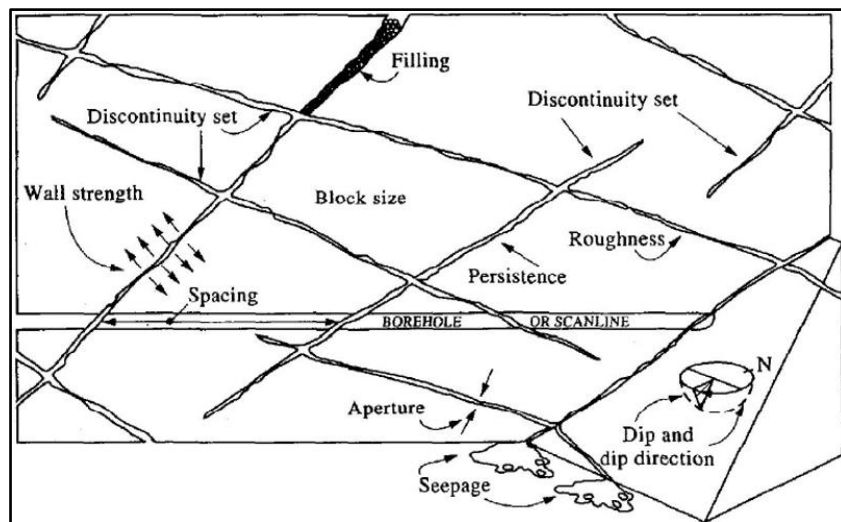
Figure 2-2 Discontinuity characteristics in the rock mass (Panthi 2006)

Even if rock mass is itself strong or impermeable or both, joint system may cause substantial weakness and promote fluid conductivity, which in turn enhances weathering (Goodman 1993).

2.1.1.2 Weakness and fault zones

Weakness zone is a zone or layer, whose mechanical properties are significantly less as compared to surrounding rock masses and has different hydrogeological condition than that of overall rock masses (Goodman 1993). It can be faults, shears/shear zone, thrust zone and weak mineral layers, among others. As per Panthi (2006), there are two types of weakness zones in general. One of them is a zone of weak rock or highly schistose rock within the series of hard rock and consists of weak material like clay, talc, graphite, mica or chlorite, pegmatite, etc, which are often anisotropic, mostly ductile, highly deformable, relatively impermeable and homogeneous in nature. Other category comprises of a zone of crushed and sheared rock or fault or fracture zones, which is as a result of numerous ruptures by faulting or tectonic activities. Figure 2-3 shows both types of weakness zones. They can create a major impact on stability problems like squeezing and tunnel buckling, roof or side wall collapse, water ingress
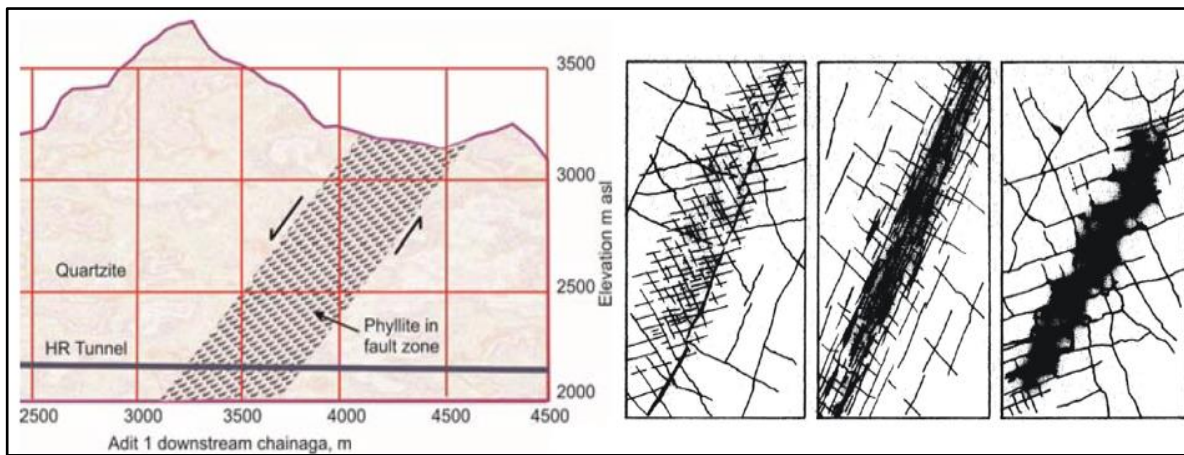
Figure 2-3 Type of weakness zone; Zone of weak rock (left) and Structural features of fracture zone (right) (Panthi 2018a)

and excavation. Stress situation of rock mass may be affected by major weakness zone (Nilsen and Palmström 2000). As seen in Figure 2-4, magnitude of minor principal stress is reduced due to the presence of shear zones. Also, during seismic events, in-situ stress of weakness zone and fault zones are permanently reduced (Panthi and Basnet 2018a). This shows that weakness zone and fault zone are the vulnerable areas during underground excavations.
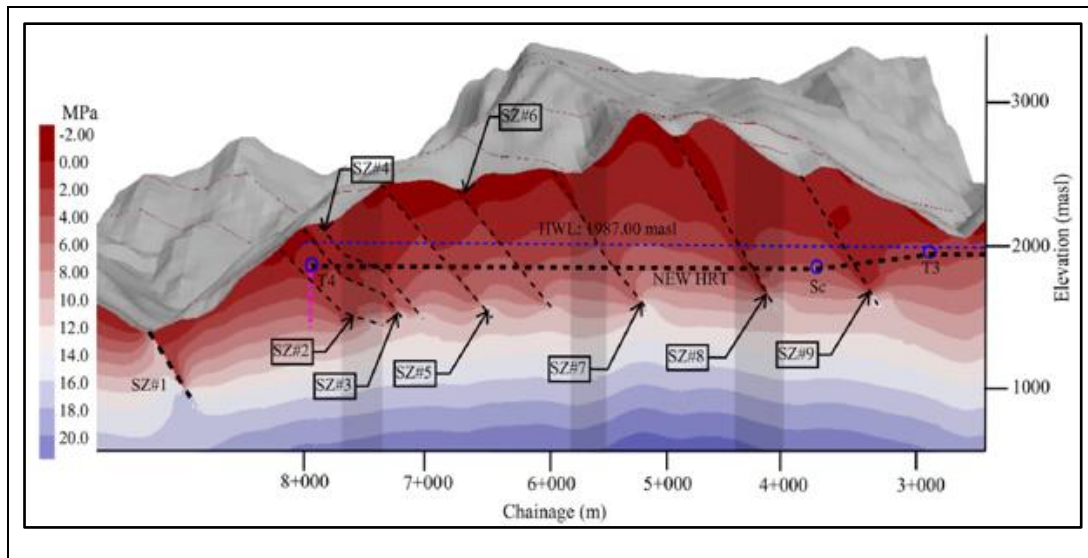
Figure 2-4 Stress attenuation near shear zones (Basnet and Panthi 2019a)

2.1.2 Rock mass strength and deformability

Information about the intact rock properties and characteristics of discontinuities is important to have reliable estimation of rock mass strength and deformability property of rock mass for underground excavation analysis (Hoek 2007).

2.1.2.1 Factor affecting rock mass strength

Principally, rock mass is a discontinuous material and its mechanical properties are scale dependent (Palmström and Stille 2010). Most methods for the estimation of rock mass strength depends on Uniaxial Compressive Strength (UCS) of selective sample of the rock mass. Different factors that influence strength of intact rock are discussed below.

1. **Scale effect**

Due to scale effect, with the increase in sample size of intact rock, significant reduction in strength takes place. As compared to crystalline un-weathered rock having small size effect, highly schistose, foliated and deformed rocks like shale, slate, phyllite and schist have substantial size as well as directional effect on their strength (Panthi 2006).

2. **Schistosity effect**

As a result of development of strong directional structure or anisotropy due to the preferred orientation of flaky or sheet minerals like mica and chlorite, many metamorphic and sedimentary rock show different rock properties in different directions of loading and present difficulties in the determining UCS. As shown in Table 2-1, the degree of anisotropy is governed by the quantity and arrangement of certain flaky and prismatic or anisotropic minerals like mica, chlorite, talc, graphite, etc., which significantly reduces the rock strength because of

easier sliding along the coated joint surface or cleavage (Palmström and Stille 2010). Rock mass in Himalaya are highly directional to strength and deformability, as of result of which, severe stability problems have been confronted during tunneling. Based on rock mass from Himalaya and other parts of the world, it has been found that UCS of intact rock is smallest when the schistosity plane is inclined at around an angle of 30 degree from direction of loading. And UCS of the intact rock is highest when schistosity plane is perpendicular to direction of loading (Panthi 2006).

Table 2-1 Classification of rock strength anisotropy (Panthi 2006)

Class	Descriptive class	Strength anisotropy index (I_a)	Typical rock types
I	Isotropic or close to Isotropic	1.0 – 1.2	Rocks having platy/prismatic minerals < 10% with shape factors <2 and platy minerals in random orientation. *Rock Types: Most of the igneous rocks and very high grade metamorphic rocks, i.e. diorite, granite, gabbro, quartzite, granitic gneiss , granulite etc.*
II	Slightly anisotropic	1.2 – 1.5	Rocks having platy/prismatic minerals 10 – 20 % with shape factors 2-4 and platy minerals in compositional layering. *Rock Types: High grade metamorphic rocks and some strong sedimentary rock, i.e. quartz-feldspatic gneiss, marble, migmatite, sandstone, limestone, etc.*
III	Moderately anisotropic	1.5 – 2.5	Rocks having platy/prismatic minerals 20 – 40 % with shape factors 4-8 and foliation plane distinctly visible. *Rock Types: Medium-high grade metamorphic rocks, i.e. mica gneiss, quartzitic schist, mica schist, biotite schist, etc.*
IV	Highly anisotropic	2.5 – 4.0	Rocks having platy/prismatic minerals 40 – 60 % with shape factors 8-12 and very closely foliated. *Rock Types: Low - medium grade metamorphic rocks such as phyllite, silty slate, etc.*
V	Extremely anisotropic	>4.0	Rocks having platy/prismatic minerals >60 % with shape factors >12 and fissile rocks. *Rock Types: Low grade metamorphic and argillaceous sedimentary rock, i.e. slate, carbonaceous phyllite, shale, etc.*

UCS measured diametrically and axially to weakness plane may possibly give false impression of an isotropic material as both give approximately same maximum strength (Broch 1983)

3. Weathering and alteration of rocks

Weathering and alteration lead to mechanical disintegration to form large number of joint and chemical decomposition to affect joint condition and rock material (Nilsen and Palmström 2000). Both processes affect the walls of the discontinuities, deteriorate rock material and

reduce the strength and deformation properties of rock mass. ISRM (1978) in Panthi (2006) has classified weathering grade into six different categories and is presented in Appendix A1.

In Himalaya, deep weathering has resulted due to combined effect of compressional tectonic movement and tough climatic conditions, which causes significant reduction in both strength and deformability and affects the stability. Impact of weathering on reducing UCS can be observed in Figure 2-5. Likewise, similar impact of weathering takes place in the reduction of elasticity modulus (Panthi 2006). Thus, in Himalaya, weathering impact should be considered during rock mass quality assessment and stability analysis of underground excavation.
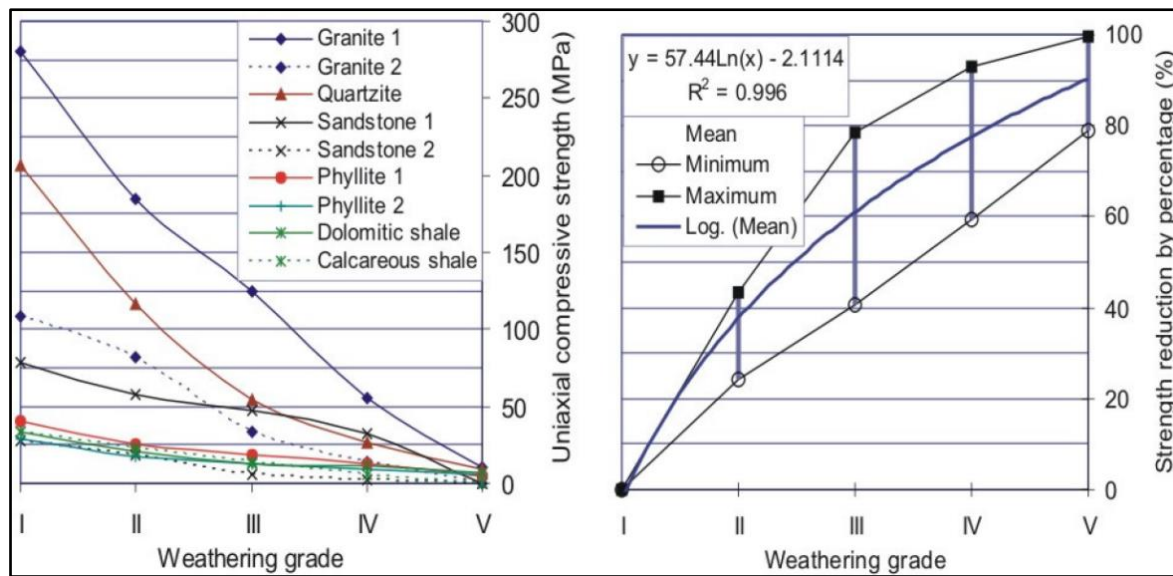
Figure 2-5 Compressive strength of rock (left) and percentage reduction in strength (right) based on weathering grade (Panthi 2006)

2.1.2.2 Rock mass strength and its estimation

As described by Panthi (2006), rock mass strength is an ability to resist stress and deformation. As it is generally not practical and impossible to measure the strength of an in-situ rock mass by laboratory type testing, rock mass strength has to be estimated from geological observation and from the test result of intact rock or rock surfaces (Hoek 2007). UCS-test is the most popular test for determining uniaxial compressive strength. Since, this test is time consuming and is limited to relatively unbroken and hard rocks that can be machined into regular sample, strength can be determined approximately by point load test, Schmidt hammer, simple field hammer test, etc (Nilsen and Palmström 2000).

Estimating the strength of rock mass is a major problem faced by designers in rock engineering. Usually, intact core sample obtained from better and stronger sections are strong and

homogeneous with few discontinuities and are much stronger than rock mass. However, strength of rock mass is different than intact rock strength. Due to this difficulty in determining rock mass strength directly, different empirical formula has been proposed by different authors for estimating rock mass strength as shown in Table 2-2.

Table 2-2 Empirical formula for estimation of rock mass strength

Proposed by	Empirical relationship
Beiniawski (1993)	$$\sigma_{cm} = \sigma_{ci} * \exp\left(\frac{RMR - 100}{18.75}\right)$$
Singh et al. (1992)	$$\sigma_{cm} = 0.7\gamma Q^{1/3}$$
Hoek et al. (2002)	$$\sigma_{cm} = \sigma_{ci} * \frac{\left(m_b + 4s - a(m_b - 8s)\right) * (\frac{m_b}{4} + s)^{a-1}}{2(1+a)(2+a)}$$
Barton (2002)	$$\sigma_{cm} = 5\gamma * Qc^{\frac{1}{3}} = 5\gamma * \left[\frac{\sigma_{ci}}{100} * Q\right]^{\frac{1}{3}} = 5\gamma * \left[\frac{\sigma_{ci}}{100} * 10^{\frac{RMR-50}{15}}\right]^{\frac{1}{3}}$$
Panthi (2006)	$$\sigma_{cm} = \frac{\sigma_{ci}^{1.5}}{60} \text{ for highly schistose and deformed rock mass}$$
Panthi (2017)	$$\sigma_{cm} = \frac{\sigma_{ci}^{1.6}}{60} \text{ for strong and brittle rock mass}$$

Where; σ_{cm} is the unconfined compressive strength of rock mass in MPa, γ is the rock density in t/m3, Q is rock mass quality value, σ_{ci} is the uniaxial compressive strength of intact rock in MPa, m_b is a reduced value of the material constant m_i, s and a are the material constant related to Hoek-Brown failure criteria, Qc is the normalized rock mass quality rating, RMR is the Bieniawaski's rock mass rating.

2.1.2.3 Estimation of rock mass deformability

Deformability of rock mass is an important engineering parameter for the design of underground structures and for the stability analysis, which explains the mechanical behavior of rock mass. Different direct in-situ deformability tests (plate bearing, flapjack test, etc.) are time consuming, costly and difficult to carry out. Likewise, value determined by these methods usually vary from one another drastically and there is a need of expertise for its interpretation. Similarly, due to discontinuities, it is particularly sensitive to a scale effect (Palmström and Singh 2001).

Due to these difficulties, modulus of deformation (E_{rm}) is usually estimated from empirical equation that are proposed by different authors. Table 2-3 shows empirical methods that have been used in the thesis. Panthi (2006) is based on elasticity modulus (E_{ci}) and intact rock strength (σ_{ci}), instead of classification system, which is subjective. Also, the estimation done at planning stage may deviate from actual ground conditions. Thus, Panthi (2006) will be useful for estimating rock mass deformation modulus of schistose, foliated and bedded rock mass having low σ_{ci}. Hoek and Diederichs (2006) is used during numerical modelling in RocData.

Table 2-3 Empirical formula for the estimation of rock mass deformation modulus

Proposed by	Empirical relationship
Hoek and Diederichs (2006)	$E_{rm} = E_{ci} * \left[0.02 + \dfrac{(1 - \frac{D}{2})}{1 + e^{(\frac{60 + 15D - GSI}{11})}} \right]$
Panthi (2006)	$E_{rm} = E_{ci} * \left(\dfrac{\sigma_{cm}}{\sigma_{ci}} \right)$

Where, D as a factor represents the degree of disturbance caused by blast damage and stress relaxation in rock mass and GSI is Geological Strength Index (GSI= RMR-5)

2.1.3 Failure criteria

Over the years, several failure criteria have been developed in order to study failure condition in rock masses. Among different failure criteria, Hoek-Brown criterion and Mohr-coulomb criterion are commonly used.

2.1.3.1 Hoek-Brown failure criterion

This criterion is widely used and accepted throughout the world. It is a non-linear criterion useful for jointed and schistose rock mass of homogeneous character and is based on triaxial test. As per Hoek et al. (2002), several amendments were made on original empirical criteria by Hoek and Brown (1980), particularly considering very weak and jointed rock masses. Later in 2002, Generalized Hoek-Brown criterion was developed for jointed and isotropic rock masses, which is expressed as equation 2-1.

$$\sigma'_1 = \sigma'_3 + \sigma_{ci} \left(m_b \frac{\sigma'_3}{\sigma_{ci}} + s \right)^a \qquad \qquad \text{2-1}$$

Where σ'_1 and σ'_3 are maximum and minimum effective stress at failure, m_b is a reduced value of the material constant m_i and is expressed by equation 2-2. Similarly, s and a are the rock mass constants expressed by equation 2-3 and 2-4.

$$m_b = m_i \exp\left(\frac{GSI - 100}{28 - 14D}\right) \qquad \text{2-2}$$

$$s = \exp\left(\frac{GSI - 100}{9 - 3D}\right) \qquad \text{2-3}$$

$$a = \frac{1}{2} + \frac{1}{6}\left(e^{-\frac{GSI}{15}} - e^{-\frac{20}{3}}\right) \qquad \text{2-4}$$

Guidelines for estimating D and m_i are given in Appendix A3 and A4.

This criterion is applicable in Rock masses which have sufficient number of closely spaced discontinuities with similar surface characteristics that exhibits isotropic behavior. In addition, it is applicable in rock mass with block size smaller than structure being analyzed (Hoek 2007). Figure 2-6 (left) explains the kind of failure criterion to be used in different rock mass condition.
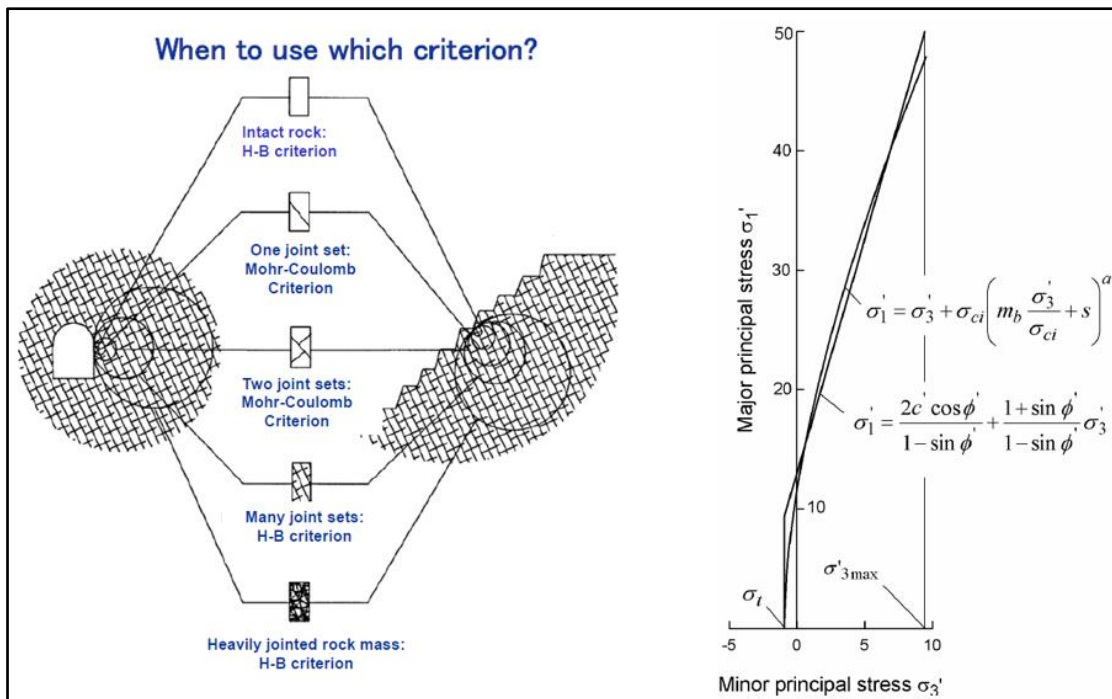
Figure 2-6 Selection of failure criterion based on rock mass condition (left) and relationships between major and minor principal stresses for Hoek-Brown and equivalent Mohr-Coulomb criteria (right) (Panthi 2018a)

2.1.3.2 Mohr Coulomb failure criterion

It is a classical approach of defining rock mass strength and is a linear criterion useful for block fall analysis and stability assessment of tunnels situated in rock mass having one or two joint set as shown in Figure 2-6 (left). In this criterion, cohesive strength c' and angle of friction angle φ' defines the strength of rock mass. In order to find the equivalent angles of friction and cohesive strengths for each rock mass and stress range, average linear relationship was fitted to the curve generated by solving equation 2-1 for a range of minor principal stress values defined by $\sigma_t < \sigma_3 < \sigma'_{3max}$, see Figure 2-6 (right).

2.1.4 Post failure behavior

Estimates of post failure characteristic is important in numerical modelling to study progressive failure of rock mass. While carrying out modelling to study rock mass behavior after failure, Hoek and Brown (1997) suggest the post failure characteristics as shown in Figure 2-7.
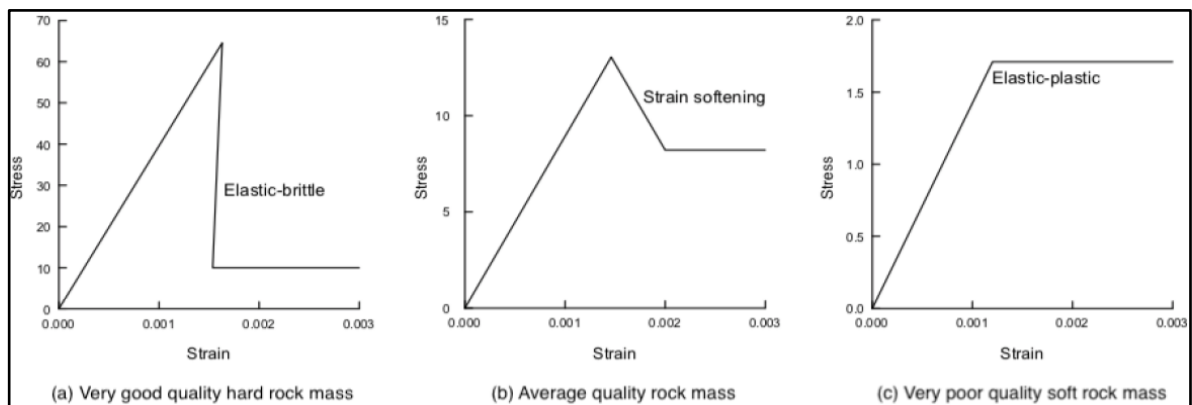
Figure 2-7 Suggested post failure characteristics for different quality of rock mass (Hoek and Brown 1997)

For an average quality rock mass, post failure characteristics are to be estimated by reducing the GSI value or peak parameters. As per discussion with Supervisor (30/03/2020), residual parameters for plastic analysis have been assumed as 1/4th of the peak value. For very poor quality rock mass which behaves as elastic-perfectly plastic and is already at residual state, Hoek and Brown (1997) and Crowder and Bawden (2004) suggest to keep post peak or residual properties same as that of peak properties with dilation equal to zero.

2.2 Rock stress

In-situ rock stresses may have significant impact on the stability of underground opening if redistributed stress around an excavation surpass the rock mass strength. However, even low

stress induces stability problem (Nilsen and Palmström 2000). If the magnitude and direction of in-situ stresses and geometry of the openings are known, then the magnitude and direction of redistributed stress around an opening can be evaluated. In addition, if rock mass parameter are known, it is possible to analyze potential stability problems and leakage problems due to stresses, need of rock support requirement and the optimization of excavation geometry (Nilsen and Thidemann 1993). Thus, it is important to know about the magnitude and directions of in-situ stresses for the analysis of stress induced instabilities.

2.2.1   In-situ stresses in rock mass

According to Nilsen and Thidemann (1993), virgin in-situ stresses in rock mass is due to the combination of following components:

- Gravitational stresses- result of gravity alone
- Topographic stresses- caused by topographic effects
- Tectonic stresses- caused by plate tectonics
- Residual stress- due to locked stress into the rock material during earlier stages of its geological history

As per Panthi (2006), gravity induced vertical stress (σ_v) may be calculated as:

$$\sigma_v = \gamma * H \qquad\qquad 2\text{-}5$$

Where, σ_v is in Mpa, γ is the specific weight in MN/m³, H is the depth in m.

Due to tectonic stress, the total horizontal stress in most cases is much higher than the horizontal stress induced by gravitation, resulting the ratio (k) of average horizontal and vertical in-situ stress to be greater than 1. Based on stress measurement from various parts of the world, this situation is especially evident at shallow and moderate depths as illustrated in Figure 2-8. However, the ratio (k) is less than one and approaches a fixed value at higher depth. Variation of stresses highlight the importance of measurement of in-situ stress as per individual cases.
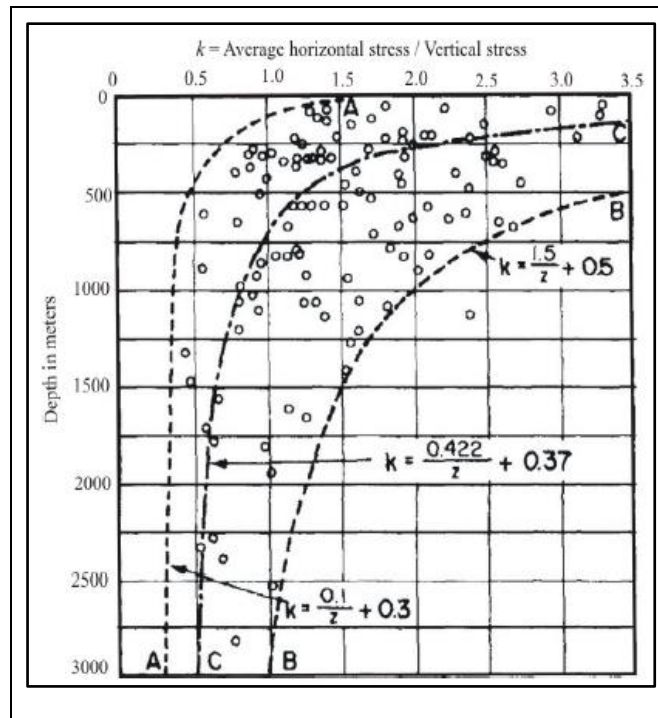
Figure 2-8 Variation of ratio (k) of average horizontal to vertical stress with depth below ground surface (Panthi 2006)

According to Panthi (2012), the magnitude of total horizontal stress can be calculated by equation 2-6, where v is the poisson ratio and σ_{tec} is the tectonic horizontal stress (locked-in stress)

$$\sigma_h = \frac{v}{1-v} * \sigma_v + \sigma_{tec} \qquad\qquad 2\text{-}6$$

Similarly, if underground excavation is placed in high valley sides, resulting stresses around an opening will be dominated by the topographic effects with major and minor principal stress being more or less parallel and perpendicular to the slope of the valley, respectively.

2.2.2   Rock stress distribution around a tunnel

Due to excavation of tunnel, in-situ stress state in rock mass gets disturbed and then, load initially carried by excavated rock mass must be transferred to the remaining rock mass around the opening. These induced stresses depend upon the magnitude and direction of principal stresses and geometry of opening, which set up in the form of tangential (σ_θ) and radial stresses(σ_R) around the opening (Shrestha 2014).

In case of circular excavation in an idealized condition in homogeneous and isotropic elastic material in isostatic virgin stress (σ), tangential stress increases rapidly close to contour and induces with twice the magnitude of the isostatic stress all around the periphery and decreases

gradually as illustrated by Figure 2-9 (right), In contrast, radial stresses will be zero at periphery of openings.
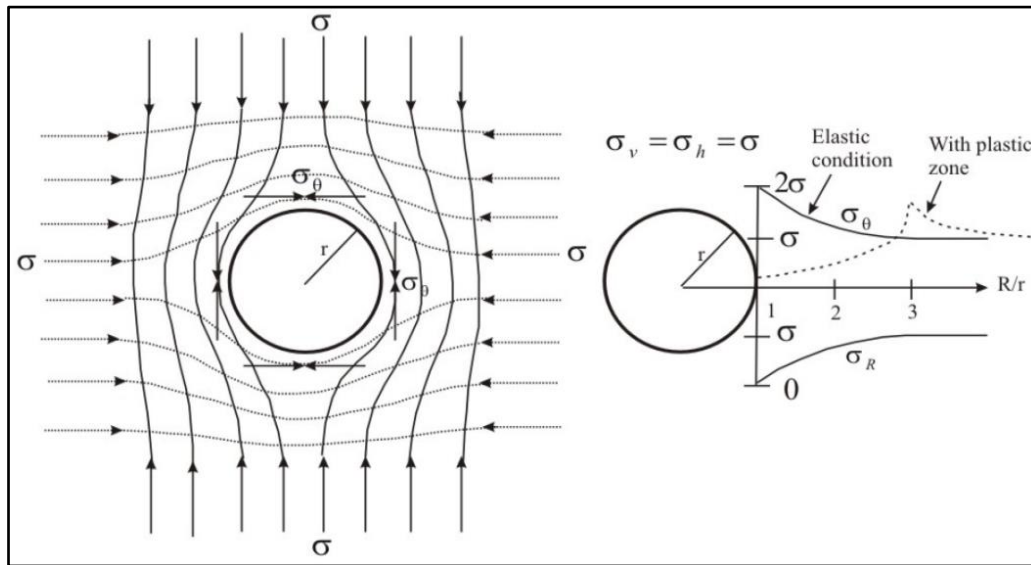
Figure 2-9 Stress trajectories in rock mass surrounding a circular opening (left) and tangential and radial stress distribution in elastic and non-elastic conditions (right) (Panthi 2006)

However, in-situ stresses are often highly anisotropic. As a result, tangential stress does not remain same around the periphery and varies as per the extent of stress anisotropy. As per Kirsch, the tangential stress will reach its maximum value ($\sigma_{\theta max}$) where σ_1- direction is a tangent to tunnel contour and its minimum value ($\sigma_{\theta min}$) where the σ_3- direction is a tangent to tunnel contour (Nilsen and Palmström 2000). Equations for calculating maximum and minimum tangential stress values are represented by equation 2-7 and 2-8 . However, they are applicable for circular opening in a continuous, homogenous, isotropic and linearly elastic rock (Martin and Christiansson 2009).

$$\sigma_{\theta max} = 3\sigma_1 - \sigma_3 \qquad\qquad 2\text{-}7$$

$$\sigma_{\theta min} = 3\sigma_3 - \sigma_1 \qquad\qquad 2\text{-}8$$

In case of non-symmetrical geometry and sharp corners, magnitude of tangential stress will be higher and in extreme cases, concentration of stresses may become more than 10 times the major principal stresses (Nilsen and Palmström 2000). In theory, magnitude of induced maximum tangential stresses varies as per the shape of underground opening and is independent of its size. Nevertheless, size impacts zone of influence directly. Apart from these, deformation properties and method of excavation determine the distribution of tangential stresses as well.

In-situ rock stress measurements in good quality homogeneous rock mass in Norway shows that stresses stabilize at a fixed level (actual virgin stress) at a distance approximately half the tunnel width from tunnel contour. In contrast, in soft and fractured rock mass, as indicated by dotted curve in Figure 2-9 (right), stress peak is relatively flat and maximum stress is located at certain distance away from tunnel contour. Similar situations will occur in most drill and blast tunnels as a result of blast damage. According to Panthi (2006), tangential stresses in weak and anisotropic rock mass drives the zone of broken rock deep into the contours forming a plastic zone and maximum tangential stresses are moved further until the elastic zone is reached.

2.3   Groundwater inflow and leakages

Intervention of groundwater during underground tunneling is one of the major challenges. Specially, it causes serious stability problems in crushed or sand like materials or when associated with other forms of instability (Nilsen and Palmström 2000). This may result in face and roof collapse and may severely affect support system due to build up high pore pressure behind tunnel periphery. Groundwater mainly affects stability of underground opening by reducing the strength of rock material and shear strength of discontinuities. Similarly, water inflow and leakage during construction and operation, respectively, cause significant problems.

As most of the intact rock has poor communication between individual pores and has low permeability, permeability of rock mass is determined by degree of jointing and character of other discontinuities in the rock mass. Jointing makes rock mass anisotropic and inhomogeneous in terms of conductivity. With increase in depth from the surface, joint aperture reduces and spacing between joints increases, which ultimately reduces the conductivity of rock mass. In order to evaluate rock mass conductivity, jointing frequency, its continuity and its interconnection with other permeable joint, joint infilling conditions, joint aperture and its orientation to valley slope need to be evaluated. In unlined/shotcrete lined tunnel, it is important to understand the behavior of rock mass when exposed to water pressure (Basnet 2018).

2.4   Instabilities issues and analysis methods in underground openings

Due to variation of stresses and rock types along the alignment, rock stress problems or instability as well varies accordingly (Palmström and Stille 2010). Thus, assessment of failure mode of rock mass along the alignment is a prerequisite so that necessary change in alignment, excavation method and support measures can be made as early as possible. As per Nilsen and Palmström (2000), instability of the ground, i.e., the rock masses surrounding an underground opening, is classified into two main categories, i.e., Block failure and Stress failure.

2.4.1 Block or Structurally controlled failure

Shallow depth tunnels with jointed rock masses, which are affected by weathering and fracturing and where in-situ stress magnitude are low, often faces block failure (Panthi 2018b). This failure mode involves free movement of pre-existing wedge or blocks from roof or sliding out of sidewalls as a result of excavation and low normal stress on joints. Both orientation of major discontinuity sets and shape, size and orientation of the opening determine the shape and size of potential wedges (Hoek 2007).

2.4.2 Stress controlled failure

In case of deep-seated tunnels, rock mass stresses are high and anisotropic that they may locally exceed the strength of the rock mass. This situation will lead to rock bursting, squeezing or other stress related instability problems (Selmer-Olsen and Broch 1977). Similar problems can be faced in tunnels, where stresses due to topography are high and anisotropic. Problems due to overstressing are usually limited to areas of maximum tangential stress (Nilsen and Thidemann 1993).

The severity and the type of overstressing induced instability are governed by rock type and its mineralogical composition, strength and quality, geometry of the underground opening and the in-situ stress state (Panthi 2018b). In case of overstressing in relatively unjointed and massive strata, instability is mainly related to rock spalling or rock bursting. However, if rock mass is weak, schistose, sheared, deformed and thinly foliated/bedded, squeezing is most likely to occur. These instabilities are faced during both excavation and operation of the tunnel.

2.4.2.1 Brittle failure

In hard and brittle rock mass, if rock mass strength is exceeded by induced maximum tangential stress, fracturing parallel to tunnel contour takes place. In case of significant maximum tangential stress, this fracturing process is accompanied with loud noises with big slabs and with release of energy in the order of earthquake intensity and is generally denoted as Rock burst. However, in case of moderate stress levels, fracturing results in loosening of thin rock slabs, which is generally called as rock slabbing or spalling (Nilsen and Thidemann 1993). Rock spalling commonly results in asymmetric tunnel profile, known as "Keel formed overbreak" as shown in Figure 2-10.
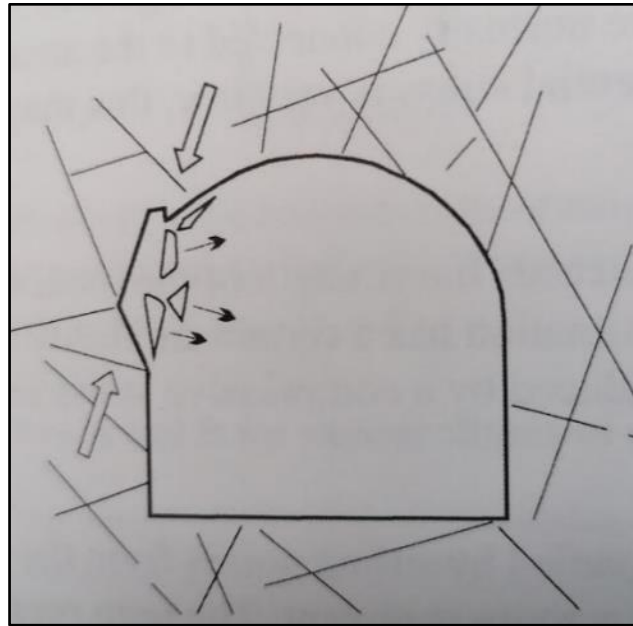
Figure 2-10 Brittle failure in hard and massive rock (Nilsen and Palmström 2000)

As compared to softer rock with significantly lower stress, there will be stress concentration in stiff rocks. Thus, as illustrated by Nilsen and Palmström (2000), tunnel section passing through hard rock like gneiss rock with more quartz and feldspar content faces rock burst or spalling and in contrast, tunnel section with mica rich gneiss are generally characterized by stress relief.

2.4.2.2 Brittle failure analysis

Analysis of extend of rock burst or spalling is one of the key design issues in planning, designing and construction of underground projects. Different methods have been developed by many scientists to assess rock burst activities. According to Panthi (2017), four widely used empirical or semi-analytical methods for prediction of brittle failure are: Norwegian rule of thumb, Stress problem classification-part of Q-system, Uniaxial compressive strength and tensile strength approach and Maximum tangential stress and crack initiation strength approach.

1. **Norwegian rule of thumb**

In 1965, Professor Rolf Selmer Olsen of Norwegian Institute of Technology (NTH) studied over 60 tunnels, which faced rock burst and rock spalling and were passing parallel with valley-side slope. Based on this study, potential brittle failure can be assessed with respect to vertical height between the tunnel and top of valley-side slope (h) and horizontal distance between tunnel and top of valley-side slope(L) as shown in Figure 2-11. This rule of thumb for hard rocks states that if h>500m and angle between tunnel location and plateau exceeds 25 degree, one should be ready for stress induced stability issues. In case of tunnels located on high valley

side, high stress anisotropy exists due to the topographic effect, which strongly influences the stability of tunnel.
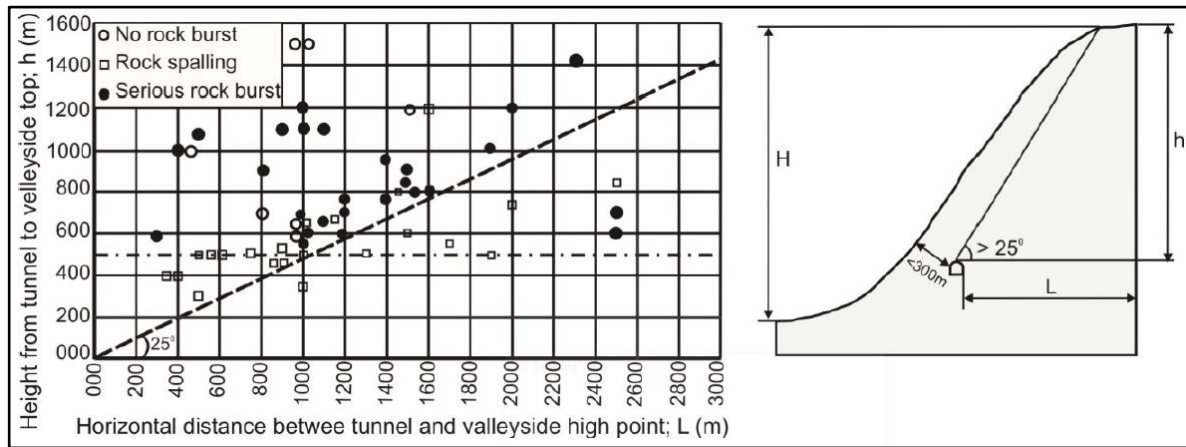
Figure 2-11 Tunnels having rock burst, rock spalling and severe rock burst plotted against height from tunnel to top of valley-side slope i.e., plateau, and horizontal distance between tunnel and valley-side top (Panthi 2017)

As per Panthi (2018b), this approach gives indication of potential rock spalling/rock burst for those tunnels, which are aligned parallel with valley side slope with a location within 500m distance from valley side slope topography. However, this simplified approach does not consider the influence of tectonic stress, but still represents experience from large number of Norwegian projects situated in valley sides (Nilsen and Palmström 2000).

2. Stress problem classification

As per Q-system, which will be discussed in 2.4.2.4, instability issue related to stresses are considered by SRF parameter. Based on three input parameters, i.e., compressive strength of intact rock (σ_{ci}), the major principle stress (σ_1) and the maximum tangential stress ($\sigma_{\theta max}$), SRF categorizes rock spalling/rock burst potential in a tunnel build in hard strong rock as shown in Table 2-4.

Table 2-4 Stress problem class in competent rock mass based on Q-system (Panthi 2017)

Stress Class	Description of potential stress induced instability	Ratio - intact rock strength and Major principle stress (σ_{ci} / σ_1)	Ratio between maximum tangential stress and intact rock strength ($\sigma_{\theta-max} / \sigma_{ci}$)
SC 1	Low stress, near surface, open joints	>200	<0.01
SC 2	Medium stress, favorable stress conditions	200 - 10	0.01 – 0.3
SC 3	High stress, very tight structure, usually favorable to blasting except for wall	10 - 5	0.3 – 0.4
SC 4	Moderate spalling after > I hour	5 - 3	0.5 – 0.65
SC 5	Spalling and rock burst after few minutes	3 - 2	0.65 - 1
SC 6	Heavy rock burst and immediate strain failure	<2	>1

3. Uniaxial compressive and tensile strength approach

It is more indirect, subjective, quick and qualitative method for assessing spalling/rock burst in rock mass. Proposed by Diederichs (2007), this approach is linked with uniaxial compressive strength (UCS) and tensile strength (T) of the intact rock, see Figure 2-12. This approach assumes that crack initiation in the rock mass is due to internal heterogeneities and strain
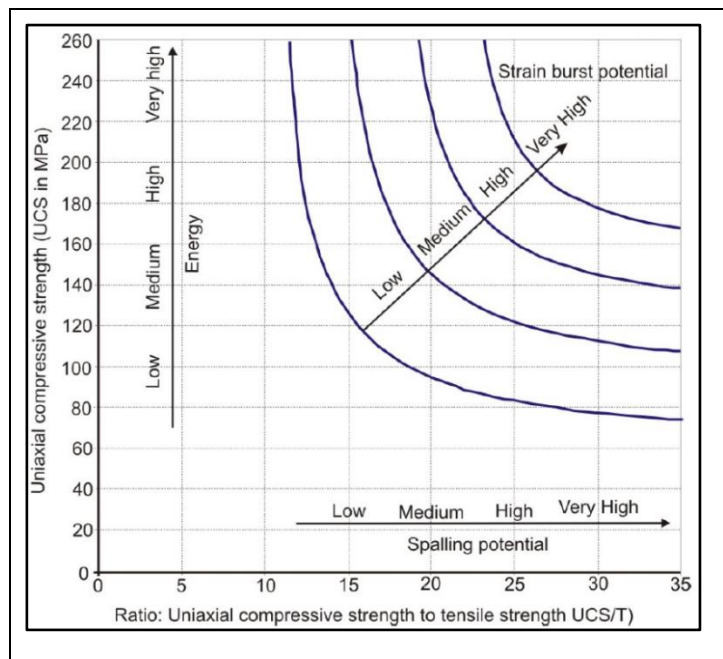
Figure 2-12 Classification of potential rock spalling/rock burst based on compressive and tensile strength of rocks (Panthi 2017)

anisotropy in the hard, strong and brittle rock mass under compression and crack initiation is strongly affected by the internal tensile strength. The major weakness of this approach is that it

does not consider the prevailing in-situ stress. Thus, while using this approach, one should also evaluate on the basis of in-situ stress (Panthi 2017).

4. Maximum tangential stress and rock spalling strength approach

Three approaches described above only assess rock burst/spalling qualitatively and does not give an idea about severity of rock burst or spalling (depth impact) into the rock mass. As per Panthi (2017), Martin and Chritiansson (2009) proposed an equation 2-9, which assesses extent of rock spalling/rock burst depth -impact in the tunnel wall (S_d) as illustrated in Figure 2-13.

$$S_d = r * \left[0.5 * \frac{\sigma_{\theta max}}{\sigma_{sm}} - 0.52 \right] \qquad 2\text{-}9$$

Where, S_d = depth of spalling measure from boundary of tunnel (m), r = Tunnel radius (m), $\sigma_{\theta max}$ = Maximum tangential stress calculated by Kirsch's equation in MPa and σ_{sm} = Rock mass spalling strength in MPa, see Figure 2-13.
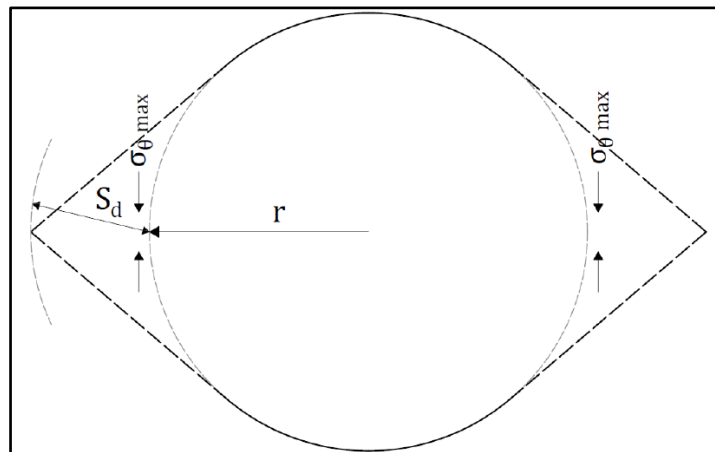
Figure 2-13 Potential depth impact in the wall of a circular tunnel caused by a major induced tangential stress (Panthi 2019)

This assessment helps in making strategy related to rock support application, especially in deciding length and type of rock anchor or bolts. Martin and Christiansson (2009) have proposed the magnitude of in-situ spalling strength for glacially eroded massive Scandinavian Crystalline rocks, which lies between 55-65% of intact rock strength while the laboratory tested crack initiations strength may be between 40-50% of intact rock strength (Panthi 2017). Experience shows that in coarse to medium grained, homogeneous and strong to very strong rocks, crack initiation starts forming once the specimen exceeds the threshold of approximately 0.3 of the intact rock strengths. Also, Panthi (2017) suggests replacing rock spalling strength

with rock mass strength, which can be estimated by Panthi (2017) from Table 2-2 for homogeneous, massive and brittle rock mass.

2.4.2.3 Plastic deformation

As per Panthi (2006), weak and soft rocks of plastic nature react in different way than that of stronger and isotropic rocks when subjected to tangential stresses. High degree of schistosity, especially the extent of thin foliation, is dominating characteristic of weak rock (Panthi 2013a). In these rocks, when induced maximum tangential stresses along the tunnel periphery is higher than strength of rock mass, micro cracks are generated gradually along the schistosity or foliation plane. This causes to form visco-plastic zone of micro-fractured rock mass deep into the walls and shifts the induced maximum tangential stress outside the plastic zone, see Figure 2-14. The final result is the inward movement of rock material towards the tunnel, which is known as tunnel squeezing (Panthi 2006).
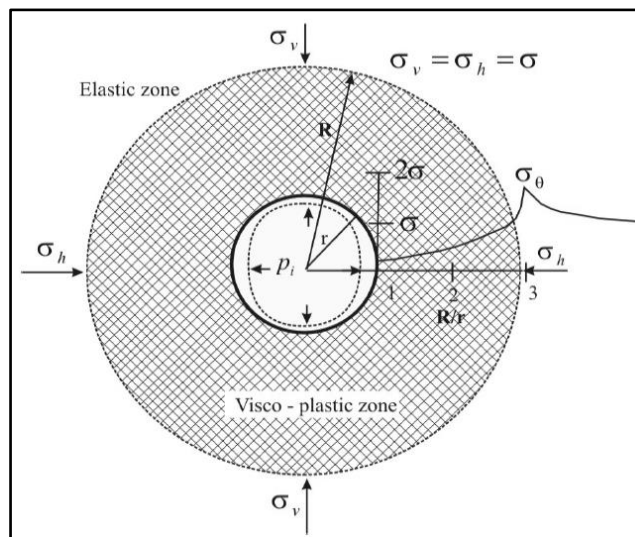
Figure 2-14 Squeezing in circular tunnel (Panthi 2006)

As per Shrestha (2014), plastic deformation, known as squeezing in weak and schistose rock mass, is the summation of instantaneous deformation or time independent and time dependent deformation. Time independent deformation takes place instantaneously after the excavation and before the applied support comes into effect. In an unsupported tunnel, tunnel face acts as a column offering fictious support. As tunnel face advances ahead, time independent deformation increases and reaches its maximum value once tunnel face advances by more than four times the tunnel diameter (Panthi and Shrestha 2018). At this instant, it is assumed that the face effect has ceased. This time independent deformation is the most dominating and usually the most crucial part of the plastic deformation. As face effect decreases, time dependent

behavior becomes dominant (Shrestha 2014). Weak and schistose rocks continue to deform as time advances due to creep effect, which is a time dependent behavior of rock mass in which, without an increase of stress on rock mass, strain rises. Deformation may stop during construction or may continue over a long period of time. As per Barla (2005), the magnitude of tunnel convergence due to squeezing, deformation rate and extent of yielding zone depends upon the geological and geotechnical conditions, in-situ stresses relative to rock mass strength, ground water flow, pore pressure and rock mass deformability characteristics. If in-situ stress is anisotropic, magnitude of deformation differs both along the tunnel alignment and also along the periphery of tunnel wall (Panthi and Shrestha 2018). If rock mass is very weak, then, deformation in tunnel is unavoidable and takes place to such an extent that it is irreversible. In order to control it, adequate support measure should be provided at the right time.

Severe squeezing has taken place in Nepal Himalaya, especially in tunnels constructed in Siwalik and Lesser Himalaya zone. These zones have weak and highly deformed rock mass like shale, mudstone, slate, phyllite, schist, schistose gneiss and highly sheared fault gouge/weakness zone. When they are overstressed as compared to their strength, they undergo severe squeezing. Even the tunnel passing through highly sheared fault zones with low rock cover of about 75m has suffered severe squeezing (Panthi 2006).

2.4.2.4 Plastic deformation analysis

Severe squeezing is a major challenge and threat to stability of underground opening, when tunneling through tectonically active Himalayan rock mass. Any misjudgment while designing rock support leads to costly failures (Hoek 2007). Thus, reliable prediction of squeezing rate and its extent should be done as accurately as possible in advance, to formulate a proper plan for controlling large deformation induced by squeezing and to carryout successful tunneling in difficult ground situations as like in the Himalaya (Panthi 2006).

Several methods have been developed by different authors for the determination of potentiality and estimation of large tunnel deformation in weak rocks. Basically, these approaches include empirical methods like Singh et al. (1992), Q-system (Grimstad and Barton 1993), Goel et al. (1995), Palmstrøm (1995), semi-analytical methods like Hoek and Marinos (2000), Kovari (1998), Aydan et al. (1993) and Panthi and Shrestha (2018) and analytical methods such as Convergence confinement methods like Carranza-Torres and Fairhurst (2000). Apart from these, numerical methods like 2-dimensional RS2 finite element program can be used for analysis. Among the different approaches described above, Singh et al. (1992), Q-system (Grimstad and Barton 1993), Goel et al. (1995), Hoek and Marinos (2000), Panthi and Shrestha

(2018) and RS2 have been used for squeezing analysis as per the discussion with Supervisor (14/03/2020).

At an early stage of tunnel design, empirical methods give an idea about whether squeezing takes place in overstressed tunnel using available information. However, in order to determine the degree of severity or magnitude of potential squeezing in a tunnel, semi-analytical methods can be used. Selected empirical and semi-analytical methods are discussed below.

1. Singh et al. method

Singh et al. (1992) proposed an empirical approach based on case histories from Himalayas and by collecting data on Barton et al. (1974). This approach has put forward a demarcation line as shown in Figure 2-15, above which squeezing probability can be expected. The equation of demarcation line is given as equation 2-10. Prediction of squeezing is made with reference to Q-value and overburden (H) of rock mass.

$$H = 350Q^{1/3} \hspace{4cm} 2\text{-}10$$

Based on this approach, it can be said that if the overburden depth of the rock mass above tunnel section exceeds $350Q^{1/3}$, corresponding tunnel section is likely to be affected by tunnel squeezing. As per Panthi (2006), this approach has considered stress effect twice, since rock mass Q-value has already been considered for rock stress effect (SRF).
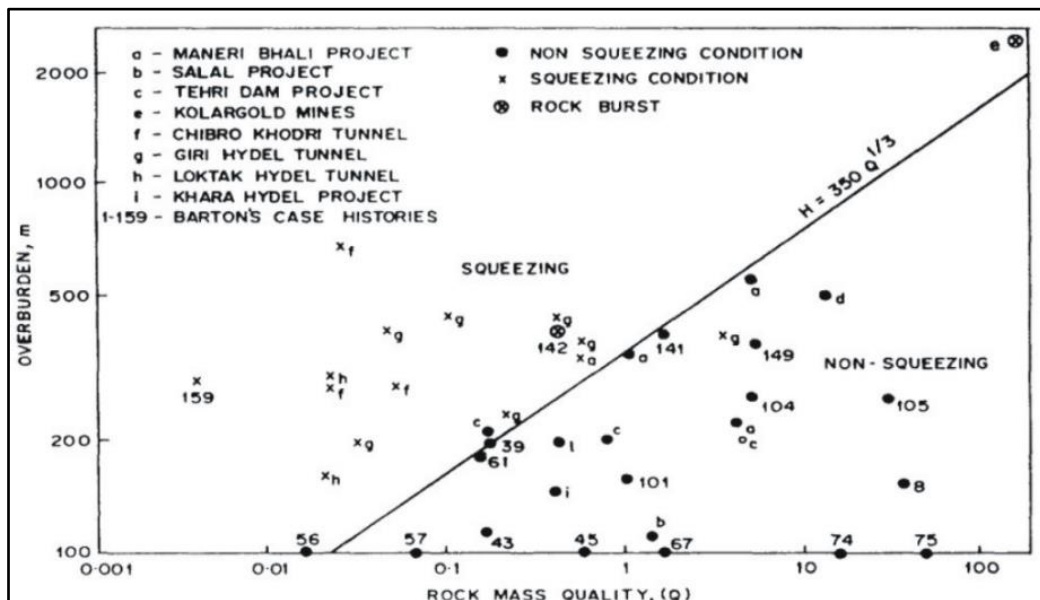
Figure 2-15 Criteria for predicting squeezing suggested by Singh et al. (1992) (Panthi 2006)

2. Goel et al. method

In order to avoid the contradiction discussed in Singh et al. approach , Goel et al. (1995) suggested the new squeezing criteria for the rock mass using rock mass number (N), tunnel depth (H) to consider stress or SRF indirectly and tunnel span (B) to consider strength reduction of rock mass with size. This approach is based on data collected from wide variety of ground conditions, varying from highly jointed and fractured rock masses to massive rock masses (Singh and Goel 2012a). The squeezing criteria is given by equation 2-11 as indicated by line AB in Figure 2-16, which separates squeezing and non-squeezing cases. Here, N is the Q-value without considering SRF value. Criteria to classify different degree of squeezing using N is presented in Appendix A2.

$$H = 275N^{0.33} * B^{-0.1} \qquad\qquad 2\text{-}11$$
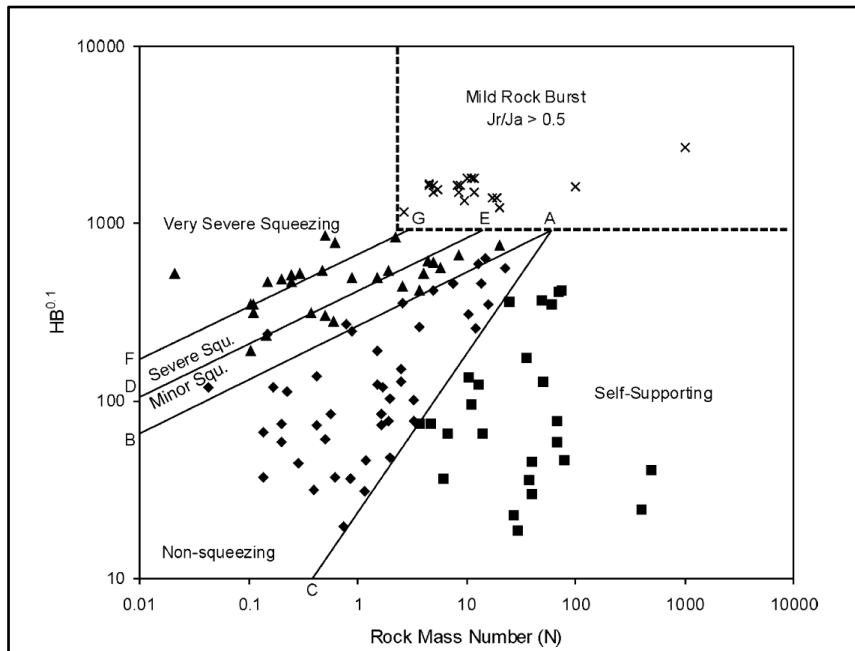
Figure 2-16 Criteria for predicting squeezing suggested by Goel et al. (1995) (Singh and Goel 2012a)

3. Q-system

Q-system was proposed by Norwegian Geotechnical Institute (NGI) by Barton et al. (1974) for quality rating as well as for rock support estimation. Later, it was updated by Grimstad and Barton (1993) by including more than 1000 cases. It is a quantitative classification system for the estimation of tunnel support based on numerical assessment of rock mass quality using six parameters, namely, Rock Quality designation (RQD), Number of Joint sets (Jn), Roughness of

most unfavorable joint (Jr), Degree of alteration or filling in joint (Ja), Water inflow (Jw) and Stress Reduction factor (SRF).

The numerical value of Tunneling Quality Index (Q) of rock mass is defined by:

$$Q = \frac{RQD}{Jn} \times \frac{Jr}{Ja} \times \frac{Jw}{SRF} \ (0.001 \leq Q \leq 1000) \hspace{2cm} 2\text{-}12$$

In 2002, it was further updated by Barton (2002) based on more than 900 new cases from Norway, Switzerland and India. SRF, a part of the Q-classification system, explains problems due to weakness zones and rock stress problems. It accounts for squeezing rocks based on the ratio of $\sigma_{\theta max} / \sigma_{cm}$. Based on Barton (2002), squeezing condition is given in Table 2-5.

Table 2-5 Squeezing condition as per Q-system (Barton 2002)

Squeezing rock: Plastic flow of incompetent rock under the influence of high rock pressure	$\sigma_{\theta max} / \sigma_{cm}$	SRF
Mild squeezing rock pressure	1-5	5-10
Heavy squeezing rock pressure	>5	10-20

4. Hoek and Marinos approach

As per Hoek and Marinos (2000), convergence of tunnel can be related to ratio of rock mass strength (σ_{cm}) and vertical stress (p_o) and this ratio determines whether or not the deformation induces stability problems. Based on closed form analytical solutions carried out by Duncan-Fama (1993) and Carranza-Torres and Fairhurst (1999) for circular tunnel in isostatic stress field, Hoek and Marinos (2000) found that there exists a good correlation between the ratio of rock mass strength and vertical stress and tunnel convergence (strain) as shown in Figure 2-17(left).

For this, Monte Carlo simulations were carried out for wide range of rock mass properties and in-situ stress conditions. However, this analysis considers only cases of tunnel and does not consider stability of face (Hoek 2001). This analysis can be extended to cover tunnels in which an internal pressure is used to simulate the effects of support. Using curve fitting process, equation 2-13 and 2-14 were found to evaluate total tunnel deformation and size of plastic zone, respectively.

Although the method is very crude, it provides with first degree estimate of potential squeezing problems in weak rock having squeezing condition. Figure 2-17(left) shows that when ratio of

σ_{cm}/p_o goes below 0.2, strain increases asymptotically, which indicates onset of instability and may cause collapse of both tunnel and face without adequate support (Hoek 2001). Thus, in addition to tunnel, tunnel face has to be stabilized, so that safe working condition can be established, and tunnel can be advanced safely. Likewise, Figure 2-17(right) gives an idea about the degree of difficulty that can be confronted during tunnel excavation.
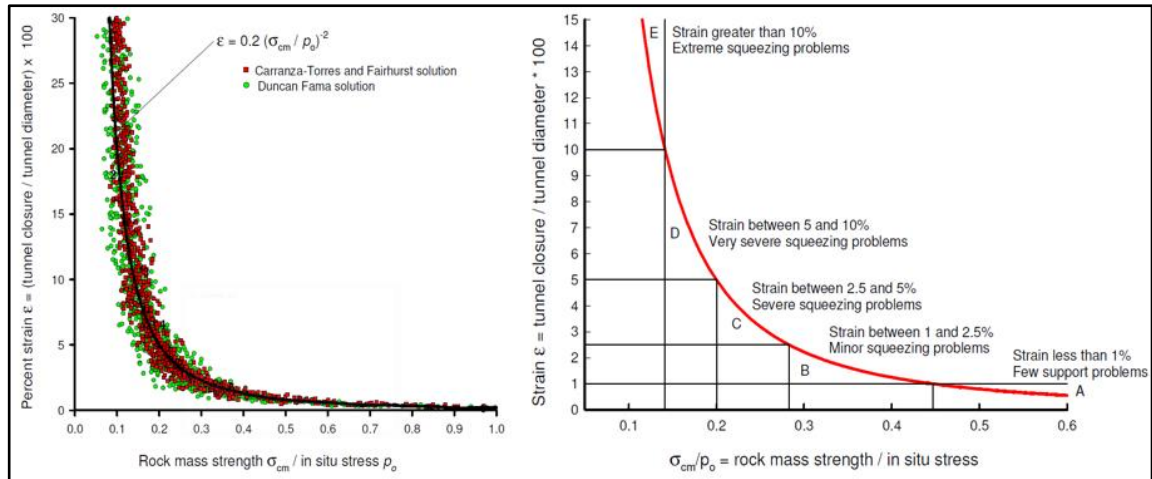
Figure 2-17 Tunnel convergence against the ratio of rock mass strength and in-situ stress (left) and tunnel convergence against degree of difficulties associated with tunnel squeezing (right) (Hoek and Marinos 2000)

$$\varepsilon = (0.2 - 0.25 * \frac{p_i}{p_o}) * (\sigma_{cm}/p_o)^{(2.4 * \frac{p_i}{p_o} - 2)} \qquad \text{2-13}$$

$$\frac{d_p}{d_o} = (1.25 - 0.625 * \frac{p_i}{p_o}) * (\sigma_{cm}/p_o)^{(\frac{p_i}{p_o} - 0.57)} \qquad \text{2-14}$$

where, ε is the total inward tunnel strain in percentage, p_i is Internal support pressure (MPa), p_o is in-situ stress= depth*unit weight (MPa), d_p is the plastic zone diameter (m) and d_o is the original tunnel diameter (m)

5. Panthi and Shrestha approach

In most of approaches used for assessing plastic deformation in tunnel, stress anisotropy in non-circular tunnel has not been considered and is a common limitation (Panthi and Shrestha 2018). High stress anisotropy exists in most of the tunnels and prevails in the Himalayan region. In case of tunnel locating at high depth and low total in-plane horizontal stress, high stress anisotropy takes place. Panthi and Shrestha (2018) carried out analysis using convergence law proposed by Sulem et. al (1987) on three completed projects from the Nepal Himalaya, which

recorded moderate to large tunnel deformation. Rock mass were weak and schistose and were subjected to anisotropic stress condition. It was found that there exists a good correlation between the tunnel strain, rock mass shear modulus, support pressure, vertical stress and ratio of horizontal to vertical stresses, see Figure 2-18. Based on this analysis, equation 2-15 and
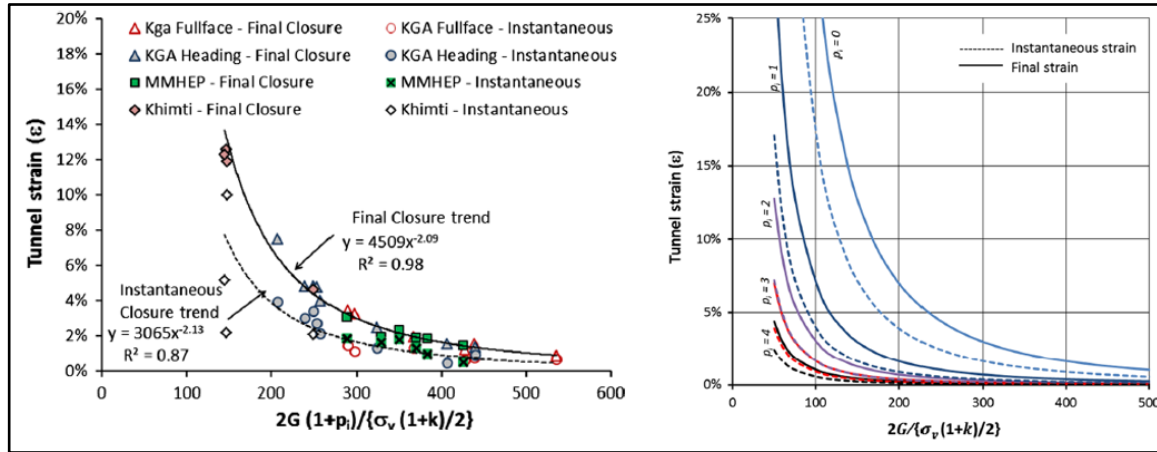
Figure 2-18 Correlation of instantaneous and final/total tunnel closure with rock mass property, support pressure and in-situ stress (left) and tunnel strain versus rock mass shear modulus, in-situ stress for different support pressure magnitude (right) (Panthi and Shrestha 2018)

2-16 are proposed to calculate both instantaneous strain (ϵ_{IC}) and final/total tunnel strain (ϵ_{FC}) with and without using support pressure. It is suggested to use this relationship to estimate plastic deformation in tunnels passing through highly schistose rock mass as of in the Himalaya.

$$\epsilon_{IC} = 3065 * \left[\frac{\sigma_v * (1 + k)/2}{2G(1 + p_i)}\right]^{2.13} \qquad \text{2-15}$$

$$\epsilon_{FC} = 4509 * \left[\frac{\sigma_v * (1 + k)/2}{2G(1 + p_i)}\right]^{2.09} \qquad \text{2-16}$$

$$G = \frac{E_{rm}}{2 * (1 + \vartheta)} \qquad \text{2-17}$$

$$E_{rm} = E_{ci} * \left(\frac{\sigma_{cm}}{\sigma_{ci}}\right) \qquad \text{2-18}$$

Where, σ_v is vertical stress (MPa), k is stress ratio, G is the rock mass shear modulus.

2.4.2.5 Numerical Modelling

Since, empirical methods have limited use and assumption made by semi-analytical methods do not exactly represent the real scenario, Numerical methods are widely used in rock

engineering structures in complex nature of rock mass. It is used basically for characterization of stress states, analyzing stability of excavations, prediction of rock failures and for analyzing deformations on non-circular tunnel with non-hydrostatic in-situ stresses in both 2D and 3D conditions. Thus, this makes it possible to predict tunnel behavior reliably and helps to optimize the rock support. In case of weak rock masses, which show squeezing behavior, application of continuum representations of medium subjected to excavation is reasonable (Barla 2005). However, due to uncertainties in input parameter for modelling, complex methods like numerical modelling does not necessary produce a precise model. Thus, the interpretation of the result obtained is very important and thus obtained result should be compared with result obtained from empirical and semi-analytical methods. In this thesis, numerical modelling using RS2 (Rocscience 2020) has been used in both brittle failure and plastic deformation analysis.

2.5 Rock support estimation

According to Nilsen and Thidemann (1993), approaches that are used for estimation of rock support requirement and support design are Empirical methods, Classification systems and Analytical methods. All these three approaches are used in the thesis for determining optimum support. Q-system support chart as Classification system by Grimstad and Barton (1993) has been used for the estimation of preliminary support, see Appendix A5. Likewise, Numerical models as analytical method has been used for evaluating and refining rock support.

2.5.1 Empirical methods

Different empirical formula to calculate different types of support are listed in Table 2-6.

Table 2-6 Empirical formula for estimation of rock supports

Description	Formula	Reference
Bolt length (L_b)	$L_b \geq d_f + 1$, $L_b \leq 0.5*H$ or B	(Li 2017)
Bolt spacing (S)	$S < L_b/2$	
Bolt length for large cavern's roof in weak rock	$L = 2+0.15*B$	(Hoek and Moy 1993)
Bolt length for large cavern's wall in weak rock	$L=2+0.15*H$	
Cable length for large cavern's roof in weak rock	$L=0.4*B$	
Cable length for large cavern's wall in weak rock	$L=0.35*H$	

2.5.2 Support pressure estimation

In order to find the equivalent support pressure of the supports provided in the numerical modelling (RS2), different formulas have been used (Carranza-Torres and Fairhurst 2000), so that calculated support pressure can be used in Hoek and Marinos (2000) and Panthi and Shrestha (2018) approach to compare the total tunnel deformation determined from numerical modelling and from these methods.

2.5.2.1 Shotcrete or concrete lining

Maximum support pressure (p_s^{max}) provided by closed ring of shotcrete or concrete lining is given by;

$$p_s^{max} = \frac{\sigma_{cc}}{2} * \left[1 - \frac{(R - t_c)^2}{R^2}\right] \qquad \text{2-19}$$

And the elastic stiffness (K_s) is given by;

$$K_s = \frac{E_c}{(1 - \vartheta_c) * R} * \frac{R^2 - (R - t_c)^2}{(1 - 2\vartheta_c) * R^2 + (R - t_c)^2} \qquad \text{2-20}$$

Where, σ_{cc} is unconfined compressive strength of the shotcrete or concrete (MPa), R is external radius of support (m), t_c is thickness of ring (m), E_c is the young modulus of shotcrete or concrete (MPa), ϑ_c is poisson's ratio for shotcrete or concrete (MPa)

2.5.2.2 Ungrouted bolts

Maximum support pressure of mechanically anchored bolts installed in circular tunnel is given by

$$p_s^{max} = \frac{T_{bf}}{s_c * s_l} \qquad \text{2-21}$$

The stiffness is given by;

$$\frac{1}{K_s} = s_c * s_l * \left[\frac{4 * l}{\pi * d_b^2 * E_s} + Q\right] \qquad \text{2-22}$$

Where, T_{bf} is ultimate load obtained from pull out test (MPa), S_c and S_l are circumferential and longitudinal bolt spacing (m), l is bolt length (m), d_b is bolt diameter (m), E_s is young's modulus for bolt (MPa) and Q is a deformation-load constant for the anchor and head (m/MN)

When more than one support is installed at the same location, their combined effect can be determined by adding stiffness of combined supports. Combined support system is assumed to fail at a point where one of the supports reaches its maximum deformation. Thus, support with lowest maximum deformation (u_r') determines the maximum support pressure (p_s^{max}) of combined support system and is calculated by (Carranza-Torres and Fairhurst 2000);

$$p_s^{max} = K_s * u_r' \qquad\qquad 2\text{-}23$$

Where, K_s is the stiffness of combined supports.

Support in this approach is assumed to act over entire surface of circular tunnel as a closed ring. Likewise, this approach assumes a perfect symmetry under hydrostatic loading of circular tunnels with no bending moments in supports (Hoek 2007). However, shape of tunnel in this project is simple Horseshoe tunnel. Also, asymmetric loading on supports creates some bending moments, which reduces the support capacities. Similarly, it is practically difficult to install support with the quality standard assumed during analysis. Thus, Maximum support pressure of the combined support system calculated by the above approach has been reduced by 30% to address these issues in 7.3.3.2.

Chapter 3: Planning and Design of Underground Openings

3.1 Introduction

Waterways are optimized based on topography and geology of the project area and are adjusted to better location of powerhouse, tailrace outlets and adits (Edvardsson and Broch 2002). Decision in selecting tunnel alignment and design during planning and design phase has direct influence on the overall cost of any tunneling project (Panthi 2019). Thus, based on geological investigation, it is important to plan and design underground elements in optimal way. According to Selmer-Olsen and Broch (1977), different stages of design procedure for underground opening are described below, which are necessary to obtain both cheapest and safest underground openings.

3.1.1 Location

Decision regarding location determines the quality of rock mass to be excavated and thus, if decision is taken too early on an uncertainty basis, it may impose greatest risk for technical and economic calamities. Based on detailed surface mapping and core drilling, underground elements should be favorably located, especially in project with limited area (Nilsen and Palmström 2000). Unfavorable rock mass like young sedimentary rocks should be avoided as they might cause severe stability problems. In case of shallow-seated tunnels and caverns, tunnel should be located at sufficient depth in order to have adequate un-weathered rock above the roof, which provides sufficient normal stress for self-supporting roof capacity. In Scandinavian hard rock with shallow weathering depth, un-weathered layer of 5m is considered as reasonable for spans up to 20m, see Figure 3-1(left).
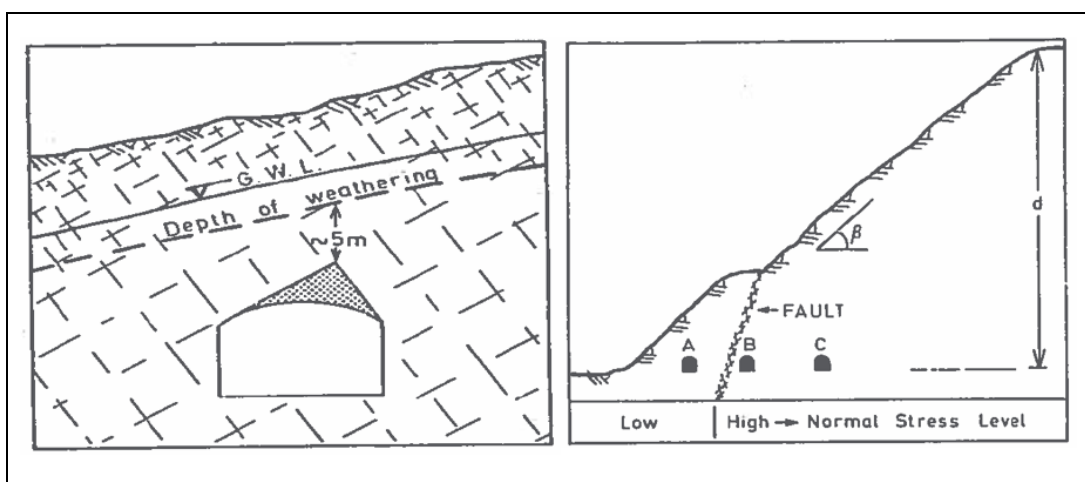

Figure 3-1 Minimum rock cover for shallow seated underground opening (left) and stress situation in steep valley side with fault zone (right) (Selmer-Olsen and Broch 1977)

However, in other geological and climatic environments, weathering and alteration depth can be as deep as 100m in large area (Stefanussen 2017). In case of deep-seated tunnel, destressed area such as protruding "noses" in deep valleys and area outside faults, gouges or crushed zone with strike parallel to the valley and dip steeply towards valley, should be assessed, see Figure 3-1(right). It would be best to avoid and not to intersect major weakness zones during excavation. If cannot be avoided, then, crossing should be made as short as possible and small crossing angles should be avoided. Likewise, steep-dipping and flat-lying discontinuities impose stability problems in walls and roofs, respectively. As per Hoek and Moy (1993), effect of surface topography in the in-situ stress field has to be considered, while locating underground powerhouse in mountainous area. Particularly minimum principal stress is altered significantly near slope face as compared to far field stress and these local changes in in-situ stress field affect the induced stresses in rock mass surrounding an underground cavern. Cavern has to be located away from slope such that the overstressed zones are smaller and less or modest support for stabilisation of rock mass surrounding cavern is required as compared to cavern locating near slope surface.

3.1.2   Orientation of tunnel and cavern alignment

Orientation of tunnel and cavern alignment with respect to the attitude of discontinuities determines tunnel and cavern stability to a great extent. Alignment should be chosen in such a way that it gives minimum stability problems, minimum overbreak and requires minimum heavy rock support (Edvardsson and Broch 2002). Since joints and foliation/bedding plane are quite common in rock mass and can create directional pattern of weakness, it should be considered while aligning underground opening (Hoek and Moy 1993). Particularly, large opening like powerhouse cavern should be assessed carefully in this aspect. Since foliation shear with low friction are expected to occur in any foliated rock mass, it is risky to align tunnel with small angle with foliation. Also, as per Barla (2005), parallel orientation of main discontinuities leads to significant increment in deformation. In an opening situated at shallow or intermediate depth, axis of alignment should be oriented along the bisection line of the maximum intersection angle between two dominating discontinuities directions. Stability problem increases when the angle between the tunnel axis and the predominant joint set becomes less than 25-30^0. Similarly, the angle between the long and high walls of cavern and steeply dipping smooth planes and clay filled joints should be at least 25^0 (Nilsen and Palmström 2000). Likewise, in deep-seated tunnel, direction of major principal stress is also important to be considered. Opening should be oriented in such a way that minimum of its

periphery is touched tangentially by stress plane. Most stable orientation is obtained when horizontal projection of major principal stress makes an angle of 15-30^0 to longitudinal axis of opening.

3.1.3 Shape design and dimensioning

Behavior of the rock mass surrounding the opening and its stability is influenced by both geometry and size of the excavation (Palmström and Stille 2010). Simple shape with arched roof helps to obtain evenly distributed compressive stresses along the whole periphery of the opening. In addition, simple shape can be constructed with minimum time and effort, which saves considerable time and cost (Panthi 2015). In shallow or intermediate depths, shape of opening's roof is governed by degree of jointing and characteristics of joints. In case of deep-seated openings, if stress is not so high or anisotropic, small curvature radii should be avoided. But, if stress is too high, to avoid stress problems, it is economical to provide a shape, which concentrates the stability problems and hence decreases areas that need to be supported. In strong rock mass, cavern shape is usually conventional straight-walled with arched roof. However, in weak rock masses, Hoek and Moy (1993) discuss about the elliptical cavern shape which is considered as ideal from a geotechnical point of view. However, it has some practical disadvantages related to construction difficulty and conventional shape is generally preferred to elliptical due to its simple shape and simple construction procedure. In addition, it suits the method of excavation (benching) and yields little unusable space (NFF 2016).

Depending upon the self-supporting capacity of rock mass, stability problem increases with the increase in the span of underground opening and becomes more evident when span exceeds 5-6m (Selmer-Olsen and Broch 1977). With the increase in span of the opening, in-situ strength of rock mass decreases and hence deformation increases (Palmström and Stille 2010). Thus, careful assessment should be done in the planning and design of large span like large powerhouse cavern, which requires constructive confining pressure.

To avoid the risk of transformer explosion and its consequence to machine hall/powerhouse caverns, separate transformer cavern is constructed. Although short distance between caverns benefits by reducing cost of high amperage connection, it is unsafe from the viewpoint of rock stability and it may cause unfavorable stress conditions in the pillar between the cavern (Hoek and Moy 1993). Thus, distance between them should be determined sensibly so that destressing situation between the caverns could be avoided with enough rock mass. Wall thickness or pillar width between them is determined by different factors like height of the underground opening, quality of rock mass and stress situation (Selmer-Olsen and Broch 1977). In general, vertical

separation (S) should not be less than the largest span (B) or height(H) of the adjacent caverns (NFF 2016) as indicated in Figure 3-2. In case of weak rock, Hoek and Moy (1993) suggest that pillar width (S) should not be less than the height of the larger of the two caverns and if possible, it should be slightly higher. Likewise, in case of very poor-quality rock mass, where overstressed zones are larger, pillar width should be increased to 1.5 times the height of the larger cavern.
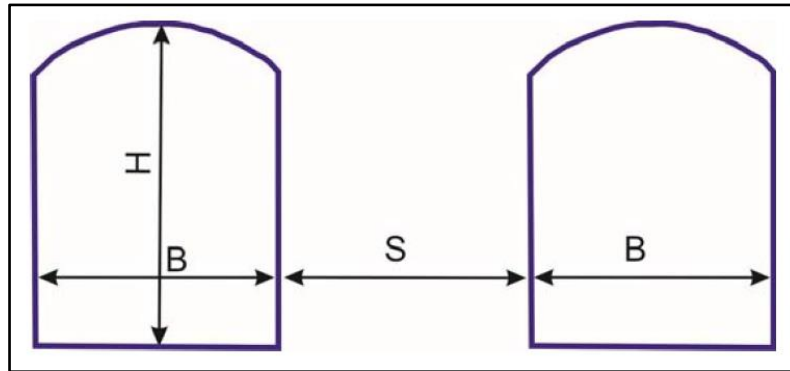
Figure 3-2 Dimensioning of two adjacent caverns (Panthi 2018a)

3.2 Unlined/shotcrete lined tunnels

Nowadays, hydropower projects construct pressure tunnels and shafts as unlined/shotcrete lined worldwide. Design philosophy of unlined tunnel is that in case of hard and durable rock mass which are not susceptible to solutioning, tunnel can be largely or fully unlined (Benson 1989). However, some special zones of minor rockfalls or weakened rock can occur, which can be treated with grouted rock bolts and shotcrete, but these minor falls or issues will not create larger issues. Since continuous concrete or steel lining is not used as permanent support, rock under direct hydrostatic pressure must be able to resist very high-water pressure itself. The concept and design principle regarding it were developed in Norway. Norwegian hydropower has more than 100 years of experience in constructing more than 4000 Km-long unlined pressure shafts and tunnels with maximum static water head of 1047m (Panthi and Basnet 2016). These experiences of design, construction and operation has led the foundation to develop design criteria and principles. Panthi and Basnet (2016) have generalized layout of successful unlined shafts and tunnels that are being used in Norway since the start of unlined concept, see Figure 3-3.
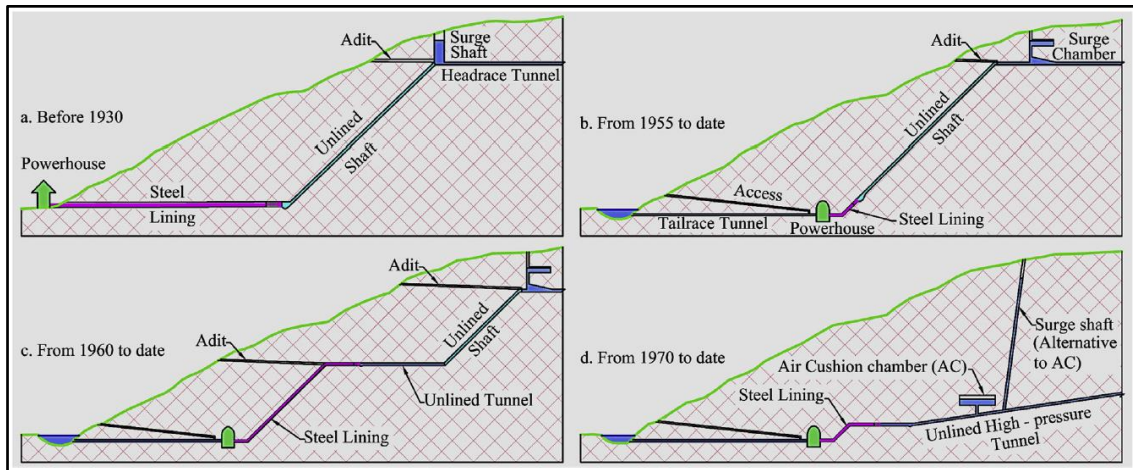
Figure 3-3 Development of unlined high-pressure shafts and tunnels in Norway (Panthi and Basnet 2016)

3.2.1 Design criteria

Since the earliest attempt in constructing Herlandfoss project in 1919, different design principles has been developed based on lessons learned from different failure cases (Basnet and Panthi 2018). In Norway, before 1968, unlined pressure shafts and tunnels were built using former "Norwegian Rule of Thumb" as shown below:

$$h > cH_w \hspace{4cm} 3\text{-}1$$

where, h is minimum required rock cover over shaft, c is constant ranging from 0.6 to 1 depending upon valley slope angle and H_w is hydrostatic head acting over shaft.

Later due to the failure of unlined pressure shaft at Byrte project in 1968, the rule of thumb represented by equation 3-1 was modified and the modified criteria and its corresponding factor of safety (FoS) are expressed by equation 3-2 and 3-3, respectively. Again, due to failure of these criteria in the design of unlined shaft at Askara in 1970, new criterion was established incorporating the slope topography to calculate the resisting ground pressure against H_w and is represented by equation 3-4 and its corresponding FoS is represented by equation 3-5. As per Broch (1984) in Benson (1989), diagrammatical correction of topography should be done to account stress attenuation caused by undulating topography, see Figure 3-4.

$$h > \frac{\gamma_w * H_w}{\gamma_r * \cos\alpha} \hspace{4cm} 3\text{-}2$$

$$FoS_1 = h' * \left(\frac{\gamma_r * \cos\alpha}{\gamma_w * H_w}\right) \hspace{3cm} 3\text{-}3$$

$$L > \frac{\gamma_w * H_w}{\gamma_r * \cos\beta} \qquad \text{3-4}$$

$$FoS_2 = L' * \left(\frac{\gamma_r * \cos\beta}{\gamma_w * H_w}\right) \qquad \text{3-5}$$

Where, h and h' is the vertical rock cover above tunnel without and with topographic correction, L and L' is shortest perpendicular distance from valley inclination line without and with topographic correction, γ_w and γ_r are the specific unit weight of water and rock respectively and α and β is the inclination of shaft/tunnel and valley side slope with respect to horizontal plane, respectively.

According to Panthi and Basnet (2016), both criteria represented by equation 3-2 and 3-4 are commonly known as the Norwegian Confinement Criteria (NCC). As criteria represented by equation 3-4 was not sufficient in some Norwegian projects, an additional criterion was established incorporating the concept of minimum principal stress after 1970s, which is a limiting confining pressure to counteract the water pressure. The criteria is the state-of-the-art in the design of unlined or shotcrete lined pressure tunnel and shaft. It states that in order to be safe against hydraulic jacking, in-situ minimum principal stress should be higher than the hydrostatic head acting on the periphery of unlined tunnel/shaft and is represented by equation 3-6 and its corresponding FoS is given by equation 3-7. Figure 3-4 represents all the criteria
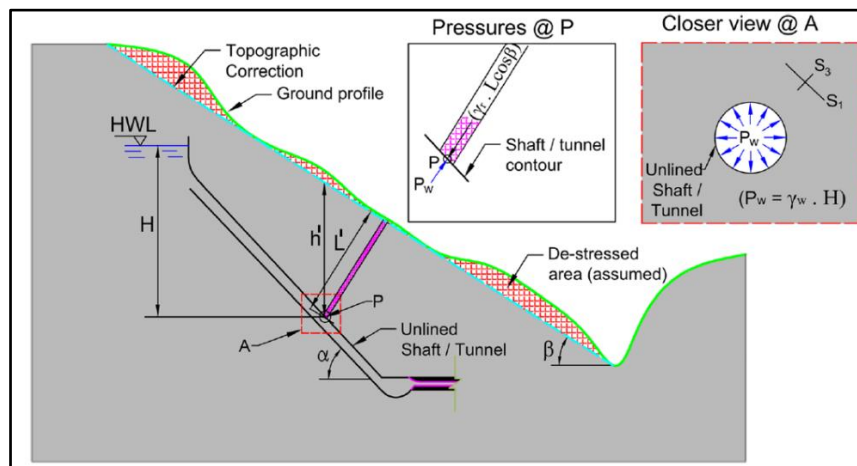
Figure 3-4 Different parameters used in different design criteria for unlined shaft/tunnel, S_3 or σ_3 is the minimum principal stress, modified from Basnet and Panthi (2019a)

discussed here and indicates the different parameter used for it. For the tunnels lying along valley sides and operating under static normal operation, Benson (1989) has recommended to use FoS of 1.3 in order to prevent hydraulic jacking. However, in case of water hammer

transients, it is not necessary to meet normal FoS as hydraulic stress during water hammer transients is too short for jacking.

$$S_3 \text{ or } \sigma_3 > \gamma_w * H_w \tag{3-6}$$

$$FoS_3 = \frac{\sigma_3}{\gamma_w * H_w} \tag{3-7}$$

Norwegian confinement criteria are established based on 2D geometry of the topography and they do not consider the engineering geology and full overview of in-situ stress state of the area (Basnet and Panthi 2018). Both aspects depend upon rock type and its properties, joints characteristics, faults and weakness zone, degree of weathering and geotectonic and geological environment of the area. There has been a few cases in Norway in which even though these criteria related to overburden and valley distance are fulfilled, there has been an initial leakage and hydraulic splitting problems (Panthi and Basnet 2017). As geological and geotectonic environments outside Scandinavia are different, Norwegian confinement criteria needs to be assessed carefully. It is emphasized that in addition to Norwegian confinement criteria, detail engineering geological assessment, stress state analysis, hydraulic jacking, hydrogeological/leakage analysis should be carried out in order to make the concept successful outside Scandinavia (Basnet and Panthi 2018). Furthermore, it is suggested that both favorable and unfavorable ground conditions should be used for the applicability of the confinement criteria beyond Scandinavia (Panthi and Basnet 2018b), see Table 3-1. In case of unfavorable ground conditions, especially in steep slope topography and faults and weakness zone, stress state of the area needs to be estimated in order to determine the safe location. Benson (1989) recommended to evaluate stress state by finite elements in area with complex geology or topography, where locally low stress may take place. Also, Benson (1989) suggests to place unlined/shotcrete lined pressure tunnel, if possible, in such a way that water table is above the hydraulic gradient line to prevent excessive leakage.

Panthi and Basnet (2017) highlights that whatsoever the design methodology is followed, unlined pressure tunnel should be safe against hydraulic splitting/jacking, should ensure that the water leakage from tunnel is within acceptable limit and should assure shot-term and long-term stability. As the design criteria for unlined tunnel does not directly account for the instabilities in tunnel, it should be carried out separately and should assure stability before the application of the unlined concept in pressure tunnels (Basnet 2018).

Table 3-1 Favorable and unfavorable ground conditions for the applicability of Norwegian confinement criteria (Panthi and Basnet 2018b)

Category	Favorable conditions	Unfavorable conditions
Topography	Relatively gentle valley slope topography	Deep, steep and complex valley slope topography
Rock mass and Jointing	Homogeneous and strong rock mass formations with no or single joint set having tight joint wall, wide spacing and anti-dip against valley slope	Weak rock mass with high degree of schistocity; Highly porous rock mass of volcanic and sedimentary origin; Jointed rock mass having more than two systematic and long persisting joint sets with one or more joint sets dipping steeply towards valley slope; Pre-existing open joints or the joints filled with sand and silt, which could easily be washed away; Sub-horizontal joints at low overburden area
Faults and weakness/crushed zones	No nearby major faults and weakness zones	Nearby fault and weakness zones that are parallel or cross-cutting to the valley slope
In situ stress state	The minimum principal stress always higher than the static water head	De-stressed area and location not far away from steep valley slope topography; Not sufficiently far away from the locally overstressed areas
Hydrogeology	Hydrostatic water line below natural groundwater table or tunnel aligned deep into the rock mass and far away from the steep valley slope restricting flow paths to reach valley slope topography	Hydro-static line above the groundwater table and relatively near from the valley side slope; Highly permeable and communicating joint sets

3.2.2 Leakage analysis

The most important aspect in the design of unlined or shotcrete lined pressure tunnel is to make sure that leakage out of tunnel during operation is within acceptable limit. The amount of allowed leakage is governed by quantity and the value of available water and probable effect of leakage on the stability of the terrain and environment (Benson 1989). As per Panthi and Basnet (2019b), maximum limit of water leakage for unlined or shotcrete lined tunnel is 1.5 l/min/m and is achievable with modern ground improvement techniques. Thus, leakage assessment is considered to be a crucial part of study if hydropower is planned with an unlined or shotcrete lined pressure tunnel. There exists a different method to estimate potential inflow and leakages in the underground opening. A semi-empirical relation is proposed by Panthi (2006) and Panthi (2010), which is based upon some Q parameters or jointing conditions, and hydrostatic head. Degree of jointing and character of rock joints along with static head has been considered in the equation and is given by (Panthi 2006):

$$q_t = f_a * h_{static} * \frac{J_n * J_r}{J_a} \qquad \text{3-8}$$

Where, q_t is specific tunnel leakage (l/min/m), f_a is the permeability factor (l/min/m^2), which depends upon connectivity of joint sets and their infilling condition, and express conductivity of joint sets and h$_{static}$ is the hydrostatic head.

According to Panthi (2006), this equation is developed based on the data records of water leakage measurement in the probe holes carried for determining the need of pre-injection grouting in pressurized shotcrete lined headrace tunnel of Khimti I Hydroelectric Project. f_a varies from 0.001 to 0.25 and can be calculated by (Panthi 2010):

$$f_a = \frac{J_p}{D * J_s}$$
3-9

Where, J_p is joint persistence, D is the shortest perpendicular distance from rock slope topography to valley side tunnel roof and J_s is the joint spacing.

Remedial measures in unlined tunnel/shaft are determined based on the amount of leakage that takes place during operation. As per Panthi and Nilsen (2005), innovative concept of systematic pre-injection and post injection grouting can play a very significant role in reducing permeability of rock mass and the water leakage from pressurized shotcrete lined tunnel. In addition, it improves the rock mass quality by cementing the cracks and joints with grout material and therefore reduces the need of rock support. Ultimately it reduces construction cost and time as compared to full concrete lining tunnel. As shown in Figure 3-5, there exists a
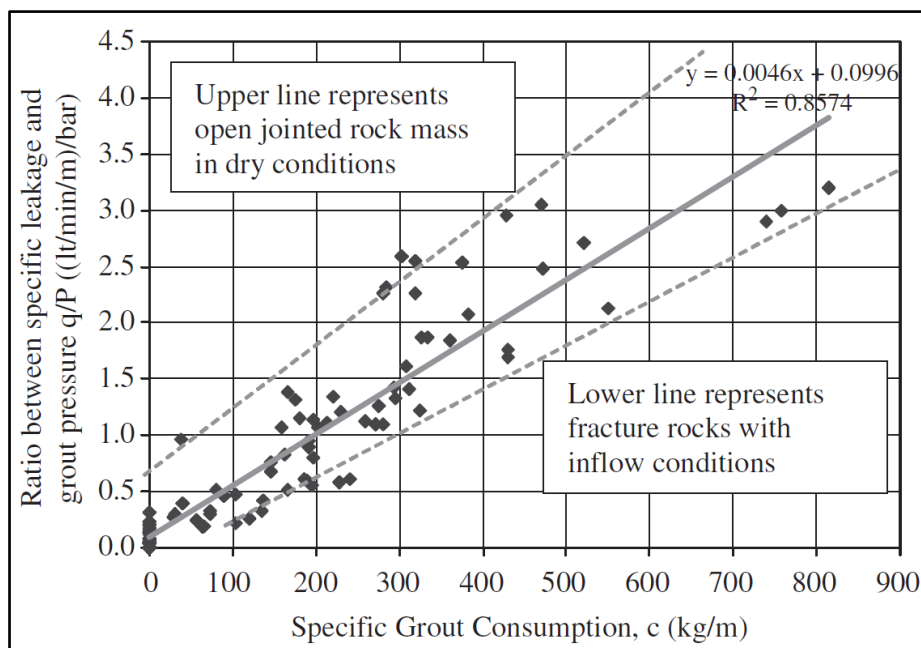

Figure 3-5 Correlation between specific leakage, grout pressure and specific grout consumption (Panthi and Nilsen 2005)

correlation between specific leakage (q), grout pressure (P, 1.5 times static pressure during operation) and specific grout consumption (c), which can be used for estimating grout consumption required for pre-injection grouting for future water conveying tunnels in similar ground condition as that in Khimti I HP (Panthi and Nilsen 2005).

3.2.3   Application in the Himalaya

Due to the favorable engineering geological and stabilized geotectonic environment of Scandinavian landscape, unlined pressure tunnel and shaft is quite common in Norway (Basnet and Panthi 2018). However, application of unlined concept outside the Scandinavia is very less due to pseudo understanding that high hydrostatic head is only bearable by Scandinavia rock mass. Many waterway systems of Norwegian hydropower run along the Caledonian mountain range, where rock types are similar to that of rock mass of Lesser and Higher Himalayan zone of Himalayan mountains. However, between Scandinavia and Himalayan mountain range, there exists a difference in geotectonic environment (Panthi and Basnet 2016). Thus, when applying Norwegian confinement criteria in Himalayan conditions, modification is required in order to consider the influential factors that affect safe location of unlined tunnel and shaft, such as topography complexity, tectonic environments and presence of weakness/fault zones. Panthi and Basnet (2018b) suggest a modification in confinement criteria for lateral valley cover and propose a modified criterion. It is believed that in most cases modified criteria provides a reasonable and safe location of unlined/shotcrete lined pressure tunnels for Himalayan geo-tectonic environment, given that ground conditions are fulfilled as mentioned in Table 3-1. A modified confinement criteria and its corresponding factor of safety was proposed by Panthi and Basnet (2018b), which is represented by equation 3-10 and 3-11 respectively. These equations can be used in the preliminary design of unlined pressure tunnel/shaft in the Himalayan region.

$$L'' > f_g * \frac{\gamma_w * H_w}{\gamma_r * \cos\beta} \tag{3-10}$$

$$FoS_4 = L' * \left(\frac{\gamma_r * \cos\beta}{f_g * \gamma_w * H_w} \right) \tag{3-11}$$

Where, L'' is the minimum later cover required to locate unlined or shotcrete lined tunnel safely, f_g is a multiplication factor, which represent either f' or f'' depending upon the project scenario, which ranges from 1.6 to 3, see Figure 3-6 (left). f' is the multiplication factor that includes stress change due to only changes in topography and f'' includes stress change due to

change in both topography and presence of weakness zone in left valley (WZ#2) as well, see Figure 3-6 (right). H_2 and H_1 indicates depth of left and right river valley, respectively from hilltop and β indicates slope angle of right valley.
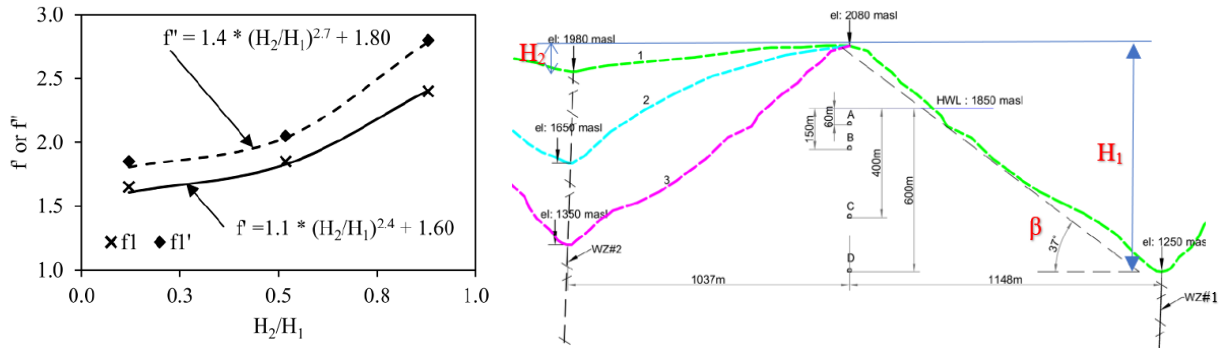
Figure 3-6 Multiplication factors at different topographic conditions (left) and different topographical conditions (1,2 and 3), tunnel locations, head water level (HWL) and weakness zone (right), modified from (Panthi and Basnet 2018b)

In Nepal, unlined or shotcrete lined pressure tunnel is being constructed at Upper Tamakoshi Hydroelectric Project (UTHP). It is different from the one which is normally fully unlined in Norwegian hydropower projects. Nevertheless, similar design criteria as that for unlined tunnels were used for shotcrete lined pressure tunnels. Due to permeable nature of shotcrete in pressure tunnel, it is considered as unlined pressure tunnel. Generally, thin layer of shotcrete (<15 cm) has porosity higher than 30%, which makes it as a highly permeable material. In addition, water tunnel with shotcrete support is provided with 1m long drain holes along the periphery in order to reduce risk of pressure that builds up between shotcrete liner and rock wall (Panthi and Basnet 2017). Both of these factors promote the direct contact between water pressure inside tunnel and rock mass. Thus, almost equal water pressure will act on rock mass as that on shotcrete lining (Basnet and Panthi 2019b).

Apart from UTHP, different projects have already been operated successfully in Nepal as shotcrete pressure tunnel. First attempt was made in 2000 at Khimti I Hydroelectric Project having medium to low pressure headrace tunnel (up to 40 bar hydrostatic pressure). Likewise, Modi khola Hydroelectric Project and Chilime Hydroelectric Project were also constructed as shotcrete lined tunnels and have been in operation since 2000 and 2003 with hydrostatic head of 30m and 20m, respectively (Basnet 2018).

Chapter 4: Tamakoshi V Hydroelectric Project

4.1   Project description

The Tamakoshi V Hydroelectric Project is a cascade scheme of the under construction 456 MW Upper Tamakoshi Hydroelectric Project (UTHP) with tandem operation. It has an installed capacity of 99.8 MW and will be located on the right bank of Tamakoshi river in Dolakha District, Nepal. Interconnection system for cascade scheme is located at Mathillo Jagat. Likewise, powerhouse site is located at Suritar. Utilizing gross head of 174 m and rated discharge of 66 m^3/s, it produces 507 GWh annual energy (NEA 2019). Project area is located approximately 170 km north east of capital city Kathmandu and approximately 40km from district headquarter of Dolakha. Construction of this project has not yet started. Since, road constructed by UTHP passes through the powerhouse and headwork site of this project, there is no need of constructing new access road. However, few kilometers of project road have to be constructed. The project area is situated within Longitude 86^{0}10'30" to 86^{0}14'30" East and Latitude 27^{0}45'00" to 27^{0}48'59" North. Location map of the project is shown in Figure 4-1.

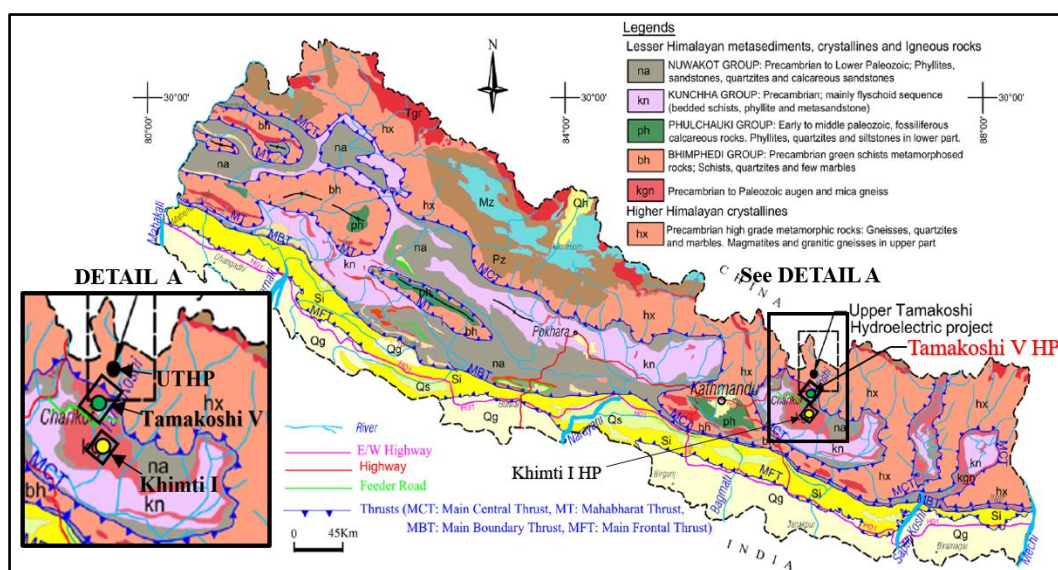Figure 4-1 Location map of the project along with other nearby projects, modified from Panthi and Basnet (2017)

4.1.1   Project layout and topography

The main civil components of the project are underground interconnection system of Headrace Tunnel (HRT) with the Tailrace Tunnel (TRT) of UTHP to divert the discharge, Headrace Tunnel, Surge Shaft, Valve Chamber, Pressure Shaft, High Pressure Tunnel, Power Station and

Tailrace Tunnel. Since, it is a cascade scheme, there is no need of separate dam and settling basin. Project layout along with existing geology is illustrated in Figure 4-2.
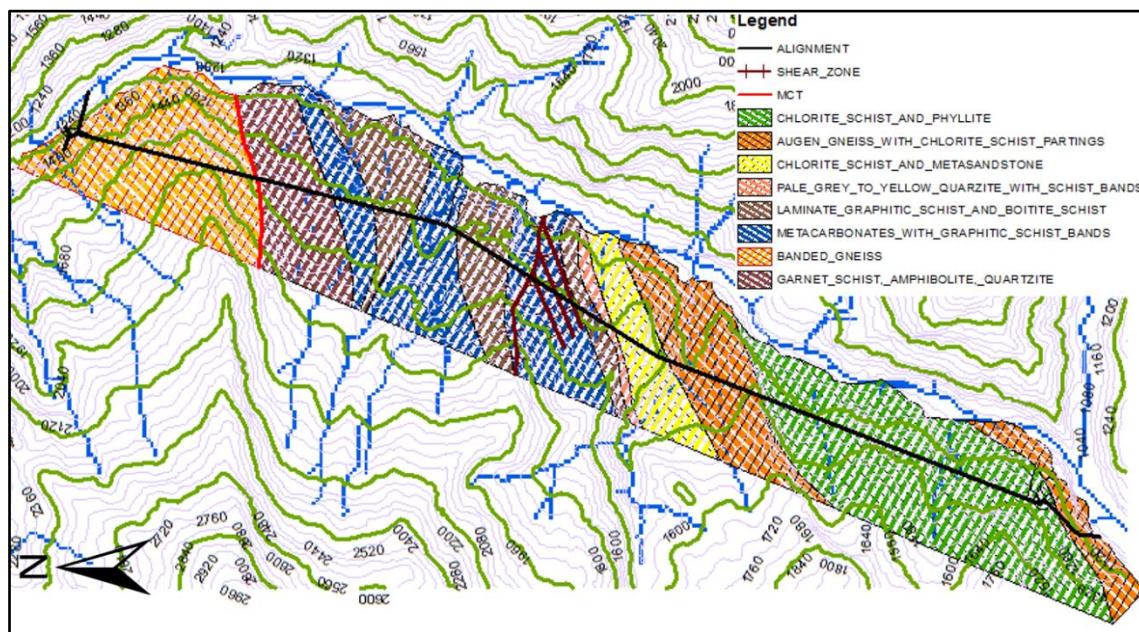
Figure 4-2 Project layout of Tamakoshi V Hydroelectric project along with the geology

Interconnection system consists of connecting tunnel, a head pond, spillway and spillway tunnel. Discharge from this system is conveyed to 8.1 km long HRT, which is a concrete lined circular tunnel of diameter 5.6m. However, excavation will be carried out as modified horse-shoe shape of diameter 6.4m. Surge tank is designed as concrete lined shaft structure with 15m diameter and 48.8m effective height. Steel lined part of waterways start from downstream of surge shaft, which is designed along pressure shaft and high-pressure tunnel with 4.2m inner diameter. Power station consists of powerhouse cavern, transformer cavern, bus duct galleries underground and terminal and ventilation building with takeoff yards, the operation and workshop building above ground in the service area. Size of powerhouse cavern is 69m long, 18m wide and 30.3m high. Similarly, transformer cavern is 47.6m long, 13m wide and 17.95 high. Powerhouse accommodates in total four turbines. Three units of Francis turbine (vertical shaft) with generating equipment of 31.6 MW each and one Francis turbine (horizontal shaft) with generating equipment of 5 MW. The water from powerhouse outlet will be released back to the same river by 440m long tailrace tunnel, designed as concrete lined with same diameter of HRT (NEA 2019). Apart from these, five construction adits will be constructed, out of which, four will be in HRT and one in TRT.

The Project area is represented by narrow valley with steep, sometimes vertical, rock slopes, narrow and deeply incised side valleys. Flat surface on ridge with soil thickness of more than 2m are used as agricultural land. Apart from it, remaining parts are covered with alpine forests and vegetation. Rocks are normally exposed on steep slopes and cliffs. The altitude in project area ranges from minimum of 983 masl on river valley of TRT outlet to maximum of 3000 masl. However, range of altitude along HRT lies between 1180 masl to 1840 masl (NEA 2019). Since most of the structures are constructed underground, there would not be direct influence on landscape.

4.2 Himalayan and Regional Geology

4.2.1 Himalayan Geology

The Himalaya is a youngest, tectonically active and vulnerable mountain chain in the world. It has formed due to collision of northward moving Indian tectonic plate with Asian tectonic plate. Due to this collision, Indian plate from south is under-thrusting the upper crust of Asian continental plates. As a result, upper part of Indian crust near plate boundary is being squeezed, thick and short and number of tectonic rupture or fault zones are formed. Out of which, most prominent are Main Frontal Thrust (MFT), Main Boundary Thrust (MBT), Mahabharat Thrust (MT) and Main Central Thrust (MCT). Due to the persistent compression caused by collision, significant amount of energy is accumulated, and this locked in stress or energy is released by frequent earthquakes through active major tectonic thrust faults and large-scale discontinuities like weakness zones, fractures, etc (Panthi and Basnet 2017). This shows that the Himalayan region has complex tectonic stress regime in terms of both space and time (Basnet and Panthi 2017).

Panthi (2006) explains that during the mountain building process, compressional and extensional faulting result in several litho-tectonic units with Northwest-Southeast general trend in the Himalayan belt. Figure 4-3 shows that Himalaya is sub-divided into five tectonic zones from South to North, which have their own special lithology, tectonics, geological structures, geological history and are made up of different rock types. Moving from South to North, these five different litho-tectonic zones are Gangetic plane/Terai, Siwalik Zone/Sub-Himalaya, Lesser Himalayan Zone, Higher Himalayan Zone and Tibetan-Tethys Zone. These zones are separated from each other by different prominent tectonic fault zones, which are dipping towards North.
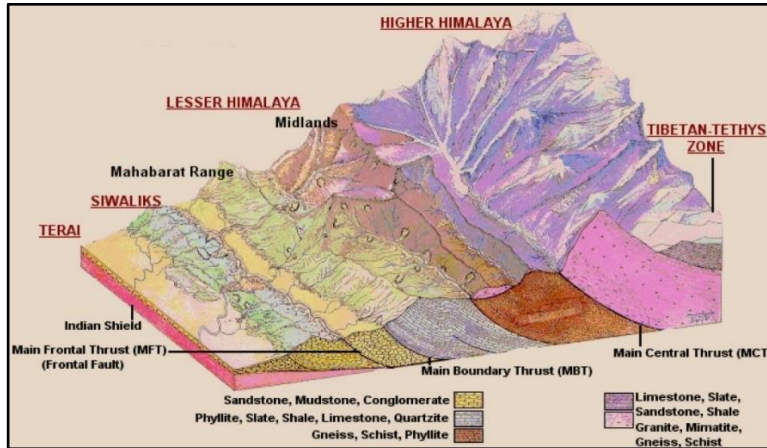
Figure 4-3 Block diagram of the Himalaya giving different litho-tectonic units (Deoja et al. 1991)

4.2.2 Regional geology

In the upper portion of Tamakoshi river, Lesser Himalayan meta-sediments constitute the footwall of the MCT, and its hanging wall comprises the medium to high grade metamorphic rocks and Micocene granites of Higher Himalayan zone. As per Dhital (2015), Schelling (1987) divided the rocks of Higher Himalayan and Lesser Himalayan zone rock into different units as shown in Figure 4-4.
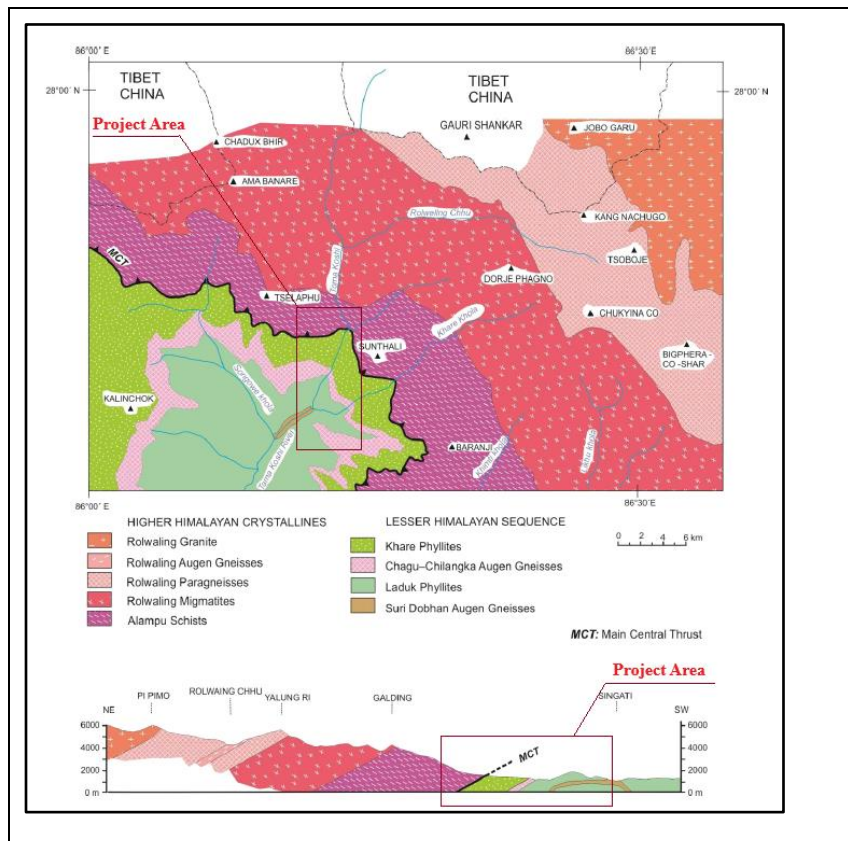
Figure 4-4 Geological sub-division of the Upper Tamakoshi Area, modified from Dhital (2015)

Higher Himalayan Crystallines

Higher Himalayan Crystallines override the Khare phyllite of Lesser Himalayan sequence steeply and consist of Rolwaling granite, Rolwaling augen gneiss, Rolwaling para-gneiss, Rolwaling migmatites and Alamphu schists from North to South. Certain starting portion of HRT lies in Alamphu schists of Higher Himalayan zone.

Lesser Himalayan Sequence

Lesser Himalayan sequence consists of Khare phyllite, Chagu-Chilangka augen gneiss, Laduk phyllite and Suri Dobhan Augen gneiss and the majority portion of the project area lies in these rock mass of Lesser Himalayan zone.

4.3   Geology of the project area

4.3.1   General geology and Engineering geological condition

The Project is located in both the Higher Himalayan Tectonic zone and Lesser Himalayan Tectonic zone of the eastern Nepal Himalayas. However, except interconnection system and first one kilometer of Headrace Tunnel (HRT), major part of the project is dominated by Lesser Himalayan zone. In general, rock mass of project can be divided into two simple categories, i.e., medium to high grade Higher Himalayan crystalline sequence and low-grade metamorphic rocks of the Lesser Himalayan rock sequence, which are separated by Main Central Thrust (MCT) as shown in Figure 4-5. Several rock masses come across the alignment of the project area. Primary rock masses of the project are augen gneiss, chlorite schist, graphitic schist, garnet
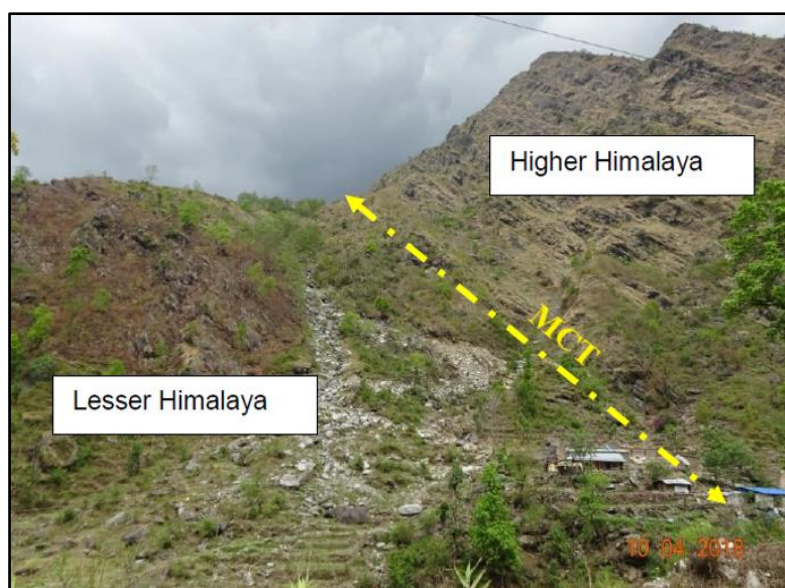
Figure 4-5 MCT at Tallo Jagat demarcating Lesser and Higher Himalayan (NEA 2019)

schist, meta-carbonate and phyllite of the Lesser Himalaya and banded gneiss of the Higher Himalaya. Rock mass in the project area are sheared, foliated, folded, schistose, anisotropic, fractured and jointed. Rock mass have been subjected to frequent intercalation and shearing with chlorite, graphite and biotite schist. As per Schelling (1992) and Supervisor (27/01/2020), rock mass downstream of MCT are tectonically disturbed, sheared and mainly destressed zone. Rock mass condition along the alignment has been evaluated as fair to extremely poor rock mass. As per NEA (2019), around 65% of rock mass in the project area belongs to Fair to poor rock mass quality. Strength of intact rock material has been designated as weak at Tatopani (Hot Spring) weakness zone to very strong at Banded gneiss section, see Figure 4-6.

Figure 4-6 Rock mass quality in the project area: weak rock mass (left) and very strong rock mass (right) (NEA 2019)

Based on surface mapping, rock masses along the alignment are anticipated to be fine to coarse grained, fresh to moderately weathered, having three major joint sets, which are closely to widely spaced with tight to moderately open joints filled with silt, sand and clay. The detail information about the project and rock mass condition along the alignment is presented in Appendix D1 to D4. Minimum and maximum rock cover of about 49.5m will be confronted at chainage (Ch.) 5+025m (approximately) in Augen gneiss with chlorite schist parting and of 690m at chainge 1+000m chainage in Banded gneiss, respectively.

Rock mass of project area lies in the northern limb of regional anticlinorium, whose core part lies in the TRT outlet structure. Rock mass at Outlet and Powerhouse area are dipping gently $(5-15^0)$ towards North-West or towards hillside along the foliation joints. The pattern of dip angle goes on increasing gradually towards north and reaches up to an angle of 65^0 to 70^0 at the headpond area. Strike of foliation joints of rock mass is WNW to ESE in head pond area, which changes gradually in anticlockwise direction as we move downstream and ends up with strike of WSW to ENE at tailrace tunnel.

The main geological structures encountered along the alignment are Main Central Thrust as a tectonic fault and Tatopani weakness/shear zone.

1. Main Central Thrust (MCT)

MCT is presumed to be confronted at chainage 1+078m in the boundary between Banded gneiss and Garnet schist (NEA 2019). As per Schelling (1992), MCT is the tectonic discontinuity or fault along which the Higher Himalayan thrust sheet have been thrust to south-southeast over lesser Himalayan meta-sediments. In addition, it has been explained that due to the thrusting along both Sunkoshi thrust and Tamar khola thrust in eastern Nepal, MCT has been breached and offset. Since then, it has been inactive and called as an inactive thrust fault. Similarly, as per Sunuwar (2016), field observation along Tamakoshi river shows that MCT is inactive and instead it is represented by high grade metamorphic rocks on hanging wall and low-grade metamorphic rocks on footwall. Besides this, based on the observation on the surface terrain using google map (Google Earth Pro), cross-sections and plan of project of the project area, no any morphological features like depression, saddle, deep gulley, landslides, etc has been noticed, which are useful in identifying fault/shear/weak zone. Also, rock mass in both upstream (u/s) and downstream (d/s) side of MCT is strong to very strong and mostly fair in quality. Likewise, as per NEA (2019), no any sheared and crushed rocks in and around the MCT zone has been found during field observation. Based on these information and discussion with Supervisor (3/02/2020), it has been concluded that MCT is an inactive seismic zone and is not problematic for underground structures.

2. Tatopani (Hot spring) weakness/shear zone

It is anticipated that Tatopani weakness/shear zone will be confronted between chainage 3+121m to 3+863m for around 100m in Meta-carbonates with graphitic schist parting (NEA 2019). Rock mass is bluish gray, primarily dolomites that consists of weak layer of graphite and talc intercalation. This shear zone passes through deep gorge at Tatopani area and has been characterized as sheared, moderately weathered and fractured rock mass consisting of dolomite, graphitic schist and biotite schist. Soft materials are found evident in shear zone along with colluvium deposit. At bore hole (HB1') at shear zone, rock core is mainly found fractured and filled with chlorite, mica, clay, stained and silt as shown in Figure 4-7, see Appendix D2 for the location of bore hole HB1' and HB2' along the HRT. As per NEA (2019), strength anisotropy index (I_a) of this rock sample is found to be around 4, which as per Table 2-1, is classified as highly anisotropic consisting of weak, platy/prismatic minerals up to 60%.

Figure 4-7 Rock core sample from HB1' at chainge 3+717m (NEA 2019)

4.3.2 Engineering geological investigation

During Feasibility stage and Detail design stage, different surface and sub-surface engineering geological investigations have been carried out at different locations of the project. Details about the different investigations have been summarized in Table 4-1.

Table 4-1 Summary of engineering geological investigation at Tamakoshi V HP

Investigation type	Description	Location
Core drilling and in-situ test	9 exploratory boreholes of length 547m in total. Standard penetration, Dynamic cone penetration and Lugeon test.	Spillway portal area, HRT/Tatopani Shear zone interaction (HB1'), HRT/Orang khola intersection (HB2'), Powerhouse area, TRT and Tailrace structure.
Seismic refraction Tomography	16 different seismic refraction profiles of total length 1875m.	Along the Tamakoshi river at Jamune, Suritar and Tatopani shear zone.
2D-Electrical resistivity tomography	Total length of completed profile is 2788m.	Along the HRT and TRT alignment, outlet area and Test Tunnel portal area.
Test Tunnel and In-situ test	Size: 2.5m *2.5m and of length 176m. Shear test, plate load test and Hydrofracture test	Along the Powerhouse area. But Hydrofracture test was incomplete due to poor rockmass condition.
Surface mapping	Detail surface mapping with Q and RMR system	Along the Tamakoshi river in the exposed rock mass

4.4   Evaluation of existing design layout

The overall layout of underground elements in a Hydropower project plays a significant role in terms of the stability, support requirements and ultimately the construction cost. All the elements of the project are underground. Headrace tunnel (HRT) is designed with mild slope of 0.42% as low-head pressure tunnel (maximum static water head of 46m at the downstream end) and is aligned on right bank of Tamakoshi river valley sides and is placed above river valley bottom. Tunnels are located at a lateral distance of around 320m at downstream stretch to 500m at upstream stretch from surface and have an average rock cover of 280m. The rock cover ranges from minimum of 49.5m at Chainage 5+025m (Augen gneiss with chlorite schist parting) to maximum of 690m at chainage 1+000m (Banded gneiss). Deep weathering is frequent due to active monsoon, high temperature variation and active tectonic movement in the Himalaya (Panthi 2006). This may result in the increment in destressed depth and have ultimate effect (especially in low cover section) in the confinement caused by in-situ stresses. Tunnel at around chainage 3+769m crosses Tatopani weakness zone, where rock cover is around 310m. It is almost aligned perpendicular to tunnel axis and extends for around 100m. It may create serious stability problems at crown and walls. Since, weakness zone is perpendicular to river valley and extends deep into the rock mass, there is no other option to avoid it and special attention is required during excavation and support installation.

Figure 4-8 shows the joint rosette with orientation of joint sets and HRT at left side and TRT and Powerhouse cavern at right side. Both HRT and TRT tunnels are aligned in Northeast/Southwest direction ($N13^0$ to 45^0E). In terms of discontinuity patterns, there are mainly three major joint sets, including foliation joint. Strike of main foliation joint (J_f) has
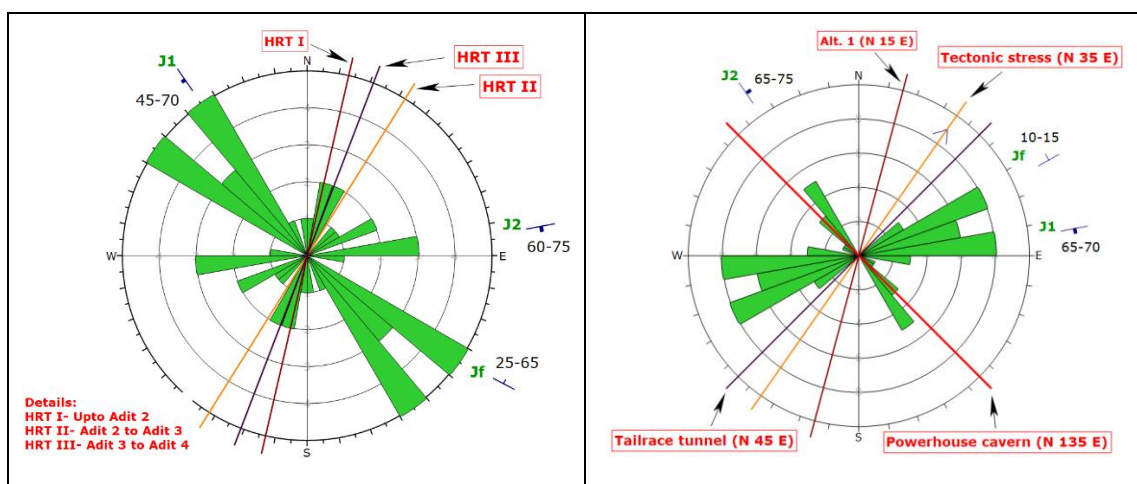

Figure 4-8 Orientation of main joint sets of Tamakoshi V HP along with Headrace tunnel alignment (left) and Tailrace tunnel and Powerhouse cavern (right)

been found varying from N65^{0}E at TRT to N120^{0}E to N125^{0}E at HRT. This might be due to the fact that HRT lies at northern limb of regional anticlinorium, whose core part lies in the TRT. J$_f$ are dipping gently at angle less than 15^0 at TRT, which changes gradually towards north dipping steeply at angle upto 65^0 at HRT. In HRT, J$_f$ is almost oriented perpendicular with respect to HRT axis and is considered to be a favorable orientation. However, J$_f$ at TRT makes an angle less than 25^0 with tunnel axis (around 20^0) and this may create slight stability problem at tunnel roof as it is dipped almost horizontal. Similarly, the orientation of other two dominating joint system as well are in favorable orientation with respect to both HRT and TRT. Some of random joints in HRT are striking almost parallel to HRT axis and found dipping towards river valley. This could be potential exfoliation joints, which might not be noticed along the excavated HRT.

As mentioned earlier, the excavation shape of tunnel is a modified horseshoe shape in the project. The magnitude of stress that are set up in the rock mass surrounding the opening and the corresponding stability problem is influenced by the shape of the openings (Nilsen and Palmström 2000). As per Hoek (2007), modified horse-shoe shape is more appropriate for poor quality rock mass. However due to construction practicality in Drill and Blast tunnels, modified horse-shape tunnels shape is usually ended up with simple horse shape (Panthi 2015), see Figure 4-9 right. Rock mass along the alignment ranges from strong rock mass to poor rock mass. Thus, as per discussion with Supervisor (30/03/2020), D-shape tunnel has been considered in upper section up to chainage 1+769m and for the remaining section, simple horse-shoe shape is considered for further analysis as shown in Figure 4-9.
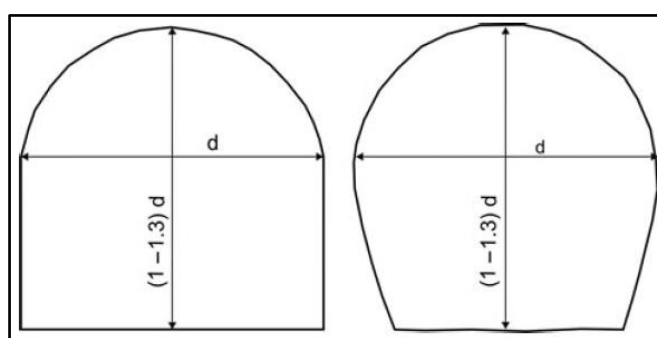
Figure 4-9 Recommended tunnel sections for hard-left and poor rock mass (Panthi 2015)

Powerhouse Cavern size is 69m*18m*30.3m (l*b*h), with conventional straight wall and is aligned almost perpendicular to river valley direction, see Appendix D3 and D4. Rock cover is between 150m to 194m along the length. Cavern roof is almost located at same level as that of river valley bottom, indicating possibility of relatively higher magnitude of tectonic stress than

along the headrace tunnel. The Powerhouse Cavern is aligned at $N135^0E$. As per Figure 4-8 (right), cavern is favorably aligned with respect to foliation joint (J_f) and Joint set 1 (J_1). However, another dominating joint set 2 is striking almost parallel to cavern axis, which is undesirable in case of large openings. In addition, it is dipping steeply making an angle of 15^0 to 25^0 with high wall. Similarly, after excavation, re-distribution of stress leads to decrease in confinement stress in walls, which is mainly due to horizontal tectonic stress (see Figure 4-8 right) that is almost perpendicular to longitudinal axis. This ultimately leads to the reduction in wall stability. On the other hand, in case of roof, re-distribution of tectonic stress provides better confinement for roof stability. Thus, taking tectonic stress direction and J_2 into consideration, alternative alignment (Alt. 1, $N15^0E$) has been proposed, which is oriented along the bisection line of the maximum intersection angle between J_f and J_2 and makes an angle of 20^0 with tectonic stress as shown in Figure 4-8 (right). This adjustment provides better confinement in both high walls and roof, confines stress related problem to small area of cavern and is more favorable in terms of avoiding structurally induced instabilities.

Pillar width between Powerhouse cavern and Transformer cavern is 30m, which is almost equal to height of powerhouse cavern. As per Hoek and Moy (1993), it satisfies the minimum criteria of weak rock mass and is generally acceptable in terms of busbar length. However, it is always better to carry out numerical modelling to study interaction of stress surrounding two caverns and analyze overstressed zone, especially potential tensile failure zone, in the pillar, which may cause excessive strain in the rock mass causing instability.

Chapter 5: Establishment of Input parameter

5.1   Introduction

For the assessment of potentiality of unlined or shotcrete lined tunnel and stability analysis of underground openings of Tamakoshi V HP, rock mass parameters of different rock mass along the alignment and corresponding in-situ stress are very much essential. This chapter presents the information about rock mass parameters, in-situ stress and hydraulic conductivity that would be used in next three chapters.

5.2   Rock mass mechanical properties

Rock mass parameters are quantified based on the detail surface mapping and laboratory test carried out by project for certain sections. Banded gneiss, which lies upstream of MCT has no laboratory test data. It is similar in nature to that of Banded gneiss of UTHP as both lie in same geological region and are very close to each other as shown Figure 4-1. Thus, for banded gneiss section, rock mass parameters are obtained from UTHP, where laboratory testing in sample was carried out in Rock mechanical laboratory at NTNU. However, for those selected rock mass lying downstream of MCT with no laboratory test data, information has been estimated from different literatures such as scientific papers, Doctoral thesis ((Panthi 2006) and (Shrestha 2014)), books, lecture notes, reports of nearby project, internet, etc. and has been verified with Supervisor (18/03/2020). While estimating, consideration has been given for similar case histories, rock types, rock mass conditions, etc. in combination with information from geological report. For the stability analysis of Powerhouse cavern, rock mass parameters have been finalized referring information obtained from Test Tunnel such as tunnel face mapping and in-situ test and referring laboratory test results of intact rock sample obtained from nearby powerhouse cavern. Based on all these, input parameters have been summarized in Table 5-1 for different chainages along the HRT, TRT and for Powerhouse cavern, see Figure 5-1. These parameters have been used in the shotcrete lined tunnel assessment and stability analysis of tunnel and powerhouse cavern as per the requirement.

Hoek and Brown constant, m_i is determined as per Appendix A4. Drill and Blast (D&B) method is most dominating in Nepal. Blasting are generally uncontrolled in nature, which result in poor contour blasting. Hence, disturbance factor (D) has been selected as 0.8 for all the analysis carried out in this thesis. In some of selected sections, instead of having fixed Q value, ranges of Q value for particular rock mass is available. In these cases, average rock mass quality has been determined using formula, $(Q_{max} \times Q_{min})^{1/2}$, for the analysis (singh and Goel 2012b).

Establishment of Input parameter

Table 5-1 Input parameter for different assessments

Section no.	Chainage, m	Rock type	Rock cover, m	Intact rock strength, MPa	Elasticity modulus, GPa	m_i	Unit weight of rock, MN/m^3	Poisson's ratio	Q	RMR	GSI
A-A	HRT 1+050	Banded gneiss	652	90	40	23	0.0275	0.25	4.00	65	60
B-B	HRT 1+590	Garnet schist, Amphibolite, Quartzite	364	70	25	16	0.0273	0.20	3.00	59	54
C-C	HRT 1+945	Metacarbonates with Graphitic schist	315	36	20	12	0.0293	0.14	2.15	54	49
D-D	HRT 2+717	Metacarbonates with Graphitic schist	138	36	20	12	0.0293	0.14	2.15	54	49
E-E	HRT 3+026	Graphitic schist and biotite schist	310	20	10	12	0.0273	0.10	0.67	37	32
F-F	HRT 3+769	Metacarbonates with Graphitic schist parting (Tatopani Shear Zone)	310	36	20	10	0.0293	0.14	0.13	34	29
G-G	HRT 4+563	Chlorite mica schist with metasandstone bands	401	35	23	15	0.0286	0.10	0.42	38	33
H-H	HRT 5+025	Augen gneiss with chlorite schist parting (Orang Khola)	49	28	33	20	0.0273	0.14	4.00	58	53
I-I	HRT 6+103	Chlorite schist and phyllite	68	25	14	10	0.0273	0.10	0.24	39	34
J-J	HRT 6+487	Chlorite schist and phyllite	194	25	14	10	0.0273	0.10	0.24	39	34
K-K	HRT 7+205	Chlorite schist and phyllite	77	25	14	10	0.0273	0.10	0.24	39	34
L-L	HRT 7+846	Chlorite schist and phyllite	270	25	14	10	0.0273	0.10	0.24	39	34
M-M	HRT 8+098	Chlorite schist and phyllite	161	25	14	10	0.0273	0.10	0.24	39	34
N-N	TRT 0+171	Augen gneiss with chlorite schist parting	187	41	48	23	0.0265	0.10	0.50	46	41
O-O	TRT 0+455	Augen gneiss with chlorite schist parting	132	48	32	23	0.0274	0.15	0.70	49	44
P-P	Powerhouse cavern	Augen gneiss with chlorite schist parting	178	41	48	23	0.0265	0.1	1.5	46	41

GSI is determined referring RMR value and using formula defined in 2.1.2.3.
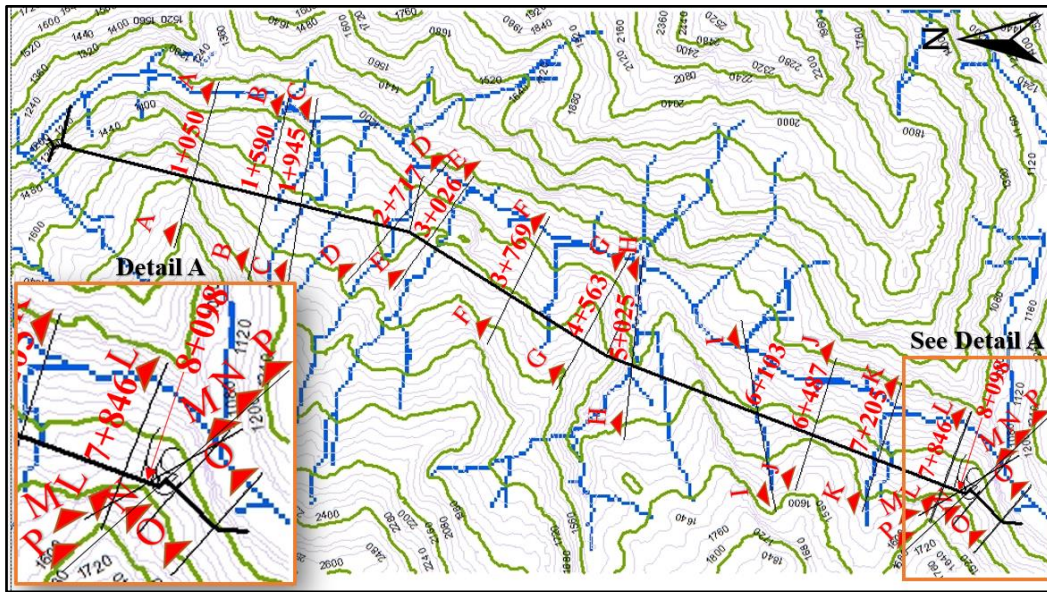
Figure 5-1 Project layout along with selected section for both stability assessment and shotcrete lined tunnel assessment

5.3 Rock mass strength calculation

Rock mass strength (σ_{cm}) has been calculated using different formula given in Table 2-2 and has been presented in Figure 5-2. Input parameter for the calculation is referred from Table 5-1. However, in chainage 3+769m (Tatopani shear zone), rock mass has been found sheared, fractured and moderately weathered. Deep weathering may result in complete change in mechanical properties and behavior of rock (Palmström and Stille 2010). Thus, considering Figure 2-5 for moderate weathering (II to III) and discussion with supervisor (18/03/2020), unconfined compressive strength (σ_{ci}) and modulus of elasticity (E_{ci}) of rock mass at chainage 3+769m has been reduced by 50%.

Figure 5-2 highlights that estimation of σ_{cm} is relatively high with Singh et al. (1992) approach and Barton (1993), except in chainage 1+050. In contrast, Bieniawaski (1993) estimates relatively low value. However, both Hoek et al. (2002) and Panthi (2006 and 2017) estimate almost similar σ_{cm} value, which lies almost between Barton (1993) and Bieniawaski (1993) for most of the sections. Most of the approaches are based on rock mass classification system. During the planning phase, rock mass classification such as Q and RMR are mostly done based on surface observation and borehole data, which are not as reliable as during construction (Panthi 2006).

As Panthi (2006) and Panthi (2017) is relevant for the Himalayan region with anisotropic rock mass and estimate σ_{cm} using intact rock strength as input parameter rather than Q-value, they have been used for estimating σ_{cm} for Q system and Panthi and Shrestha (2018) approach, which are required for Squeezing analysis. Similarly, Hoek et al. (2002) has been used in Hoek and Marinos (2000) approach.

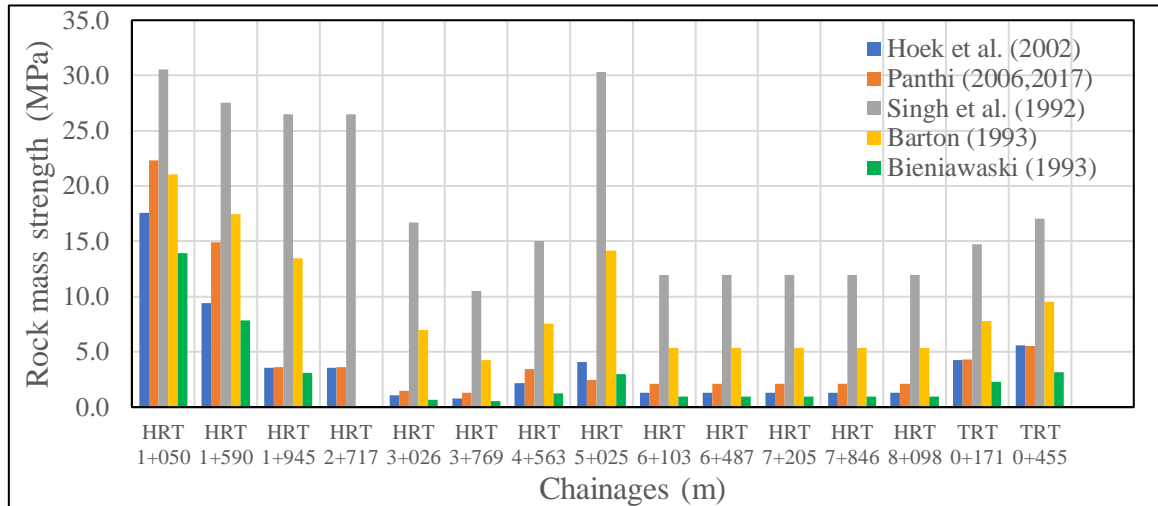Figure 5-2 Comparison of rock mass strength using different empirical methods

5.4 Rock mass deformation modulus calculation

Rock mass deformation modulus (E_{rm}) has been calculated using Panthi (2006) and Hoek and Diederichs (2006) based on formula of Table 2-3 and are shown in Figure 5-3. As it can be seen
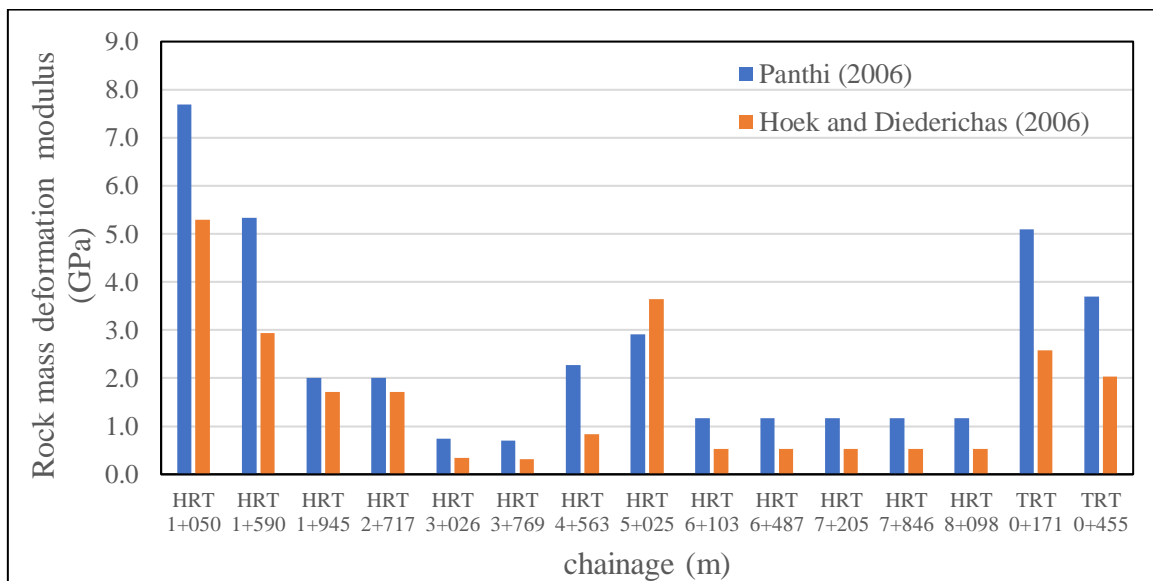

Figure 5-3 Comparison of rock mass deformation modulus using Panthi (2006) and Hoek and Diederichs (2006)

that except in chainage 5+025m, Panthi (2006) estimated higher E_{rm} as compared to estimation done by Hoek and Diederichs (2006). For Panthi and Shrestha (2018) approach, E_{rm} is calculated using Panthi (2006). Hoek and Diederichs (2006) has been used in numerical modelling as software RocData calculates E_{rm} based on it.

5.5   Hydraulic conductivity

Based on water pressure (Lugeon) test, Lugeon value and the hydraulic conductivity for two sections along HRT is given in Table 5-2. This would be used during leakage assessment in 6.5.2.

Table 5-2 Rock mass permeability data at Tatopani shear zone and Orang khola (NEA 2019)

Bore hole no.	Approximate Chainage (m)	Location	Lugeon value l/min/m at 10bar	Hydraulic conductivity m/s
HB 1'	3+717	Tatopani shear zone	16	$1.5*10^{-6}$
HB 2'	5+030	Orang Khola	5	$4*10^{-7}$

5.6   Tectonic stress

According to Hudson and Harrison (1997) in Panthi (2012), meaningful assessment of instability caused by induced stresses in underground openings can only be achieved by determining magnitude and direction of in-situ stresses. As the project area lies in Himalayan region, tectonic activity and the orientation of tectonic stress affect the total component of horizontal stress. Based upon geographical location, geological environment and distance from main tectonic fault system, magnitude of tectonic horizontal stress varies significantly (Panthi 2012). Since, in-situ stress test carried out in project was not successful, it is necessary to determine the value of tectonic stress from nearby project with similar geotectonic environment, which then can be used for determining in-situ stress in required sections. Rock mass lying u/s of MCT is relatively stronger and massive and is similar to that of UTHP. Similarly, rock mass d/s of MCT and up to chainage 1+769 is relatively stronger. As per Panthi (2014), contribution of tectonic stress in total horizontal stress is considerable in case of relatively unjointed, massive and strong rock mass. Also, Nilsen and Palmström (2000) explain that concentration of stresses takes place in stiff and strong rock and in soft rock, stresses are low. Thus, it has been assumed

that similar tectonic stress as prevailed in stronger rock mass of UTHP acts along the rock mass section mentioned above in Tamakoshi V HP as well (up to chainage 1+769m). However tectonic stress value for rock mass lying d/s of chainage 1+769m, which are relatively weak, sheared, fractured and destressed, has been evaluated low and is discussed later on.

In-situ stress in Test Tunnel (TT) of UTHP has been measured in 2008 using 3D overcoring at three different locations TT1, TT2 and TT3 as shown in Figure 5-4 (left). General trend of tectonic stress orientation nearby UTHP is in the direction of approximately N20^0-40^0E as shown in Figure 5-4 (right). Out of measured stress data at three different locations, trend of
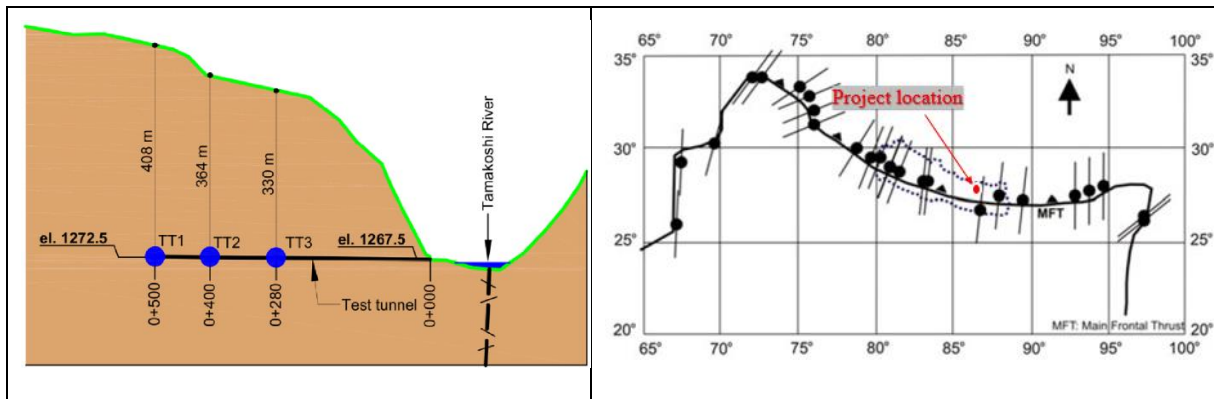
Figure 5-4 Stress measurement location at Test Tunnel of UTHP (left) and approximate horizontal tectonic stress orientation (right), modified from (Basnet and Panthi 2019b)

stress data measured at TT3 is found to be comparable with general trend as discussed above (Panthi and Basnet 2017). Thus, stress data at TT3 is used as reference for determining tectonic stress and is presented in Table 5-3. Based on Figure 5-4 (left), topographic model (2D plain strain RS2 model) has been prepared, see Figure 5-5. Measured 3D stress at TT3 is transformed using "Stress transform" function (Rocscience 2020) to obtain equivalent plain strain principal stress field aligned with axes of topographic model (aligned as N120^0E), see in Table 5-3. After creating the model, different combinations of tectonic stress magnitudes (5 MPa to 11 MPa), orientations (N30^0E to N45^0E), in-plane and out-plane stress ratio are used until the simulated stress (see Figure 5-5) in RS2 model converged to corresponding transformed σ_1' and σ_3' field stress and angle as given in Table 5-3.

Table 5-3 Measured 3D stress values and transformed stress values for RS2 at TT3

Stresses	Measured stress			Transformed stress	
Principal Stresses	MPa	Trend	Plunge	Stresses	MPa
σ_1	21.6±2.2	N21.1^{0}E	10.4^0	σ_1'	12.63
σ_2	12.6±2.8	N116.5^{0}E	27.2^0	σ_3'	6.92
σ_3	6.4±2.7	N272.2^{0}E	60.6^0	σ_z	20.75
σ_1', σ_3' and σ_z' are major in-plane, minor in-plane and out of plane field stress respectively in RS2 plain strain model. Angle is measured between positive x-axis and direction of σ_1'.				Angle	155^0
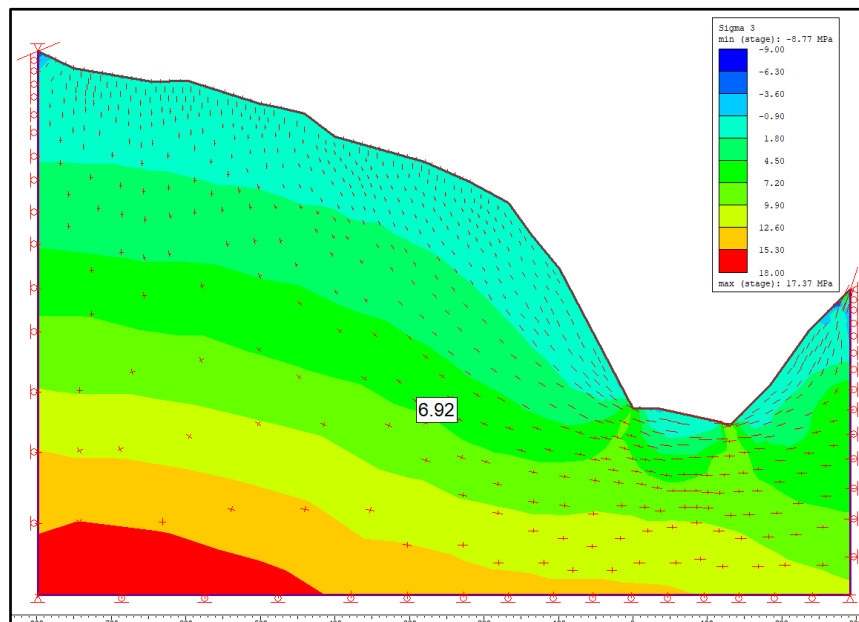
Figure 5-5 Simulated minor in plane stress (σ_3') at TT3

Based on this approach, tectonic stress of magnitude 7 MPa and direction as N35^{0}E has been found to simulate σ_1, which converges to transformed σ_1' stress as shown in Figure 5-6. However, in Figure 5-7, tectonic stress of magnitude 7 MPa with direction N40^{0}E has been found to simulate σ_3, which converges to transformed σ_3' stress. The magnitude of tectonic stress is quite comparable to tectonic stress of 7.5 MPa at Parbati II project in the Himalaya with almost similar geotectonic condition (Panthi 2012). Also, as per Panthi and Basnet (2018b) 15 MPa of tectonic stress acting along direction of N35^{0}E has been found out in 3D model using

FLAC3D for UTHP. However, this high value of tectonic stress is acting at the base of model (0 masl) and the value gradually decreases above the valley level due to stress attenuation. Thus, this obtained tectonic stress of magnitude 7 MPA aligning in direction N35^{0}E has been considered reasonable and has been used for HRT section until chainage 1+769m.

Rock mass lying downstream of chainage 1+769m is weak, sheared, foliated, schistose and fractured. In these kind of rock masses, destressing takes place and the tectonic contribution to the total horizontal stress magnitude decreases extremely (Panthi 2014). According to Nepal (1999) referred in Shrestha (2014), tectonic stress magnitude in Nepal Himalaya varies between 3 and 4 MPa if rock mass is schistose and sheared. Based on different paper reviews, it
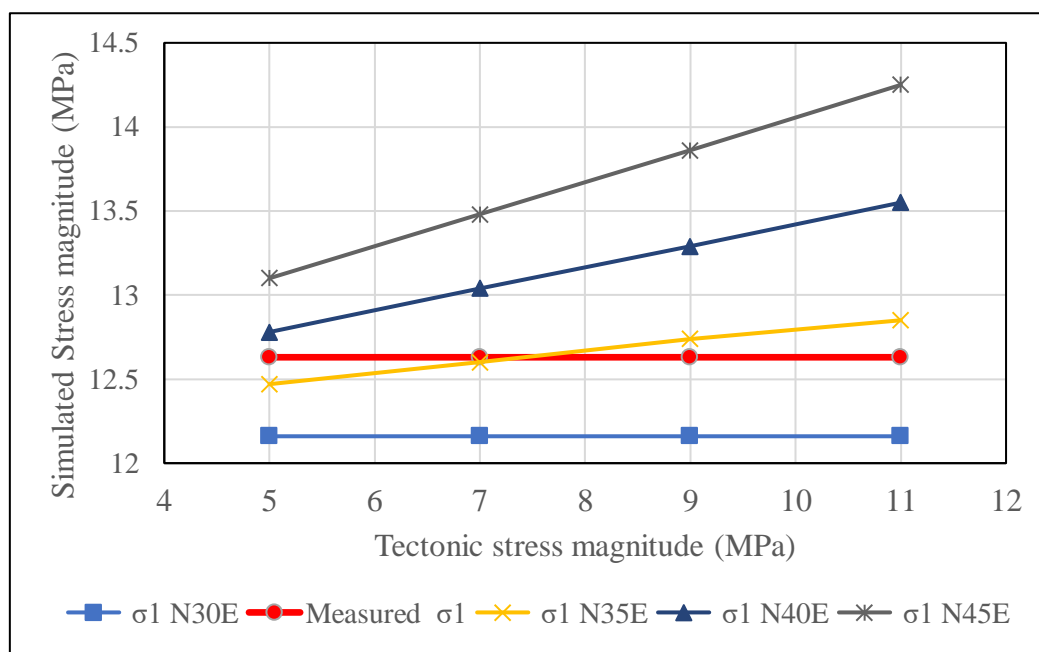
Figure 5-6 Comparision between measured/transformed and simulated stress (σ_1)

has been found out that magnitude of tectonic stress in different projects lying between MCT and MBT in Nepal lies between same range mentioned above. Likewise, in Khimti I HP, which is located close to Tamakoshi V HP (see Figure 4-1), tectonic stress has been evaluated as 3 MPa (Shrestha 2014). However, Tamakoshi V HP lies relatively close to MCT as compared to Khimti I HP and can be assumed that the destressing effect is relatively high as compared to Khimti I HP resulting lower tectonic stress. Similarly, HRT is situated above the river valley due to which topographic impact on in-situ stress or tectonic stress takes place (Panthi and Basnet 2018a). Tectonic stress increases rapidly below river valley level and decreases as elevation increases. Thus, considering these all aspects and as per discussion with Supervisor (22/02/2020), tectonic stress magnitude of 2.5 MPa has been finalized for the
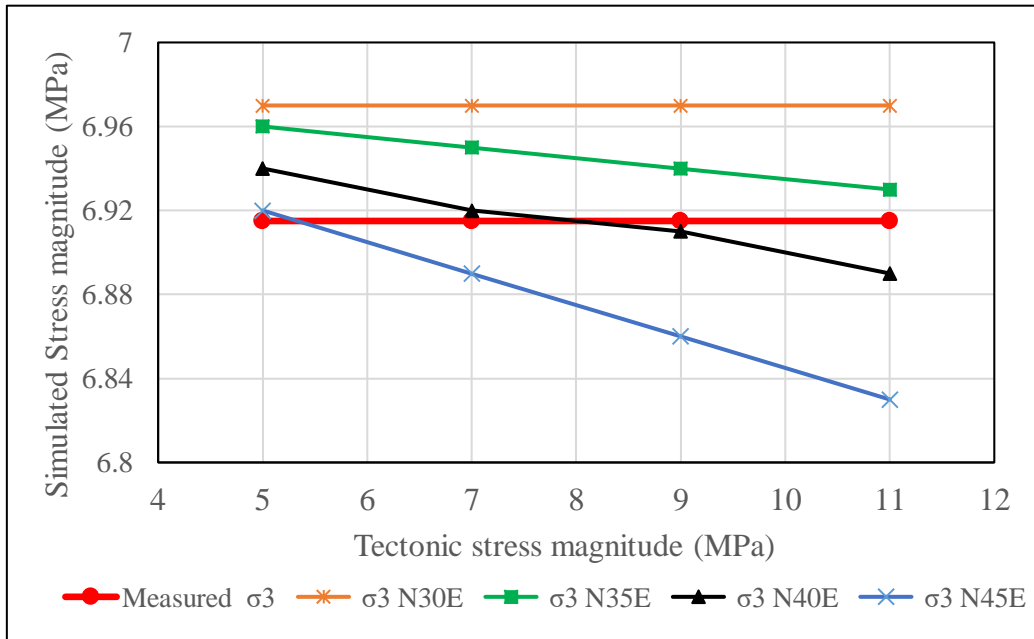
Figure 5-7 Comparison between measured//transformed and simulated stress (σ_3)

rock mass lying d/s of chainage 1+769m and for Powerhouse as well. However, in case of Tatopani sheared zone, tectonic stress of 1.5 MPa has been used. This is due to fact that although tectonic push of Indian plate towards north produces significant horizontal tectonic stress, intense seismic activity or earthquake destresses the accumulated stress along the weakness/sheared zone and active major tectonic faults (Panthi 2014). Regarding tectonic stress direction, similar direction as obtained above (N35^{0}E) has been used for rock mass lying d/s of chainage 1+769m and for Powerhouse as well.

Chapter 6: Shotcrete lined pressure tunnel assessment

In the Himalayan region, underground pressure waterway system is generally designed with traditional design approach, in which full concrete lining is used to secure stability. This approach has proven to be costly solution and financially unfeasible. Therefore, there is a need of innovative, economic and optimum solution to reduce the length of full concrete lining in pressure tunnels and shafts (Panthi 2014).

One of the ways to obtain optimum design solution is to exploit rock mass as a part of support system and adopt unlined/shotcrete lined pressure tunnels to the extent that rock mass allows. This helps to reduce the overall construction cost and time. However, there are several technical, geological and geotechnical challenges related to this solution. Thus, prevailing rock mass condition and the applied sprayed concrete and systematic bolting for shotcrete lined tunnels should secure long-term stability and safety of waterway system (Panthi 2015). In addition, it should ensure that potential leakage out of tunnel during operation should be within acceptable limit. Otherwise, leaked water would cause economic loss and affect the stability of tunnel, valley sides slopes and the environment as well.

This chapter evaluates the potentiality of exploring unlined/shotcrete lined design solution in the pressurized headrace tunnel of Tamakoshi V HP. HRT of Tamakoshi V is a low to medium pressure tunnel with maximum static water head of about 46m (0.46 MPa) at the downstream end of headrace tunnel, where it connects to concrete lined surge tank and steel lined pressure shaft. Potentiality of shotcrete lined pressure tunnel has been studied by assessing the topographical conditions, in-situ stress state, overall rock engineering aspects and potential leakage along the headrace tunnel. Thus, potentiality of implementing this innovative concept has been evaluated by Rock engineering assessment, Norwegian Confinement Criteria (NCC), Modified NCC, In-situ stress state assessment and Leakage assessment.

6.1   Rock engineering assessment

Rock engineering assessment is about the rock mechanical behavior and engineering geological investigation (Nilsen and Palmström 2000). Mechanical properties of rock mass are related to its strength and deformability properties and these properties are of utmost importance when it comes to planning of unlined/shotcrete lined tunnel. Apart from it, evaluation of presence of any weakness and shear zone and 3D topography in the project area is crucial while selecting shotcrete lined pressure tunnel (Panthi and Basnet 2019a).

Strength of intact rock has been mapped as weak to very strong. As presented in Table 5-1, uniaxial compressive strength of intact rock (σ_{ci}) along HRT is strong enough to resist water pressure. Although intact rock is not vulnerable to hydraulic fracturing, schistosity developed in rock mass might make it vulnerable to hydraulic jacking. As rock mass is schistose and sheared along HRT, there exists strength anisotropy in the rock mass along the HRT. As per NEA (2019), strength anisotropy index (I_a) of the two rock samples taken from HRT at bore hole HB 1' and HB 2'is about 4 and 1.6, respectively. Based on Table 2-1, rock strength anisotropy can be classified as highly anisotropic to moderately anisotropic at bore hole HB 1' and HB 2', respectively. This indicates the vulnerability of rock mass in hydraulic jacking. In these kinds of anisotropic and schistose rock, it is difficult to determine uniaxial compressive strength since their behavior is dominated by closely spaced planes of weakness or schistosity. In case of Hard and well interlocked rock masses, Hoek and Brown (1997) recommend to use maximum value of σ_{ci}, however, in case of tectonically disturbed, poor quality rock masses, lowest value of σ_{ci} should be used. As per Nasseri et al. (2003), minimum failure strength (σ_{ci}) occurs when schistosity plane is inclined at around 30^0 from loading direction. Drilling at both boreholes is done vertically. And at bore hole locations, foliation planes are dipped within an angle of $30\text{-}35^0$. This shows that foliation angle in rock samples is between $30\text{-}35^0$ during UCS-test and hence σ_{ci} obtained from UCS test should be close to minimum possible strength.

Rock mass quality along the HRT has been mapped based on surface mapping. As per Appendix D1 and D2, rock mass quality along tunnel varies from extremely poor at Tatopani shear/weakness zone (Ch. 3+769m) to Fair at Banded gneiss, Garnet schist and Augen gneiss (Orang Khola) section. Figure 6-1 shows anticipated percentage of different types of rock mass
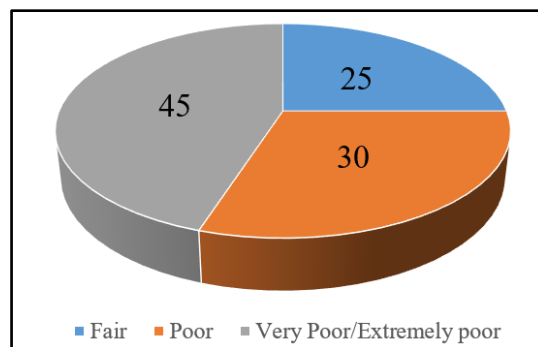

Figure 6-1 Anticipated percentage of rock mass quality along HRT

along HRT, which indicates that combined percentage of fair and poor rock mass is relatively high as compared to very poor/extremely poor rock mass. These different rock mass behave in different ways when subjected to water pressure. Very poor to extremely poor rock masses are

more vulnerable with respect to stability. Tatopani weakness zone at chainage 3+769m has rock mass quality ranging from poor to extremely poor and is even more vulnerable regarding stability. Rock mass along the downstream portion of HRT from chainage 5+000 onwards are fair in quality for short stretch of approximately 390m length. Remaining rock mass downstream of it are very poor to poor in quality for around 2850m length, which will demand extensive rock support during tunnel excavation.

The HRT alignment is above the river valley bottom, which provides an elevation difference of about 120m at end of HRT. As per Panthi and Basnet (2018b), higher the location of pressure tunnel from valley bottom, more unsafe will unlined pressure tunnel be. Based on topography, vertical and lateral cover at downstream of chainage 5+000m is less as compared to section upstream of it.

Piezometer reading at bore hole HB 2' between June and August suggests a ground water table at around 1182.6 masl, which is above the hydrostatic water level of 1158.2 masl. This condition is considered favorable for unlined or shotcrete lined tunnel as explained in 3.2.1. However, it should be noted that monsoon season in Nepal falls between June and September, during which ground water table is high above the hydrostatic water level due to high rainfall. In contrast, in dry periods, ground water table drops down to tunnel level or even below. The hydrostatic water level (h_{static}) will thus dictate the potential water leakage and is a critical parameter.

6.2   Analysis with Norwegian confinement criteria (NCC)

In order to assess whether the rock cover along the HRT are sufficient enough to counteract the static water pressure and is safe against hydraulic jacking during the operation, nine different sections along the HRT has been selected as shown in Figure 6-2, also see Figure 5-1.

Most of the sections are selected in the d/s end of HRT. This is due to the reason that the location of HRT between chainage 5+025m (Orang Khola) and end of HRT is relatively close to valley slope with low lateral cover and has low vertical rock cover. In addition, this section has high static water head as compared to sections upstream of Orang khola sections (Ch. 5+025m) (See Appendix D1 and D2). Thus, this portion of HRT is more vulnerable to hydraulic jacking as compared to upstream segment of the HRT.

Each section along the HRT are selected in such way that they are critical in a direction having relatively closer distance from valley slope surface, having low vertical cover and which might
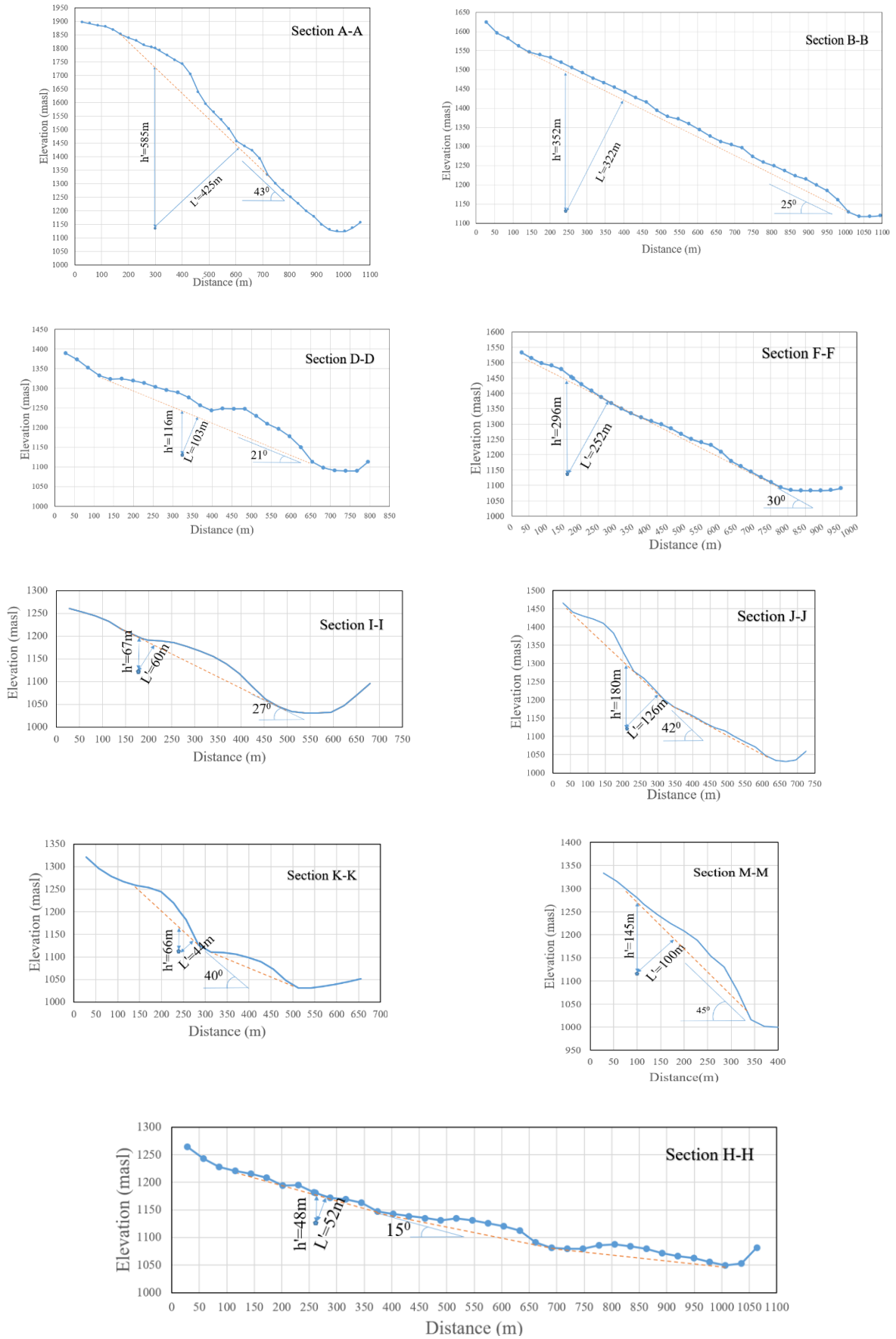
Figure 6-2 Cross section across the tunnel alignment at different locations as per Figure 5-1

potentially cause stress relief in that direction. Geometrical parameters are measured from the different cross sections as shown in Figure 6-2. Topographical correction in section with undulated ground surface has been applied assuming that their contribution to confinement is negligible. All necessary refined geometrical parameter and other relevant data for analysis are listed in Table 6-1.

Table 6-1 Analysis of HRT using NCC and Modified NCC method

Section	Chainage	H_w	P_w	h'	α	L'	β	h	L	$\frac{H_2}{H_1}$	f_g	L"	FoS_1	FoS_2	FoS_4
	m	m	MPa	m	Deg	m	Deg	m	m			m			
A-A	1+050	16	0.16	585	0.24	425	43	5.8	8.0	0	1.80	14	101	53	29.7
B-B	1+590	18	0.18	352	0.24	322	25	6.6	7.3	0	1.60	12	53	44	27.7
D-D	2+717	23	0.23	116	0.24	103	21	8.4	9.0	0	1.60	14	14	11	7.1
F-F	3+769	28	0.27	296	0.24	252	30	9.6	11.0	0	1.80	20	31	23	12.7
H-H	5+025	33	0.32	48	0.24	52	15	12.1	12.5	0	1.80	23	4	4	2.3
I-I	6+103	37	0.36	67	0.24	60	27	13.6	15.2	0	1.60	24	5	4	2.5
J-J	6+487	39	0.38	180	0.24	126	42	14.3	19.2	0	1.60	31	13	7	4.1
K-K	7+205	42	0.41	66	0.24	44	40	15.4	20.1	0	1.80	36	4	2.2	1.2
M-M	8+098	46	0.45	145	0.24	100	45	16.8	23.8	0.10	1.803	43	9	4	2.3

As it can be seen from the Table 6-1, calculated factor of safeties, FoS_1 and FoS_2 using equation 3-3 and 3-5 at different tunnel locations of HRT are as high as 101 at chainage 1+050m, which has high vertical cover (585m) and very low static water pressure head of just 16m and as low as 2.2 at chainage 7+205m with lateral cover of just 44m and static water pressure head of 42m. As the calculated factor of safeties using NCC are more than recommended factor of safety of 1.3, HRT is safe against hydraulic jacking if operated as unlined or shotcrete lined pressure tunnel.

6.3 Analysis with Modified Norwegian confinement criteria

It should be noted that NCC evaluates based on simple equilibrium principles, which only considers gravitational stress for confinement calculation against water pressure. Compared to Scandinavian rock mass, Himalayan rock mass are fractured and weathered along the topographical slopes and valleys, which ultimately lead to deep weathering and destressing. Similarly, deep valleys and multiple valley slopes attenuates in-situ stresses. In addition, due to recent tectonic evolution and ongoing mountain building process, seismic activity is very intense. As a result of which, the Himalayan region has quite complex tectonic stress regime,

both spatially and temporally (Basnet and Panthi 2017). Thus, in the project like Tamakoshi V HP with different geotectonic environment than that of Scandinavia, applicability of NCC has proven to be seldom applicable.

Panthi and Basnet (2018b) propose State of art modification in NCC as discussed in 3.2.3 in order to consider different topographical, geological and geotectonic environments that usually prevail in the Himalaya. Thus, assessment has been made using this approach as well, in addition to NCC. Himalayan river valley generally represents as a weakness zone, which may be crushed/shear zone (Basnet and Panthi 2019b). For this, Tamakoshi river valley has been considered as weakness zone (WZ#1) in all selected sections and lies in right hand side as shown in Figure 3-6 (right). Out of the selected sections, section at chainage 8+098m is almost similar to topography condition "1" as shown in Figure 3-6 (right), where slope of valley on left side of hilltop is relatively gentle than that of Tamakoshi valley on the right side. Left valley is represented by river valley called "Thulokaseri Khola/River". Based on measurement, value of H_2/H_1 has been found to be just 0.1. Thus, the multiplication factor (f_g) for section at chainage 8+098m has been chosen as f " as shown in Figure 3-6 (left) for further calculation. However, topography of the remaining sections is different as compared to topography conditions represented in Figure 3-6 (right). Remaining sections have continuous slope from Tamakoshi valley side and do not have valley on the other side as presented in topography condition 1,2 and 3 in Figure 3-6 (right). Thus, for simplicity, these remaining sections has been assumed to have flat topography on top of hill with the value of H_2/H_1 equal to zero. Hence, f_g has been chosen as f ' with no river valley on left hand side. However, sections 2+717m, 5+025m, 6+103m and 7+205m crosses rivers, which are tributary to Tamakoshi river. Thus, for these sections f_g has been chosen as f " assuming these river as weakness zone and topography with the value of H_2/H_1 equal to zero.

Based on these discussions above, values of H_2/H_1 and f_g for all selected sections have been listed in Table 6-1. With these values, the corresponding value of L" for lateral cover and its corresponding FoS_4 have been calculated using equation 3-10 and 3-11, respectively.

Figure 6-3 shows the factor of safeties calculated along the selected sections of HRT using NCC and Modified NCC. In general, FoS_1 calculated for vertical cover is higher in all sections as compared to other factor of safeties (FoS_2 and FoS_4). However, in case of shotcrete lined tunnel located in slope topography, lateral cover is more critical, and factor of safety related to it should be more emphasized. With regard to lateral cover, FoS_4 calculated by Modified NCC shows

relatively lower value as compared to NCC (FoS$_2$). It can be seen that FoS is sufficiently high in chainage 1+050m and 1+590m using both methods due to low water pressure head and high
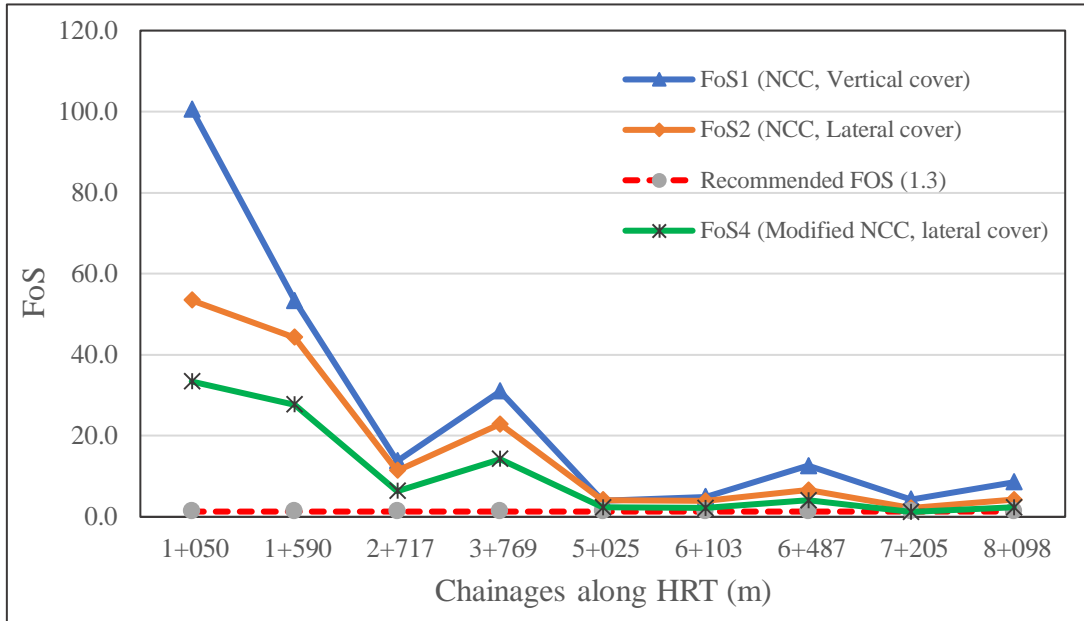
Figure 6-3 Comparison of Factor of safeties for all selected location using different methods

vertical and lateral rock cover. Also, chainages 2+717m, 3+769m and 6+487m are found to be safe against hydraulic jacking by both methods. As compared to these sections discussed above, remaining sections have relatively lower FoS and are presented in Figure 6-4 for further discussion.
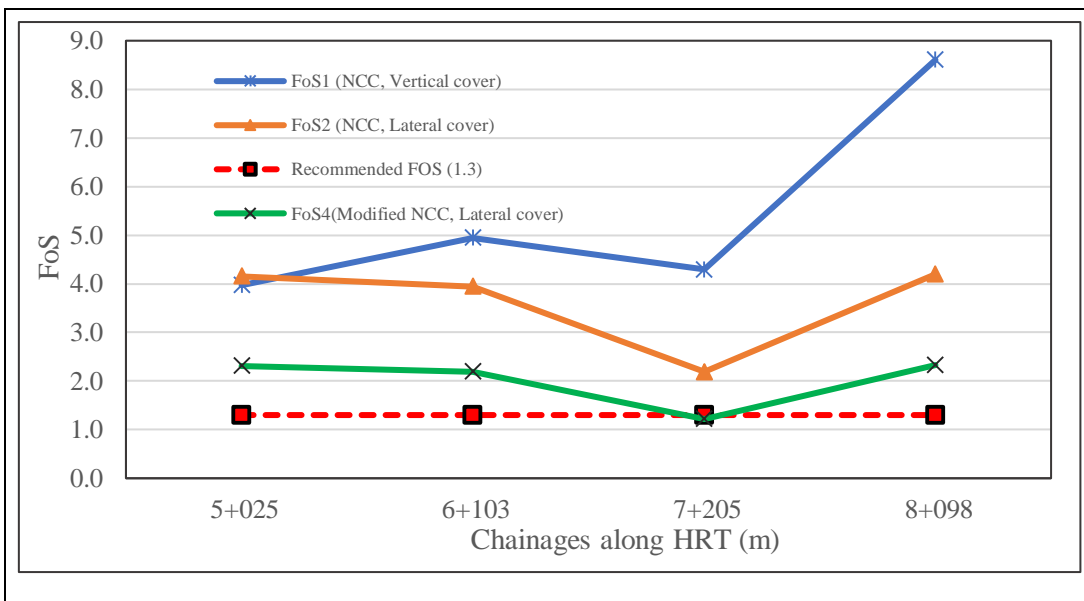

Figure 6-4 Comparision of factor of safeties for sections with lower FoS

At chainage 7+205m, FoS calculated by NCC for both vertical and lateral cover is higher than recommended FoS (1.3). However, FoS calculated by modified NCC is lower than the recommended value, which shows that tunnel location at this chainage might face potential hydraulic jacking and potential leakage problems during normal operation period. This is due to less lateral cover. In addition, this chainage represents river crossing section, which might represent crushed and sheared zone.

6.4   In-situ stress state assessment

Reliable estimation of in-situ stress state is crucial for the design and implementation of unlined pressure tunnels and shafts. In-situ stress state at rock mass is influenced by rock covers, irregular surface topography, tectonic stress magnitude and direction, depth of the valley, presence of weakness zone, location with respect to bottom valley, etc. Even within same overburden, in-situ stress varies spatially due to presence of complex topography and presence of local shear and weakness zone or destressed area (Basnet and Panthi 2019b).

Particularly, minimum principal stress is a decisive parameter in case of unlined or shotcrete lined pressure tunnel. Thus, the key for successful design of unlined or shotcrete lined pressure tunnel and shafts depends upon how correctly the in-situ minimum principal stress is evaluated (Panthi and Basnet 2019a). In order to be safe against hydraulic jacking and prevent possible leakage at any point along the pressure tunnel, minimum principal stress in adjacent rock mass should be greater than the maximum future water pressure. Thus, in order to assess minimum principal stress along the selected section, two-dimensional numerical modelling has been modelled using RS2.

6.4.1 Model setup

Quantification of input parameter is very important in obtaining better result in numerical modelling. Most of the input parameters are taken from Table 5-1 for model setup. Apart from it, remaining parameters for model set up have been summarized in Table 6-2. It should be noted in this table that there are some other sections apart from selected sections as discussed in 6.2, which would be used later, on the stability analysis in Chapter 7. Modelling process that has been used setting up model in this chapter and in Chapter 7 and 8 has been discussed here.

Topographical model has been created based on digital GIS file. Initially, in stage 1, 2D box model along with topography of selected section has been generated as shown in Figure 6-5 and later in stage 2, rock mass above valley slope topography has been excavated. As initial condition, initial element loading is considered as field stress and body force. For stiffness,

isotropic has been chosen. Failure criterion has been selected as Generalized Hoek-Brown. Furthermore, RocData software has been used to calculate input parameters for material properties using Generalized Hoek-Brown criteria. Regarding restraining, top surface is set free to move in both directions, sides are restrained in the X direction only and bottom boundary is restrained in both X and Y directions. In order to determine in-situ stress from topographical model, field stress type has been set as gravity with the use of actual ground surface since model profile have variable elevation. Beside this, material is assumed to be elastic. Modelling is carried out as plane strain analysis using Gaussian eliminator as solver type. Both in-situ stress ratio (both in and out of plane) and locked-in horizontal stress for both in and out of plane have been summarized in Table 6-2.

Table 6-2 Input parameters (loading) for RS2 model

Chainage/ Description	HRT 1+050	HRT 1+590	HRT 1+945	HRT 2+717	HRT 3+026	HRT 3+769	HRT 4+563	HRT 5+025	HRT 6+103	HRT 6+487	HRT 7+205	HRT 7+846	HRT 8+098	TRT 0+171	TRT 0+455
Direction of Tectonic stress (NE)	35^0	35^0	35^0	35^0	35^0	35^0	35^0	35^0	35^0	35^0	35^0	35^0	35^0	35^0	35^0
Direction of Tunnel alignment (NE)	13^0	13^0	13^0	13^0	32^0	32^0	32^0	21^0	21^0	21^0	21^0	21^0	21^0	45^0	45^0
Angle between tectonic stress and tunnel alignment	22^0	22^0	22^0	22^0	3^0	3^0	3^0	14^0	14^0	14^0	14^0	14^0	14^0	10^0	10^0
Stress ratio (in plane)	0.33	0.25	0.16	0.16	0.11	0.16	0.11	0.16	0.11	0.11	0.11	0.11	0.11	0.11	0.18
Stress ratio (out of plane)	0.33	0.25	0.16	0.16	0.11	0.16	0.11	0.16	0.11	0.11	0.11	0.11	0.11	0.11	0.18
Tectonic stress, MPa	7	7	2.5	2.5	2.5	1.5	2.5	2.5	2.5	2.5	2.5	2.5	2.5	2.5	2.5
Locked in stress (in plane), MPa	2.62	2.62	0.9	0.9	0.13	0.08	0.13	0.6	0.6	0.6	0.6	0.6	0.6	0.43	0.43
Locked in stress (out of plane), MPa	6.5	6.5	2.32	2.32	2.49	1.49	2.49	2.43	2.43	2.43	2.43	2.43	2.43	2.46	2.46

After determining in-situ stress state from different selected topographic models, stability analysis has been carried out in Chapter 7 and 8. For this, excavation boundaries for the selected section has been created with external boundary set as a box with expansion factor 5, assuming that it is sufficient for rock mass to normalize towards the boundary. However, for Powerhouse cavern, expansion factor has been kept 3. Also, in-situ stress determined is set as constant field stress type. To analyze displacement, rock mass failure and response of installed support, material is assumed to be plastic, which allows material and support to yield.

6.4.2   Assessment of minimum principal stress

As per the process discussed in 6.4.1 and using input data from Table 5-1 and Table 6-2, the model has been created as shown in Figure 6-5 for chainage 3+769m. This model is set up with rock mass overburden lying above the valley slope as well, which is removed in stage 2. Then,

Figure 6-5 Topograhical model at chainage 3+769m
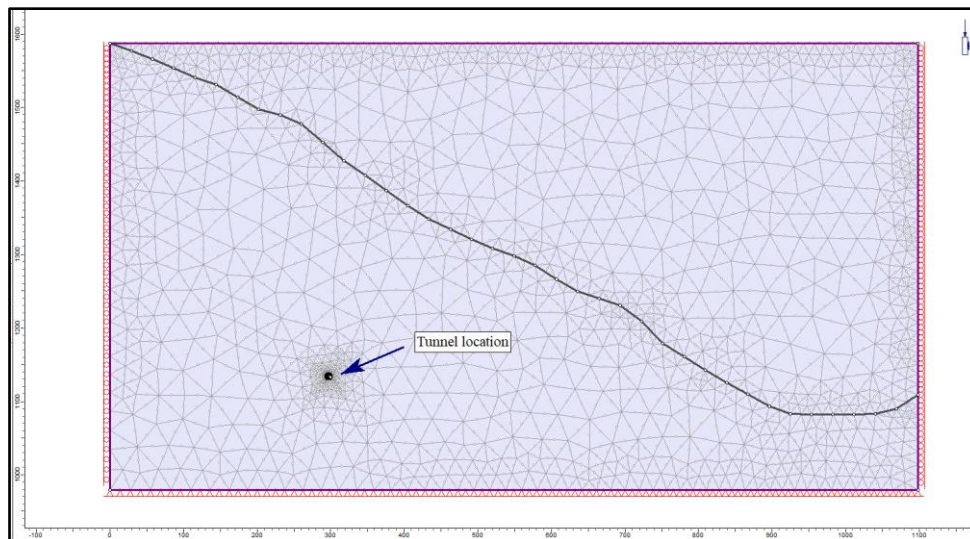
model computation is carried out in elastic mode. Based on this elastic analysis, in-situ minimum principal stress at this chainage is found to be 1.21 MPa as shown in Figure 6-6. Similar process has been followed for the rest of selected eight sections and their corresponding in-situ minimum principal (σ_3) stresses have been found out from the elastic analysis.
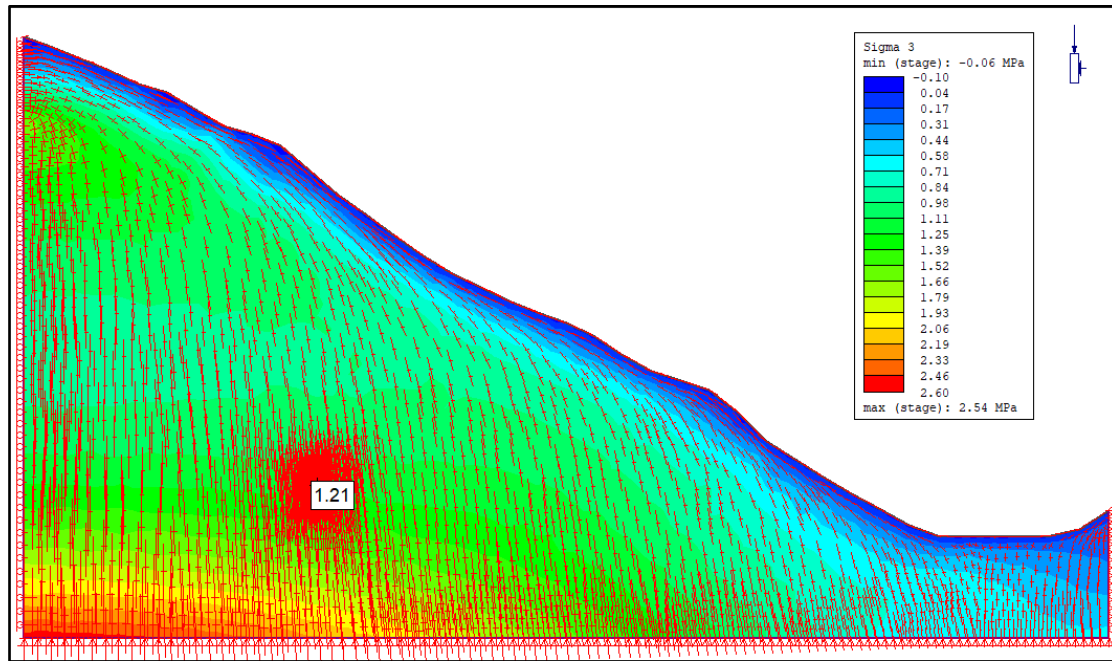
Figure 6-6 Minimum principal in-situ stress at chainage 3+769m

All the simulated in-situ minimum principal stress from different RS2 model for different chainages are listed in Table 6-3. Using static water pressure and σ_3, FoS_3 has been calculated

Table 6-3 In-situ minimum principal stress from elastic analysis at different chainages and FoS_3

Chainage	H_w	P_w	σ_3 (elastic analysis)	FoS_3
m	M	MPa	MPa	
1+050	16	0.16	6.31	40.2
1+590	18	0.18	4.04	22.9
2+717	23	0.23	1.56	6.9
3+769	28	0.27	1.21	4.4
5+025	33	0.32	0.83	2.6
6+103	37	0.36	0.85	2.3
6+487	39	0.38	1.31	3.4
7+205	42	0.41	0.92	2.2
8+098	46	0.45	1.2	2.7

using equation 3-7. The plot of the in-situ minor principal stress and hydrostatic pressure and FoS_3 is shown in Figure 6-7. As it can be seen that, σ_3 is significantly high as compared to Pw for the sections at chainage 1+050m, 1+590m and 2+717m. For remaining sections, difference in pressure between σ_3 and P_w is found to be below 1 MPa. At chainages 5+025m, 6+103m and

7+205m, difference in pressure is found to be relatively less (just 0.5 MPa) as compared to the other section. However, if the calculated FoS_3 is compared with the recommended value of 1.3, all the selected sections are found to be safe against hydraulic jacking and possible leakages.
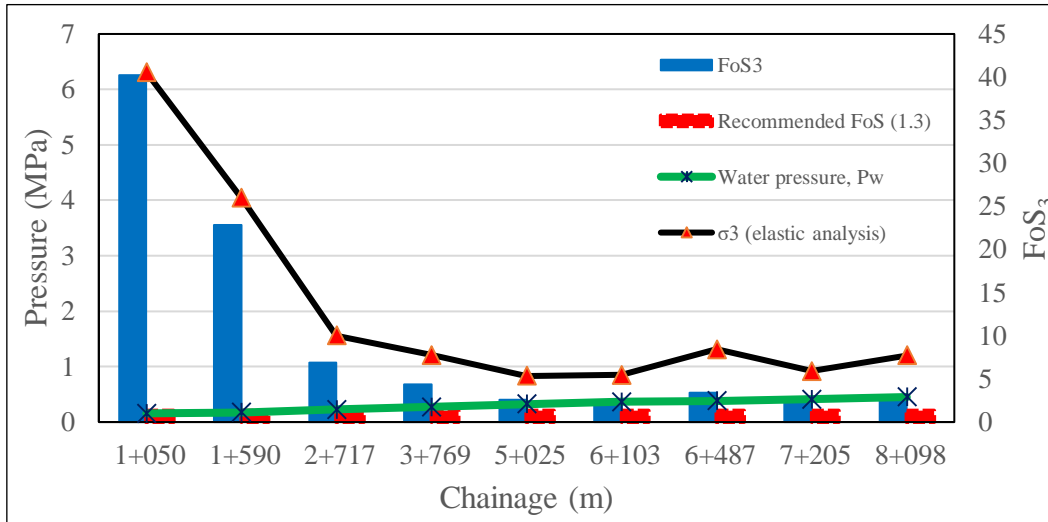

Figure 6-7 Comparison of in-situ minimum principal stress and static water pressure and FoS_3

Apart from in-situ minimum principal stress in selected chainages, it is also important to analyze redistribution of minimum principal stress around the periphery of the opening after excavation. This gives an idea about the extent of destressing that takes place into the rock mass from the periphery of the opening and helps to identify potential area, where the hydraulic fracturing might take place. For this, tunnel has been excavated on the topographic model due to which redistribution of in-situ stress takes place around the opening. Computation in the model is carried out by selecting material type as Plastic. This analysis has been carried out for all selected chainages. However, based on above analysis, three critical sections have been discussed further, i.e., chainage 5+025m, 6+103m and 7+205m. Due to presence of poor rock mass and drill and blast as a construction technique, rock mass near perimeter are weakened and stress relieved. It has been found that destressing has taken place all around the periphery and extended up to 2m to 5m into the rock mass, where σ_3 value is about 1.3 times the static water pressure. However, the natural distribution of in-situ stress has been found further away into the rock mass from this destressed zone. This destressed area could be the potential area where hydraulic jacking might occur. Among three sections, larger extent of destressed has been found to be in chainage 6+103m. At this chainage, destressed zone around the tunnel contour where σ_3 is less than $1.3*P_w$ is limited to a distance of within 5m as shown in **Figure 6-8**. Due to this reason, hydraulic jacking might take place along the existing joints in this zone. However, potentiality of leakage out of tunnel from this zone during operation depends upon

the condition of existing joints such as infilling situation, open or tight, persistence, hydraulic conductivity and its interconnection with other vulnerable existing joints, if any.
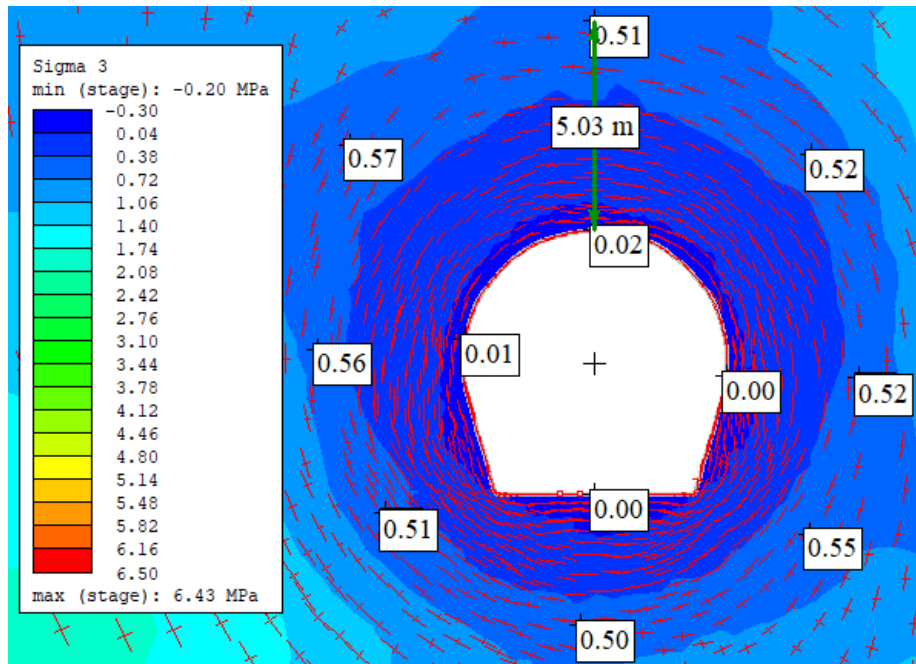
Figure 6-8 Redistribution of minimum principal stress after excavation at chainage 6+103m

6.5   Leakage assessment

In an unlined or shotcrete lined pressure tunnel, most vulnerable design issue is to make sure that the potential leakage out of tunnel during operation at full hydrostatic pressure is within acceptable limit. As per Panthi and Basnet (2019b), leakage limit for unlined or shotcrete lined water tunnel may be defined up to a maximum of 1.5 liters/minute/meter tunnel. Extent of leakage from water tunnels during operation depends upon degree of jointing, joint aperture and infilling condition, spacing of unfavorable joint set, joint persistence, hydrostatic water pressure, distance from tunnel to topography surface and orientation of joint set with respect to valley side slope. The quantitative assessment of potential leakage in shotcrete lined pressure tunnel in Tamakoshi V HP has been carried out based on the information about joint condition obtained from detail surface mapping carried out along Tamakoshi river valley and using empirical formula as discussed in 3.2.2.

6.5.1   Joint condition

Joint condition of HRT has been summarized dividing HRT into three different portions, I.e., beginning of HRT to Adit 2, Adit 2 to Adit 3 and lastly Adit 3 to Adit 4. Rock mass u/s of Adit 2 have two (plus random joints) to three major dominating joint sets (including foliation joints)

which are moderately open to tight joints filled with mostly sand and silt, moderately spaced, smooth undulating to rough planar and have medium persistence. Based on stereographic projection of the jointing system and valley slope, joint set J1 appears to be more or less parallel to the valley slope and dip steeply towards valley side as shown in Figure 6-9 (left). Similarly, rock mass between Adit 2 and Adit 3 have three major dominating joint sets (including foliation joints) which are moderately open to tight joints filled with mostly sand, silt and clay, moderately spaced, smooth undulating to rough planar and have medium persistence. Orientation of J1 as compared to valley side slope is similar in nature as described above for the first portion of HRT (See Figure 6-9, center). Lastly, rock mass between Adit 3 and Adit 4 have three major dominating joint sets (including foliation joints) which are moderately open to tight joints filled with mostly sand and silt in Augen gneiss portion and silt and clay in phyllite portion, wide (Augen gneiss section) to moderately spaced (phyllite section), smooth undulating to rough planar and have medium persistence. As per Figure 6-9 (right), there are no any joint sets which have unfavorable orientation with respect to valley slope.
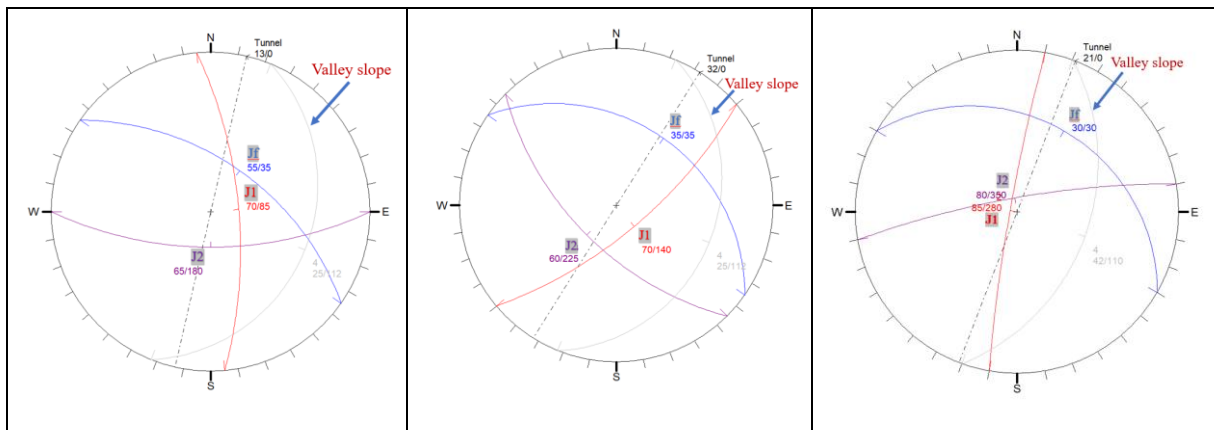
Figure 6-9 Equal area lower hemisphere stereographic projection of the jointing system. On the left for rock mass upto Adit 2, center for rock mass between Adit 2 and Adit 3 and right for rock mass between Adit 3 and Adit 4.

6.5.2 Leakage estimation

Different parameters that are used to estimate potential leakage using an empirical approach discussed in 3.2.2 are listed in Table 6-4. Input parameters are quantified based on surface field mapping and as per discussion with Supervisor (04/05/2020). Joint persistence has been mapped mainly between 3 to 10m. At chainages 1+050m, 1+590m and 5+025m rock masses have been mapped with joint spacing of 0.6m to 2m at surface. In the remaining chainages, rock masses have been mapped with joint spacing of 0.2m to 0.6m. As joints spacing increases with distance from surface, joint spacing has been set higher, than what has been mapped in surface,

Table 6-4 Assessment of leakage along the selection chainages of HRT

Chainage	J_p	J_s	D	f_a	h_{static}	J_n	J_r	J_a	q_t
m	m	m	m	$l/min/m^2$	m				$l/min/m$
1+050	7	3	425	0.005	16	6	1.5	2	0.40
1+590	5	2.5	322	0.006	18	6	1.5	2	0.50
2+717	5	1.5	103	0.032	23	9	1.5	3	3.35
3+769	7	1	252	0.028	28	9	2	3	4.67
5+025	6	2.5	52	0.046	33	6	1.5	2	6.85
6+103	5	1.5	60	0.056	37	9	2	6	6.17
6+487	5	2	126	0.020	39	9	2	6	2.32
7+205	5	1	44	0.114	42	9	2	6	14.32
8+098	5	2	100	0.025	46	9	2	6	3.45

considering the location of tunnel with respect to surface. Shortest perpendicular distance (D) from rock slope topography to valley side tunnel roof has been fixed based on the information (L') from Figure 6-2. Using equation 3-9, f_a has been calculated. In chainage downstream of 5+025m, joint alteration number has been mapped as silty or sandy clay coatings and assigned 3. However, chlorite schist and phyllite rock mass is schistose, sheared and very poor in quality with the presence of chlorite schist bands with clay infillings, thus, their permeability is comparatively less and considered impermeable with respect to water leakage. Thus, assigned number "3" is found to be inappropriate and has been replaced with "6". Finally, specific tunnel leakage (q_t) has been calculated using equation 3-8 and presented in Table 6-4.

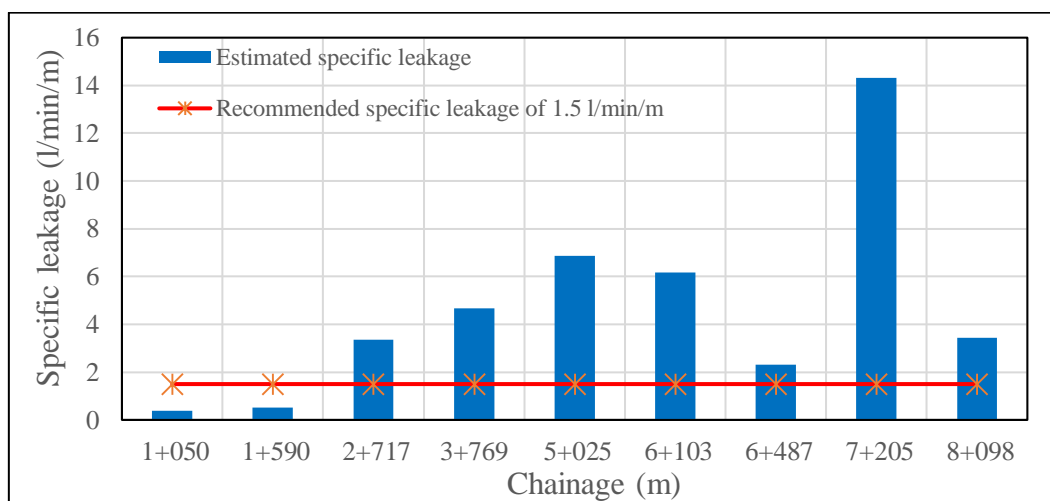As one can see in Figure 6-10, except the first two chainages, leakage estimations in the

Figure 6-10 Estimated specific leakage (q_t) from HRT of Tamakoshi V HP

remaining sections are higher than the recommended limiting value of 1.5 l/min/m. Maximum leakage of 14.32 l/min/m is estimated at chainage 7+205m and minimum leakage of 0.4 l/min/m at chainage 1+050m. Maximum leakage is estimated at tunnel stretch, where rock mass is relatively very poor in quality, subjected to high static water pressure with closely spaced and moderately open joints, and where the location of tunnel is near to the surface. And minimum leakage is estimated at tunnel stretch, where rock mass is fair in quality, subjected to very low static water pressure with widely spaced and relatively tight joints, and where location of tunnel is more than 400m from surface. Specific leakage between chainage 5+025m and end of HRT (Ch. 8+098m) is relatively high. Along this stretch, leakage possibility is high at chainage 5+025m, 6+103m and very high at 7+205m for around 300m, 525m and 380m length respectively. Tunnel at these chainages are relatively close to surface. As per Nilsen and Palmström (2000), most of leakages in a tunnel alignment normally take place in the shallowest part of tunnel, where rock mass is generally more jointed and the joints are more open than at deeper location and in those sections, which are confined in fractures, faults and weathered zone. Total leakage of water in these three stretches of around 1200m length only is around 180 l/sec, which is considerable.

As discussed earlier in 3.2.2, pre-injection as modern ground improvement technique can be used to reduce the leakage out of tunnel to allowable limit, to improve quality of rock mass and save time and money. Since, ground condition of Tamakoshi V is quite similar to that of Khimti I HP, Figure 3-5 can be used to estimate grout consumption for pre-injection in Tamakoshi V HP as well. Thus, based on specific leakage calculated in Table 6-4 and static water pressure head at different chainages, estimation of grout consumption for pre-injection grouting has been done referring Figure 3-5 and has been presented in Table 6-5. Estimated grout is for Ordinary

Table 6-5 Calculation of grout consumption for pre-injection grouting

Chainage	h_{static}	q_t	q/P	C
m	m	l/min/m	l/min/m per bar	Kg/m
1+050	16	0.40	0.16	14
1+590	18	0.50	0.19	19
2+717	23	3.35	0.97	189
3+769	28	3.11	0.74	220
5+025	33	6.85	1.38	279
6+103	37	6.17	1.11	220
6+487	39	2.32	0.40	65
7+205	42	14.32	2.27	472
8+098	46	3.45	0.50	87

Portland Cement. As tunnel is designed for water conveying purposes and not for dry tunnel like roadway, Ordinary Portland Cement is considered sufficient enough to seal open joints and reduce the cost of grouting material as micro cement is 5 times expensive than that of ordinary cement (Panthi and Basnet 2019b). Similarly, comparison between concrete lining of 350mm thickness for 100m tunnel length and grout material for same tunnel length around the chainage 7+205m has been done for simplicity. As invert will be designed with reinforced concrete, remaining wall and crown has been considered for calculation of concreting. Concentration of grout required at chainage 7+205m is used as 472 Kg/m as calculated in Table 6-5. At this stage, comparison is made based on requirement of ordinary cement only for both different design approaches. It has been found that per 100m tunnel length, 3500-3600 bags of cement (50kg) is required for concreting (1:2:4) at around chainage 7+205m. In contrast, 944 bags of cement are required for cement grouting on the same section. This shows that concrete lining is about four times expensive than the pre-injection grouting in terms of the cement alone. In addition, time required for concrete lining is also higher.

Based on water pressure (Lugeon test), it has been found that hydraulic conductivity near 3+769m and 5+025m is classified as moderate and low conductivity, respectively (Table 5-2). Leakage estimated by Panthi (2006) and Panthi (2010) in chainage 3+769m is found to be quite similar to leakage obtained by Lugeon test as shown in Table 6-6. However, at chainage 5+025m, leakage found by Lugeon test is lower than estimated by Panthi (2006) and Panthi (2010).

Table 6-6 Comparison of leakage at chainage 3+769m and 5+025m by Panthi (2006) and Panthi (2010) and Lugeon test

Chainage	Leakage in l/min/m at h_{static}	
M	Panthi (2006 and 2010)	Lugeon test
3+769	4.67	4.48
5+025	6.85	1.65

Similarly, Panthi (2006) and Panthi (2010) show that higher leakage is expected in chainage 5+025m as compared to chainage 3+769m and vice-versa by Lugeon test. This difference in leakage might be due to the fact that Panthi (2006) and Panthi (2010) approach is based on Q-parameters, which are determined on the basis of surface mapping at this stage and mapping itself is subjective. In addition, Lugeon test is only for a limited volume of rock mass around

borehole. Also, Lugeon test can be influenced by single joints and corresponding result can be misleading as well (Nilsen and Palmström 2000).

6.6   Findings

Based on the assessment carried out in this chapter, it can be said that at chainage 7+205m, potentiality of leakage by hydraulic jacking is very high. Modified NCC and Panthi (2006) and Panthi (2010) approach emphasize that this particular chainage for around 380m might face substantial leakage challenges if no any mitigation technique is adopted. Likewise, tunnel sections downstream of chainage 5+000m seem relatively vulnerable based on NCC, Modified NCC, In-situ stress state assessment, Rock engineering assessment and Leakage assessment. Likewise, at chainage 3+769m in Tatopani weakness zone, leakage potential is relatively high, which is itself weathered and sheared and consists of colluvium and landslide in these area as destressed material. Similarly, one of the joint set orientations in Tatopani weakness zone is unfavorable and is striking parallel and dipped steep to valley slope.

However, if the factor of safety calculated above is compared against recommended factor of safety of 1.3, then, HRT is safe against hydraulic jacking except at chainage 7+205m. Likewise, if compared with Table 3-1, unfavorable conditions prevail relatively more than the favorable conditions along HRT. However, use of pre-injection grouting based on estimation of grout in Table 6-5 improves the permeability condition of rock mass and hence reduces the leakage potential. Length of tunnel to be treated with pre-injection grouting as per Table 6-5 will be around 100m, 300m, 525m and 380m at chainage 3+769m, 5+025m, 6+103m and 7+205m, respectively.

Apart from assessing risk of potential hydraulic jacking and potential leakage, it is very essential to ascertain both short- and long-term stability of tunnel itself if designed for unlined or shotcrete lined tunnel. Thus, stability analysis has been carried out in Chapter 7.

Chapter 7: Stability analysis of Waterway System

In water conveying unlined/shotcrete lined pressure tunnel, two important issues have to be considered. First, it is to make sure that leakage through tunnel is kept to a minimum during operation of pressure tunnel. And second, it is to secure tunnel against any kind of stability challenges (Panthi 2013b). Depending upon the geological condition of rock mass and topographical condition in Tamakoshi V HP, stress induced instabilities has been assessed in detail in this chapter, applying both empirical and semi-analytical methods, as well as numerical modelling. However, with regard to structurally controlled failure, only discussion about possible block fall has been presented. Analysis of stability challenges along Headrace Tunnel (HRT) is important when designed as shotcrete lined pressure tunnel because design criteria of unlined or shotcrete lined pressure tunnel do not consider these instability issues. Thus, stability of HRT should be ensured in order to design it as an unlined or shotcrete lined pressure tunnel. Apart from HRT, potential stability issues in Powerhouse cavern and Tailrace Tunnel (TRT) have been evaluated as well in this chapter in detail.

7.1   Structurally controlled failure

Along the HRT at around chainage 5+025, as shown in Appendix D2, HRT passes through shallow section having rock cover of 49.5m in rock mass of augen gneiss with chlorite schist parting, which is strong to very strong rock mass and is blocky. Rock mass has three major joint sets, which are well developed as they are near to surface and are intersected to each other due to their orientation as shown in Figure 7-1. This potentially leads to the formation of wedge at
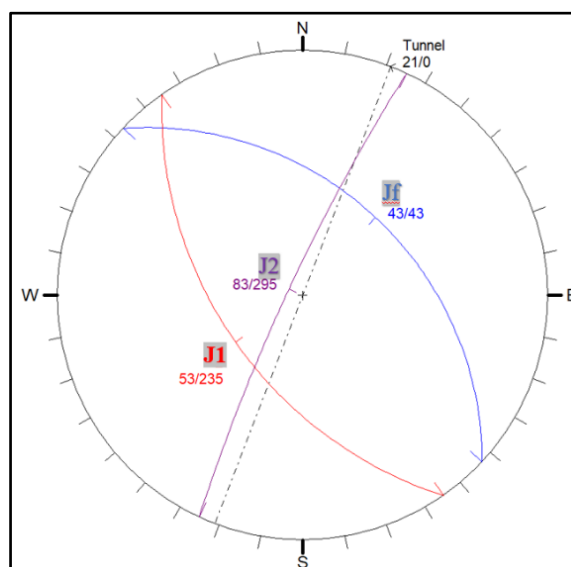

Figure 7-1 Equal area lower hemisphere stereographic projection of the jointing system (5+025m)

the roof or walls. Joints are filled with sand and silt up to 5mm thickness. Low confinement stress may lead to low normal stress on the joints. Once excavation is done, restrain from surrounding rock mass is removed. Also, ground water pressure may act along the joint plane, which further reduces the shear strength of these discontinuities and makes it vulnerable. In addition, during operation of the project, water pressure may easily wash away the filling of sand and silt and further reduce the shear strength of these joints sets and increase the probability of failure along these joint sets. Thus, it can be said that there is a high probability of having block failure at this section until and unless adequate support such as spot or sparsely spaced pattern bolting with load capacity higher than the deadweight of the potentially falling block is installed.

7.2 Brittle failure analysis

Rock mass u/s of chainage 1+769m consists of Banded gneiss and Garnet schist, amphibolite and Quartzite as shown in Appendix D1 and D2 and are mapped as strong to very strong rock mass. Banded gneiss in the region is a Precambrian high-grade metamorphic rock and is similar to Banded gneiss of UTHP. Both represent the rock mass from Higher Himalayan region, whose quality are comparable to Scandinavian hard rock mass, see 'hx' in Figure 4-1. Based on the laboratory test carried out in the rock laboratory at NTNU, rock samples obtained from UTHP consists of 63-89 % quartz (Basnet and Panthi 2019a). Also as per Panthi (2006), percentage of Quartz, Plagioclase and k-feldspar in the banded gneiss of Khimti I HP, which lies relatively close to Tamakoshi V HP as shown in Figure 4-1, is more than 85%. Thus, it can be assumed that Banded gneiss in Tamakoshi V HP as well has higher content of Quartz and feldspar. Rock stress problems in rock mass which are rich in quartz and feldspar are related to rock spalling or rock burst (Nilsen and Palmström 2000). Rock cover along the Banded gneiss ranges from 207m to 690m. Likewise, Garnet schist and amphibolite, which are formed by advanced metamorphism of basic and ultrabasic igneous rock, are very hard schistose rock (Goodman 1993). Rock cover of Garnet schist ranges from 307 to 440m. Based on these information and discussion with Supervisor (18/03/2020), rock spalling/bursting or brittle analysis has been carried out until chainage 1+769m using methods described in 2.4.2.2.

7.2.1 Norwegian rule of thumb

As discussed earlier in 2.4.2.2, this method helps to indicate potential rock burst or spalling in a tunnel, which are aligned parallel with valley side slope with a location within 500m distance from the valley side slope topography. Based on this, two sections along the HRT up to chainage

1+769m are selected, which are particularly at chainage 1+050m and 1+590m as shown in Figure 7-2 and Figure 7-3. Information from Figure 7-2 and Figure 7-3 are listed in Table 7-1.
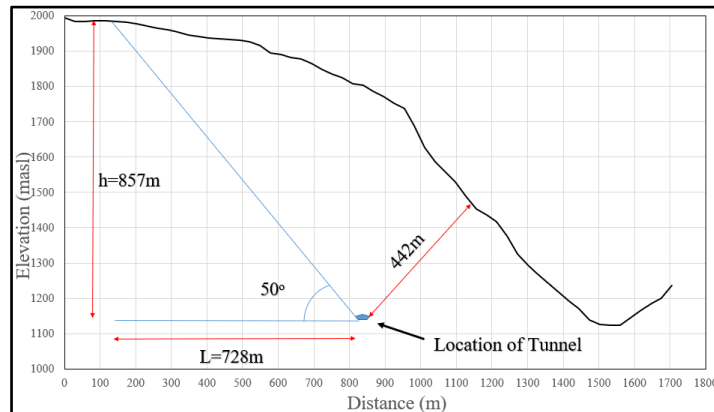
Figure 7-2 Cross-section at chainage 1+050m for brittle failure analysis
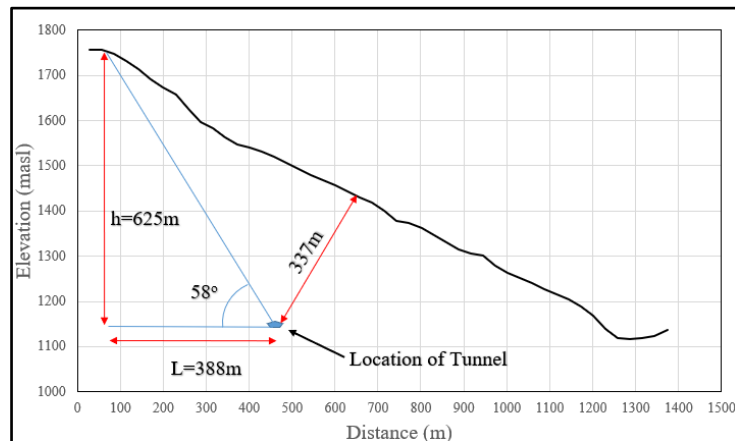
Figure 7-3 Cross-section at chainage 1+590m for brittle failure analysis

As per Norwegian rule of thumb (see Figure 2-11) and information from Table 7-1, it can be said that there is potential of having spalling on selected both sections.

Table 7-1 Analysis using Norwegian rule of thumb at chainage 1+050m and 1+590m

Description	Ch. 1+050m	Ch. 1+590m
Height from tunnel side to valley side top (h), m	857	625
Horizontal distance between tunnel and valley side high point (L), m	728	388
Distance from valley side topography, m	442	337
Angle, degree	50	58

7.2.2 Stress problem classification

Information required for this approach is in Table 7-2. Major principal stress (σ_1) has been considered as gravitational stress and maximum tangential stress is calculated using kirsch equation 2-7. σ_3 is determined using equation 2-6 and information from Table 6-2. Similar approach is used in 7.3.1 as well. Based on Table 2-4 and Table 7-2, moderate spalling can be expected in chainage 1+050m with stress class SC4. However, in chainage 1+590m, spalling potential is relatively less as compared to chainage 1+050 and stress class is found to be SC3.

Table 7-2 Analysis using Stress problem classification using Stress problem classification 1+050m and 1+590m

Description	Ch. 1+050m	Ch. 1+590m
Intack rock strength (σ_{ci}), MPa	90	70
Major principal stress (σ_1), MPa	18	9.9
ratio ($\sigma_{ci}/(\sigma_1)$)	5.00	7.04
Maximum tangential stress ($\sigma_{\theta\text{-max}}$), MPa	45	25
ratio ($\sigma_{\theta\text{-max}}/(\sigma_{ci})$)	0.50	0.36
Spalling potential	Moderate spalling after >1 hour	High stress, very tight structure, usually favorable to blasting except for wall
Stress class	SC 4	SC3

7.2.3 Uniaxial compressive and Tensile strength approach

Using the information for this approach as presented in Table 7-3 and Figure 2-12, it has been found that probability of spalling in these two sections is very less. However, it should be noted that this approach does not consider in-situ stress condition of rock mass.

Table 7-3 Analysis using Uniaxial and Tensile strength approach at chainage 1+050m and 1+590m

Description	Ch. 1+050m	Ch. 1+590m
Intack rock strength (σ_{ci}), MPa	90	70
Intack rock tensile strength (σ_t), MPa	10	9
ratio ($\sigma_{ci}/(\sigma_t)$)	9	7.8

7.2.4 Maximum tangential stress and Rock spalling strength approach

Apart from predicting potential spalling or qualitative assessment of rock burst/spalling, it is of great importance to determine the extent of damage caused by induced stress around the tunnel contour for support optimization such as determining length of bolt. Maximum tangential stress and Rock spalling strength approach provide valuable information about the severity of rock burst/spalling (depth-impact) into the rock mass behind the tunnel wall.

In order to use equation 2-9, information about rock mass spalling strength (σ_{sm}) is a prerequisite. Rock mass in these two chainages are coarse grained and strong to very strong in nature. As per the discussion in 2.4.2.2, crack initiation starts developing once specimen exceeds the threshold of approximately 0.3 of the UCS. Likewise, as per Supervisor (14/03/2020), rock spalling strength should be below 35% of intact rock strength. Thus, for depth impact analysis, σ_{sm} has been kept as 33% of σ_{ci}. Likewise, as recommended by Panthi (2017), rock mass strength has been used to replace σ_{sm} and is calculated using Panthi (2017) from Table 2-2. Thus, in total, two different approaches have been used to calculate σ_{sm}. Using these two different values of σ_{sm}, two different depth impacts are determined as shown in Table 7-4. It gives an idea that in chainage 1+050, depth impact due to spalling ranges between 0.8 to 1.6m. Likewise, at chainage 1+590m, depth impact is relatively less and ranges between 0.1 to 1m.

Table 7-4 Analysis using Maximum tangential stress and rock spalling strength approach at chainage 1+050m and 1+590m

Description		Ch. 1+050m	Ch. 1+590m
Radius of tunnel, m		3.2	3.2
Maximum tangential stress ($\sigma_{\theta\text{-max}}$), MPa		45	25
Rock mass spalling strength (σ_{sm}), MPa	33% of σ_{ci}	29.7	23.1
	Panthi (2017)	22.32	14.93
Distance from tunnel wall contour to failure point (S_d), m	33% of σ_{ci}	0.8	0.1
	Panthi (2017)	1.6	1.0

Taking this information into consideration, bolt length of approximately 3m and 2.5m are required at chainage 1+050m and 1+590m, respectively. This bolt length is obtained after adding 1.5m as an additional length to depth impact.

7.2.5 Numerical modelling

Numerical modelling for analyzing spalling has been carried out for Ch. 1+050m, which is more vulnerable as compared to Ch. 1+590m. As per elastic stress analysis carried out in topographic model at chainage 1+050m, it has been found that the stresses at tunnel locations are slightly affected by topography as shown in Figure 7-4. After determining in-situ stress state, excavation boundaries for this section has been created with external boundary set as a box with expansion factor 5, assuming that it is sufficient for rock mass to normalize towards the boundary. Also, in-situ stress determined is set as constant field stress type.
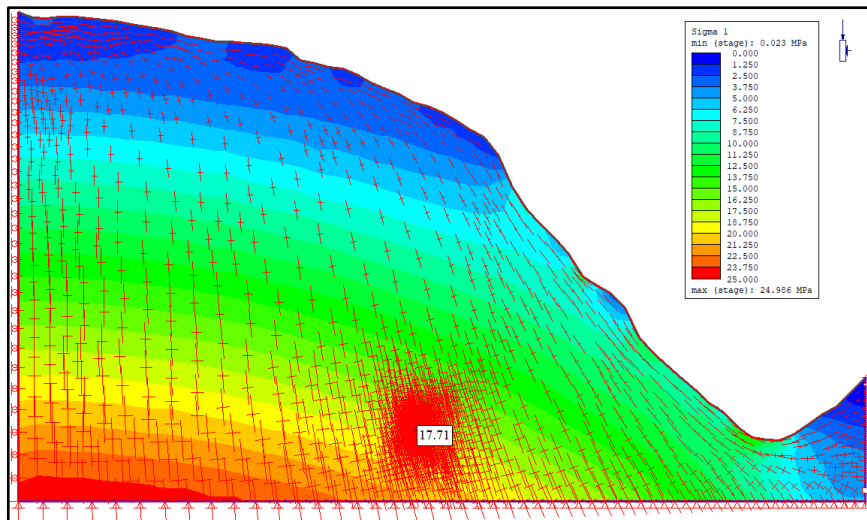

Figure 7-4 Stress situation at chainage 1+050m

Figure 7-5 (left) shows the Strength Factor (SF) around the opening after excavation, which represents the ratio of available rock mass strength to induced stress at a given point (Rocscience 2020). As per this figure, there is a zone of overstress surrounding the opening with SF less than 1. This means rock mass within this zone will fail, if left unsupported. Thus, plastic analysis is required. Also, as per elastic stress redistribution, induced stresses are high in lower right part of roof and in lower left part of wall at invert level as shown in Figure 7-5 (right). However, low stress is induced at top of roof and at invert. Location of induced maximum tangential stresses at periphery is the tangential point with respect to the direction of maximum principal stress. Induced stress at the left corner of invert is very high due to sharp bend between wall and invert. However, stress induced at lower right part of roof is quite comparable to maximum tangential stress calculated (45 MPa) by Kirsch equation. This might be due to the fact that rock mass in Kirsch equation is considered isotropic, homogeneous and

as an elastic material in circular opening. And similar is the case at this lower right part of roof in elastic model representing a segment of half circle.
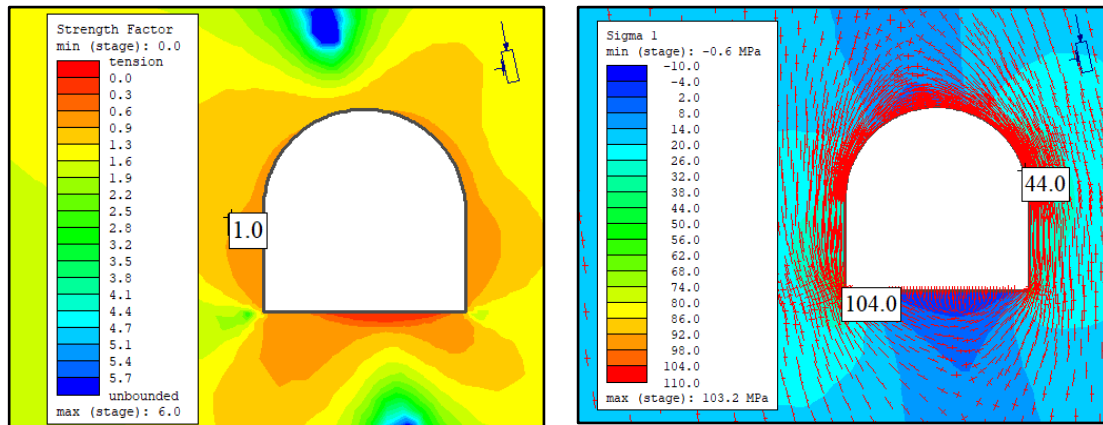

Figure 7-5 Strength factor (left) and stress distribution of Sigma 1 (right) after excavation at chainage 1+050m (Elastic model)

Plastic analysis has been carried out as shown in Figure 7-6. Extent of failure is all around the periphery (Figure 7-6, left). However, extent of failure depth is high in the lower right part of roof (around 2m), in the left wall and at invert. Extent of failure in lower right part of roof (circular part) is quite comparable with depth of impact determined in Table 7-4. However, depth of failure is relatively high at Invert. Total number of yield finite elements is 654.
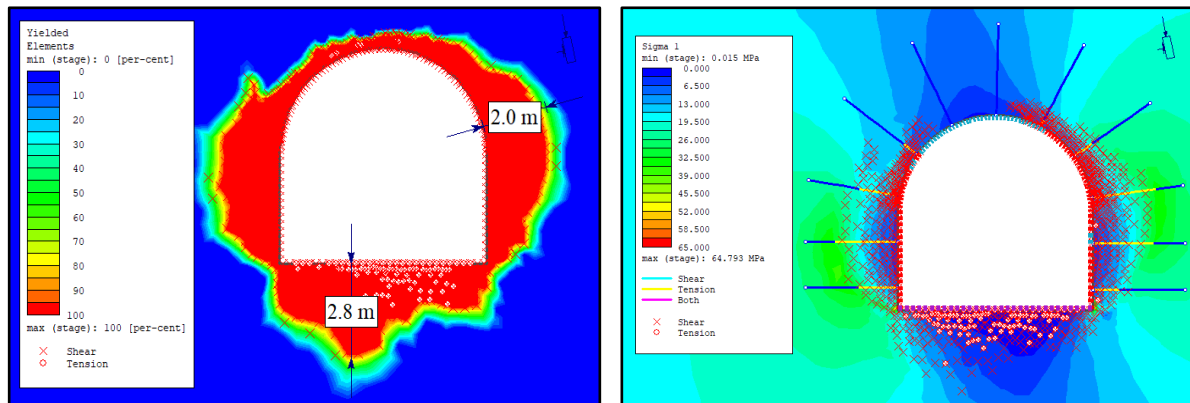
Figure 7-6 Plastic analysis at chainage 1+050m: without support (left) and with support (right)

Based on the findings from plastic analysis, findings from Table 7-4 and with the help of formula from Table 2-6, support has been proposed as indicated in Table 7-5. Figure 7-6 (right) shows plastic stress (sigma 1) analysis with yielded finite element zone and the yielded supports. Total number of yielded finite elements after support application is reduced to 540 from 654. Likewise, total number of yielded bolt and liner elements are 62 and 68 respectively.

Most of the support which are on the both wall sides and in the lower part of both roof sides are yielded. In other words, their peak capacity has been exceeded but still carries a load less than

Table 7-5 Rock support estimation at chainage 1+050m

Description	Bolt type	Bolt length and spacing	Fiber reinforced Shotcrete	Reinforced concrete
Wall and Roof	Fully grouted	3m @ 1.5m x 1.5m c/c	10 cm	-
Invert	-	-	-	400 mm

or equal to their residual capacity (Rocscience 2020). This yielding might be due to the high concentration of induced stresses along the side walls and lower part of roof. In contrast, due to low concentration of induced stress along roof top and invert, supports are not yielded but are found loaded up to its 80% capacity.

7.3   Plastic deformation analysis

In Tamakoshi V, most of the rock mass downstream of MCT, except Garnet schist, are weak, poor to extremely poor in quality, strongly foliated, jointed and anisotropic. As per Schelling (1992), rock mass downstream of MCT is a shear zone. Strongly foliated rocks can cause stability problems in underground opening (Goodman 1993). Major rock mass along the alignment are schist (Graphite, Biotite and Chlorite), phyllite and schistose augen gneiss with chlorite schist partings. HRT has an average overburden of approximately 280m, while more than 70% (approx.) of HRT has overburden more than 200m. Generally, Schist in tunnel with high overburden are susceptible to squeezing problem and this problem can be more severe in chlorite schist, graphite schist or talc schist with very low rock mass strength (Goodman 1993). Also, there is weakness zone in the HRT section, where rock mass is metacarbonate with graphite schist parting. Similarly, there exists stress anisotropy along the alignment due to high overburden, topographic effect and low contribution of tectonic stress to total in-plane horizontal stress. This is due to the orientation of tunnel alignment and tectonic stress, which are almost parallel. Likewise, the rock masses along the alignment of Khimti I HP are quite similar to the rock masses of Tamakoshi V (d/s of Ch. 1+769m), which had faced squeezing.

All these different discussions give an indication that rock mass along the alignment, especially downstream of MCT might be vulnerable for plastic deformation and this needs to be assessed.

In order to carryout plastic deformation or squeezing analysis, 13 critical and potential sections are selected based on rock cover and rock mass type along the HRT and TRT alignment. Out of these sections, some sections are from unlined/shotcrete lined pressure tunnel assessment, except chainage 1+050m and 1+590m, which are already analyzed as Brittle failure approach. Reason behind the inclusion of sections from unlined/shotcrete lined pressure tunnel assessment is to assess potential deformation issues, if there exist any. Remaining sections are selected based on rock mass, which are susceptible to deformation and have high overburden.

7.3.1 Squeezing prediction using empirical methods

Three empirical methods have been used to predict the potentiality of squeezing that might take place along the selected tunnel alignment. The findings have been presented in Table 7-6. It

Table 7-6 Squeezing prediction using empirical methods

Chainage (m)	Rock cover (m)	Q	Singh et al. (1992)		Q system (Barton and Grimstad 1993)				Goel et al. (1995)		
			Limiting cover (m)	Squeezing condition	$\sigma_{\theta\,max}$ (MPa)	σ_{cm} (MPa)	$\sigma_{\theta\,max}/\sigma_{cm}$	Squeezing condition	N	Limiting rock cover (m)	Squeezing condition
HRT 1+945	315	2.15	452	NO	25.3	3.6	7.0	Heavy	4.3	370	Non
HRT 2+717	138	2.15	452	NO	10.6	3.6	2.9	Mild	4.3	370	Non
HRT 3+026	310	0.67	306	YES	24.3	1.5	16.3	Heavy	1.7	270	Mild
HRT 3+769	310	0.13	179	YES	25.7	1.3	20.2	Heavy	0.3	148	Moderate
HRT 4+563	401	0.42	263	YES	33.0	3.5	9.6	Heavy	1.1	233	Moderate
HRT 5+025	49	4.00	556	NO	3.23	2.5	1.3	Mild	4	361	Non
HRT 6+103	68	0.24	219	NO	4.7	2.1	2.3	Mild	0.6	194	Non
HRT 6+487	194	0.24	219	NO	14.7	2.1	7.1	Heavy	0.6	194	Mild
HRT 7+205	77	0.24	219	NO	5.5	2.1	2.6	Mild	0.6	194	Non
HRT 7+846	270	0.24	219	YES	20.7	2.1	9.9	Heavy	0.6	194	Mild
HRT 8+098	161	0.24	219	NO	12.1	2.1	5.8	Heavy	0.6	194	Non
TRT 0+171	187	0.5	278	NO	14.1	4.3	3.3	Mild	0.5	182	Mild
TRT 0+455	132	0.7	311	NO	9.8	5.5	1.8	Mild	1.75	275	Non

can be seen that, prediction by three different methods are common at HRT at chainage 3+026m, 3+769m, 4+563 and 7+846m. These sections qualify for the squeezing as per the three methods. However, predictions for the remaining sections are quite mixed. As per Singh et al. (1992) and Goel et al. (1995), there would not be squeezing at seven sections out of thirteen sections. In case of sections from Unlined/shotcrete lined pressure tunnel assessment, potentiality of squeezing is at chainage 3+769m and 6+487m. And remaining sections are safe against squeezing. Likewise, in TRT, there is no any significant squeezing problem.

7.3.2 Squeezing prediction and support estimation by semi analytical methods

Quantitative assessment of potential deformation/strain in the tunnel has been analyzed using Hoek and Marinos (HM 2000) and Panthi and Shrestha (PS 2018). Details about the analysis has been presented in Table 7-7.

Table 7-7 Calculation of strain by semi-analytical methods (without support)

Chainage (m)	Rock cover (m)	Hoek and Marinos (2000), without support			Panthi and shrestha (2018), without support			
		σ_{cm}/P_o	Total strain (%)	Squeezing problems	G (Gpa)	k	Instant. strain (%)	Total strain (%)
HRT 1+945	315	0.39	1.3	Minor	0.9	0.26	1.6	3.0
HRT 2+717	138	0.88	0.3	Few support	0.9	0.39	0.3	0.7
HRT 3+026	310	0.13	12.6	Extreme	0.3	0.13	8.0	14.3
HRT 3+769	310	0.09	26.6	Extreme	0.3	0.17	12.2	21.7
HRT 4+563	401	0.19	5.6	Very severe	1.0	0.12	1.4	2.6
HRT 5+025	49	3.02	0.0	Few support	1.3	0.61	0.0	0.0
HRT 6+103	68	0.71	0.4	Few support	0.5	0.44	0.2	0.4
HRT 6+487	194	0.25	3.3	Severe	0.5	0.23	1.4	2.5
HRT 7+205	77	0.62	0.5	Few support	0.5	0.40	0.3	0.5
HRT 7+846	270	0.18	6.3	Very severe	0.5	0.19	2.6	4.7
HRT 8+098	161	0.30	2.2	Minor	0.5	0.25	0.9	1.8
TRT 0+171	187	0.86	0.3	Few support	2.4	0.13	0.0	0.1
TRT 0+455	132	1.55	0.1	Few support	1.6	0.25	0.1	0.1

Comparison of total tunnel deformation using both approaches (without support) has been shown in Figure 7-7. It shows that the squeezing problem is relatively higher at HRT as compared to TRT. The maximum deformation takes place at chainage 3+769m, which is a

Tatopani weakness zone and represents one of the sections of Unlined/shotcrete lined tunnel assessment. Total strain calculated by HM (26.6%) is relatively higher than PS (21.7%) and both indicates that this section faces extreme squeezing. Thus, substantial support is required in order to prevent convergence and possible collapse of this section. Likewise, similar extreme squeezing is likely to occur at chainage 3+026m, with total strain ranging from 12.6% to 14.3%. At chainage 7+846m and 4+563m, severe to very severe squeezing may take place with total strain ranging from 6.3% to 2.6%. In the remaining sections including TRT, total tunnel strain is less than 3.3% and most of them are less than practical limit of 2% strain (Hoek 2007).
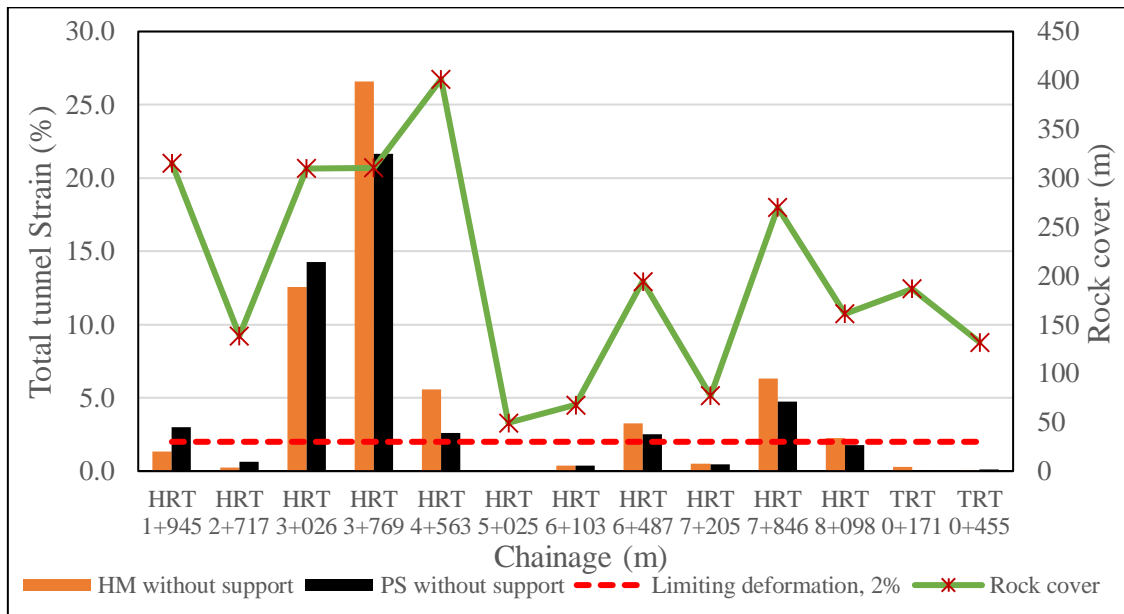

Figure 7-7 Comparison of Total tunnel deformation using both HM-2000 and PS-2018 (without support)

Despite having high rock cover at chainage 4+563m, total tunnel strain at chainage 3+769m is higher than at chainage 4+563m due to the presence of weak, sheared, fractured and destressed rock mass at this chainage. Total strain calculated by HM approach is relatively higher than PS approach in more than 50% of the sections. Similarly, instantaneous strain calculated by PS approach is relatively high at chainage 3+769m and 3+026m as shown in Table 7-7.

Both of these methods can be used to obtain first estimate of support pressure required to limit the closure of tunnel. Using equation 2-13 and 2-16, rock support pressure required to limit strain at 2% has been presented in Table 7-8. The selection of these three chainages is done based on their severity of squeezing. It can be seen that estimation of support pressure at same chainage is different due to two different methods.

In Tunnels exhibiting high degree of squeezing, it is difficult to provide support using conventional systems (Hoek 1998). In order to provide rock support pressure of around 3.1 MPa at chainage 3+769m (Tatopani shear/weakness zone), either thick concrete lining or steel ribs embedded in shotcrete or concrete is required. In addition, support that accommodate

Table 7-8 Support pressure estimation using HM and PS approach

Description	Chainage 3+026m		Chainage 3+769m		Chainage 7+846m	
	HM	PS	HM	PS	HM	PS
Total strain without support (%)	12.6	14.3	26.6	21.7	6.3	4.7
Support pressure required to limit deformation at 2% (MPa)	2.4	1.55	3.1	2.1	1.5	0.5

displacements have to be considered. However, as per NFF (2010) and Supervisor (17/04/2020), load bearing capacity of Reinforced Ribs of Shotcrete (RRS) is similar to a concrete lining with similar geometry and is an extremely flexible method, which allows deformation to occur. Besides that, it can be designed as permanent support. As per Stefanussen (2017), in many cases steel ribs have failed due to the deformation on it and it has been found that RRS is proven to be a good solution in squeezing cases with high stress and weak rock. Besides this, RRS is quicker to install, requires less material and is less expensive, and environment friendly as compared to full concrete lining (Panthi 2018a). RRS forms a good arch in combination with invert concrete lining. Invert concrete lining provides a good transition between invert and wall, protects against buckling or pressing up of tunnel floor in extreme unstable condition, limits the deformation, and acts as an additional support to wall. First approximation of support can also be obtained from the use of classification scheme. Based on lowest Q-value in the weakness zone of 0.01 and ESR of 1.6, Q system-Grimstad and Barton (1993) recommends RRS in addition to fiber reinforced shotcrete (Sfr) and bolt (B).

For the other two chainages, which require support pressure 1.5 to 2.4 MPa, rock support combination of 25mm diameter bolt with shotcrete lining (150mm-300mm) fulfills the support requirement. Table 7-9 shows the preliminary estimation of support using Q system- Grimstad and Barton (1993) for all three selected chainages.

Table 7-9 Preliminary estimation of support using Q-system- Grimstad and Barton (1993)

Chainage (m)	Q-value (lowest of the given range)	Support type
3+026	0.2	Sfr (9-12 cm thick) + B (2.1m-2.5m c/c)
3+769	0.01	Sfr (>15cm thick) + RRS + B (1.5m-1.7m c/c)
7+846	0.06	Sfr (12-15cm thick) + B (1.7m – 2.1m c/c)

7.3.3   Numerical modelling

Although empirical and semi-analytical methods are useful in determining whether tunnel require significant support and in estimating support pressures, they might not be considered sufficient for the final design purpose. Tunnels subjected to significant potential squeezing problems should be analyzed using numerical modelling (Hoek and Marinos 2000). Likewise, as per Barla (2005), numerical modelling is highly recommended if ratio of σ_{cm}/P_o is less than 0.15 and is advisable if σ_{cm}/P_o is less than 0.3. Thus, on the basis of severity of squeezing and ratio of σ_{cm}/P_o (see Table 7-7), out of total 13 sections along HRT and TRT, three critical sections along HRT are selected for further numerical modelling (chainage 3+769m, 3+026m and 7+846m), which help to optimize the design and support as well. Input data required for numerical modelling is more comprehensive as compared to empirical and semi-analytical methods. For three selected sections, all necessary input parameters are taken from Table 5-1 and Table 6-2 and model set up and further analysis has been carried out as per the process discussed in 6.4.1. Both elastic and plastic analysis has been carried out. Plastic analysis has been done with and without support to determine the response of ground and the installed support.

7.3.3.1 Elastic analysis

Typical RS2 topographical model for chainage 3+769m has been already presented in Figure 6-5. Similar model has been created for remaining two sections as well. After determining in-situ stress, model has been analyzed with elastic material. Figure 7-8 shows that Strength Factor (SF) is less than 1 around the periphery indicating overstressed zone. Similarly, SF is less than 1 for remaining two sections. Since strength factor is less than 1, tunnel suffers severe damage if left unsupported. Thus, plastic analysis is required.
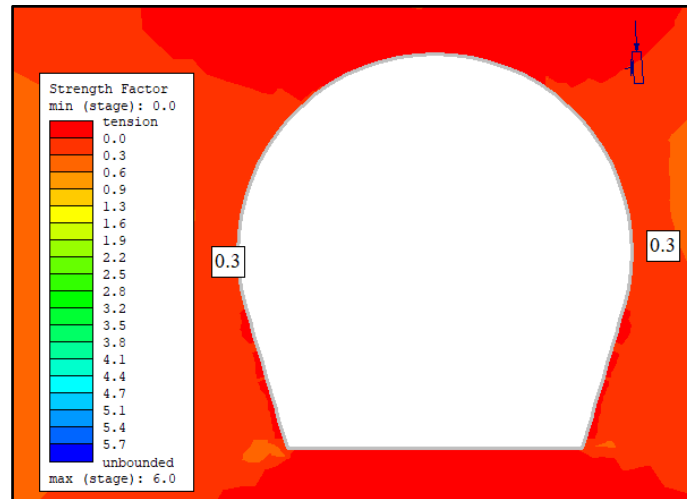
Figure 7-8 Strength factor at chainage 3+769m (Elastic analysis)

7.3.3.2 Plastic analysis

1. Without support

In order to install support in right pattern as in the real scenario in RS2, core replacement technique can be used. However, this requires radius of plastic zone. As per Figure 7-9, rock mass is yielded by both shear and tension before tunnel excavation and is extended upto surface.
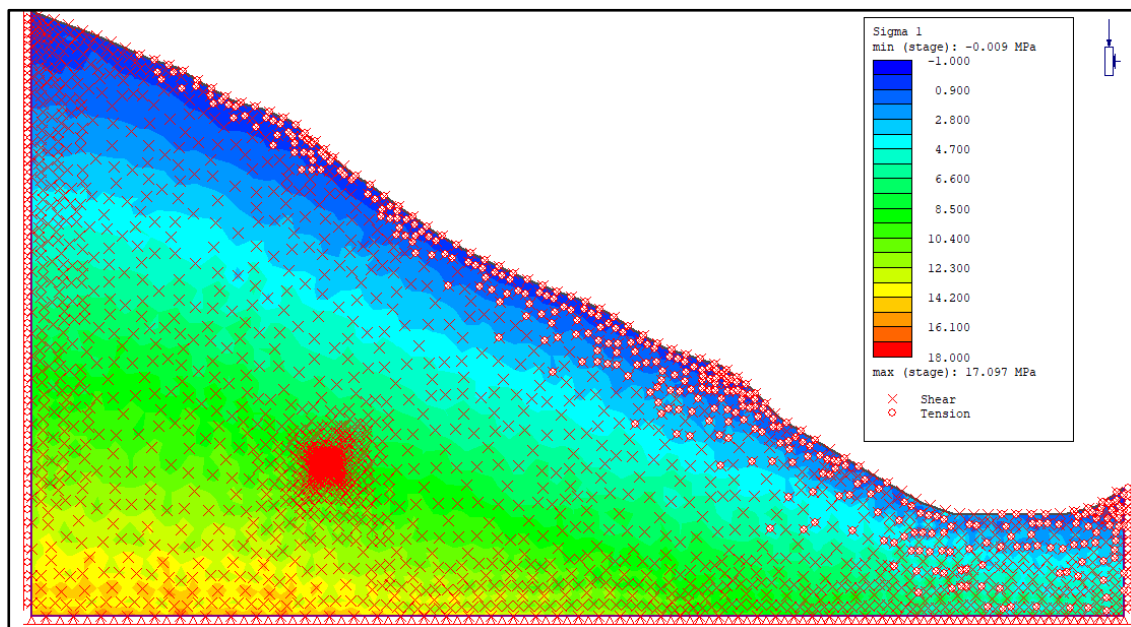

Figure 7-9 Sheared rock mass condition at chainage 3+769m after tunnel excavation

Because of this situation, it is difficult to determine radius of plastic zone in this tunnel section. Similar problems have been observed in the remaining two sections as well. This might be due

to weak rock mass and high stress anisotropy of 0.13-0.19 (horizontal to vertical stress), which is common in the Himalaya. Using core replacement technique has not been a possibility due to this reason. Thus, support is installed immediately after the excavation, i.e., at second stage in all three models.

Figure 7-10 shows that deformation around the tunnel contour is significantly high up to 0.59m at invert level. Deformation is relatively more evident in the upper and lower portion of tunnel periphery. Likewise, rock mass has mostly failed by tension in invert and roof and more on wall by shear, which might be due to the high stress anisotropy that exists because of low tectonic stress or low total in-plane horizontal stress and high vertical cover.
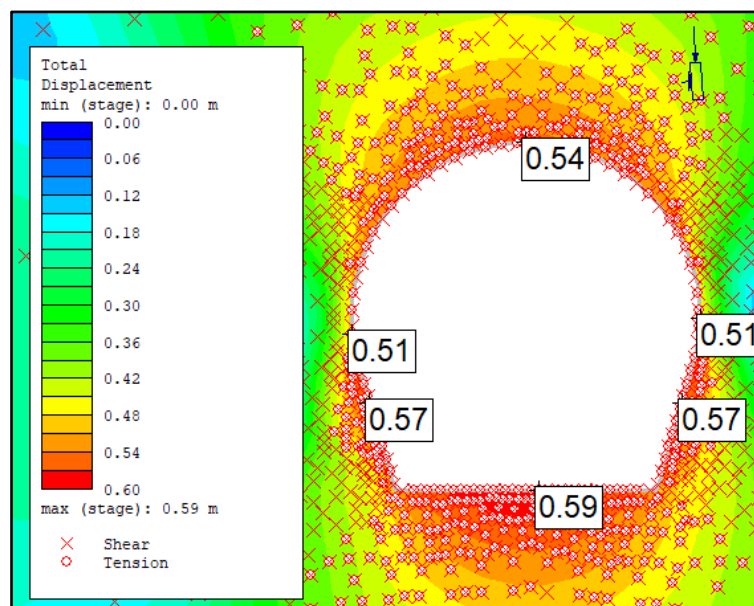

Figure 7-10 Total displacement at chainage 3-769m without support (Plastic analysis)

Similar analysis has been carried out in two other chainages as well and has been presented in Appendix C.

It can be seen in Figure 7-11 that at three different chainages, deformation from numerical modelling is relatively lower than the deformation estimated by other two methods, except at chainage 7+846m. At this chainage, deformation estimated by PS is almost similar to that of modelling. In general, HM has estimated higher total tunnel strain as compared to others, except at chainage 3+026m.
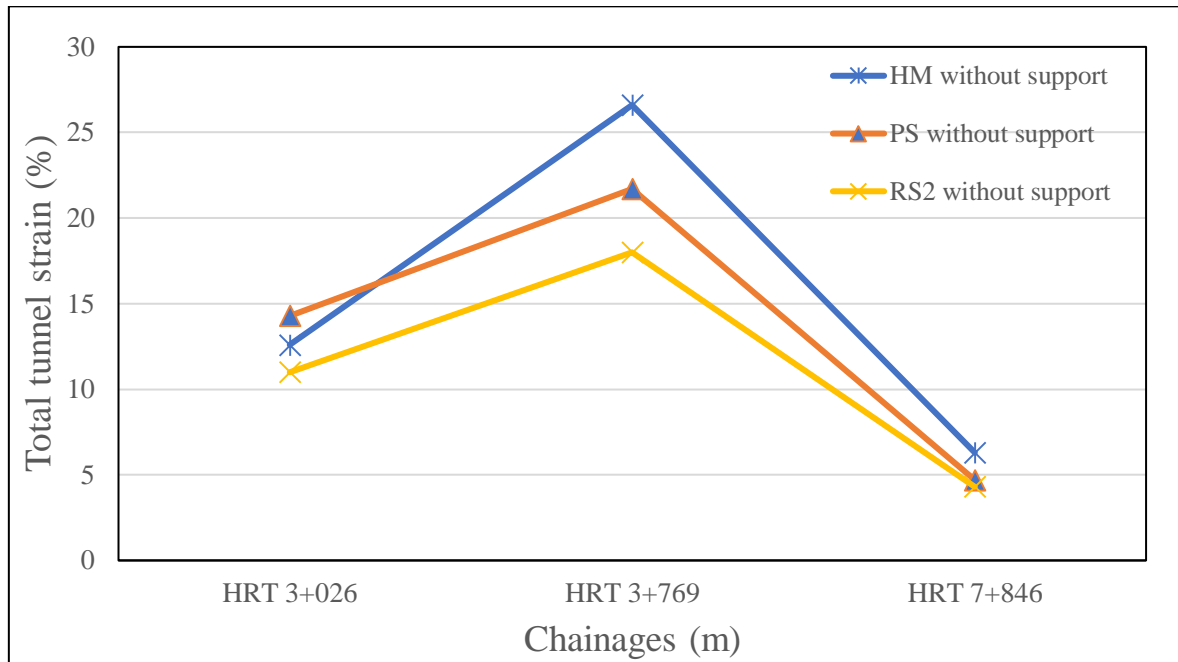
Stability analysis of Waterway System

Figure 7-11 Comparison of total tunnel deformation at selected chainages using different methods (without support)

2. With support

Preliminary support has been applied based on Q system-Grimstad and Barton (1993) (see Table 7-9). As per supervisor (3/18/2020), deformation in unlined/shotcrete lined tunnel, consisting of support system of steel fiber reinforced shotcrete and systematic bolting, should be within 5%. If deformation is higher than 5%, then one should look for full concrete lining solution. Taking this into consideration as limiting value, support systems for this selected chainage have been analyzed and revised in plastic model. Final suggested support which has limited the deformation within 5% has been presented in Table 7-10. As there is no option to define RRS directly in RS2, it is simulated in model (chainage 3+769m) by defining fiber reinforced shotcrete along with reinforced bars and radial bolts for simplicity. Its properties are

Table 7-10 Suggested support system at different chainages

Chainage (m)	Rock support		Maximum deformation (%)
	Wall and Roof	Invert	
3+026	Sfr (30 cm) + B (3m @ 1m c/c)	RC (400mm)	4.6 (roof)
3+769	Sfr (35 cm) + RRS + B (3m@1m c/c)	RC (400mm)	2.1 (invert)
7+846	Sfr (25 cm) + B (3m @ 1m c/c)	RC (400mm)	2.5 (invert and crown)

defined based on NFF (2010). Length of rock bolts has been determined based on Table 2-6. As per discussion with supervisor, invert floor is provided with invert Reinforced Concrete (RC), which will be applied throughout the tunnel alignment after completion of the excavation. Usually thickness of invert concrete is around 300mm. But due to the irregularities as a result of blasting and overbreak, final thickness has been set 400mm. Properties related to different support has been presented in Appendix B.

At chainage 3+769m, plastic analysis with support application as per Table 7-10 has been shown in Figure 7-12. Deformation around the periphery has been significantly reduced to 2.1% at invert level. Besides deformation, tension failure zone has also been reduced substantially as compared to the tunnel without support. Before, same section was analyzed with bolt, shotcrete
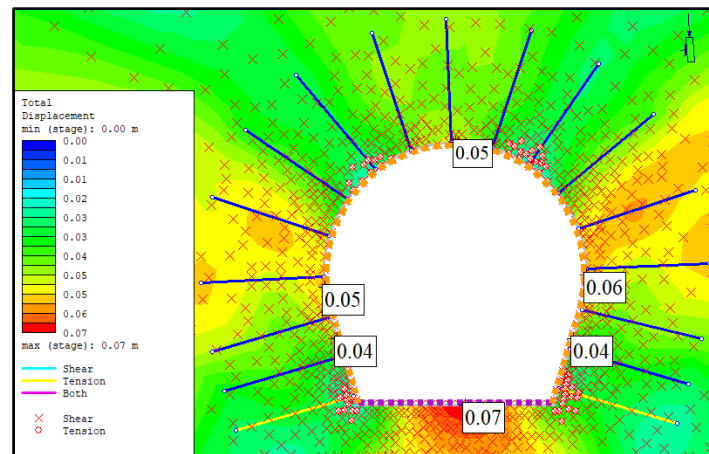

Figure 7-12 Total displacement at chainage 3+769m after support applied (Plastic analysis)

(40cm) and invert concrete (400mm). Deformation has been found to be around 7% (>5%) and almost all supports has been found yielded. As per Hoek (2007), rock support should not be stressed to failure. Thus, RRS has been introduced as rock support. Loading on support has been found to be within their peak capacity, which shows that support installed has higher factor of safety. However, in real practice as a result of practical constraints, higher factor of safety is usually not possible (NFF 2010). Plastic analysis with suggested support as per Table 7-10 for other two chainages is presented in Appendix C. At chainage 3+026m, maximum deformation at roof after support installation is 4.6 %, which is under 5%. Similarly, maximum deformation after support application at chainage 7+846m is 2.5%.

Rock support pressure of final suggested support as per Table 7-10 at different chainages is calculated based on 2.5.2. Calculations are presented in Appendix B. Corresponding support

pressure has been used in HM (2000) and PS (2018) methods to determined corresponding total tunnel strain. Figure 7-13 indicates that the final suggested support at three different critical chainages are sufficient enough to maintain total deformation within the limit of 5%.
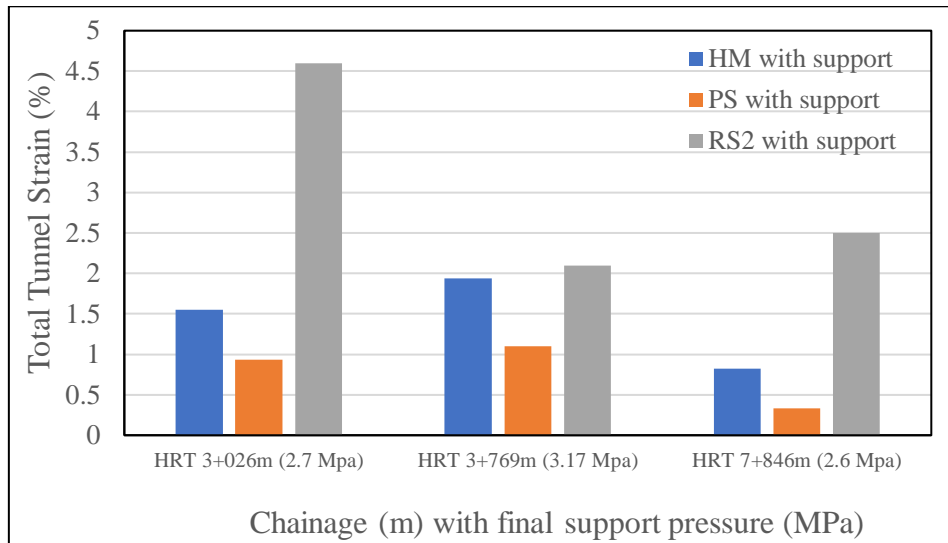

Figure 7-13 Comparison of total tunnel strain with suggested support pressure as per three different methods

For remaining selected chainages for deformation analysis, rock support consisting of fiber reinforced shotcrete of 5cm to 10 cm with systematic bolting provides support pressure of around 1 MPa, which is sufficient enough to keep deformation under 5% (see Figure 7-14). However, at chainage 4+563m at HRT, support pressure of around 2 MPa is necessary. In addition, invert concrete will be provided after complete excavation along the alignment. It can be seen that PS (2018) shows lower deformation as compared to HM (2000) for same support pressure.
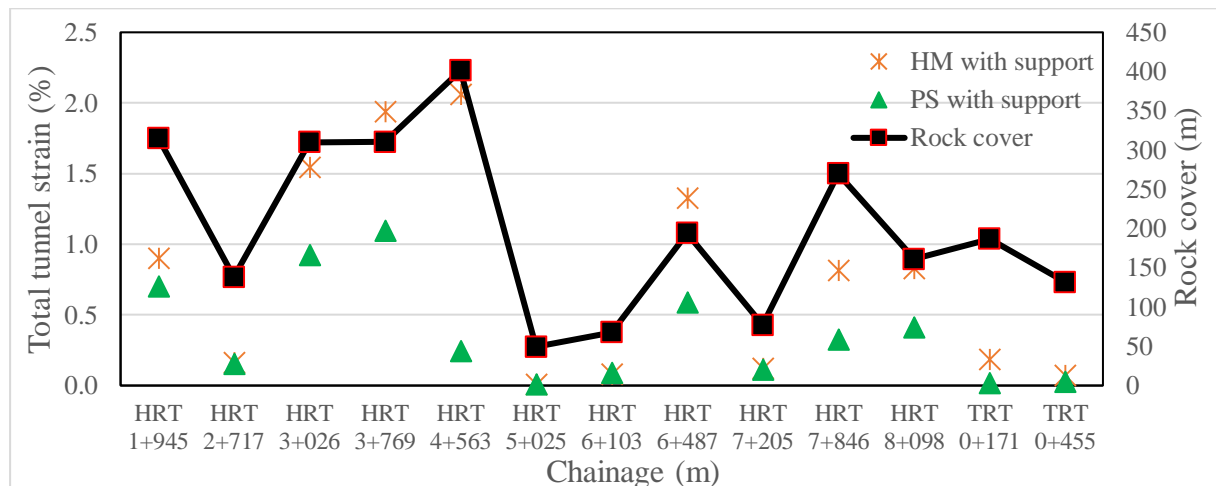

Figure 7-14 Total tunnel strain with support pressure along the selected chainages

Chapter 8: Stability analysis of Powerhouse Cavern

During the construction of large caverns in rock mass, which are heavily jointed and more deeply weathered, it is difficult to control the overbreak during excavation by drilling and blasting. After excavation, failure might extend to significant depth into the rock mass and rock mass and support installed may face severe deformation of up to 50 or 100mm at excavation surface. Thus, while designing powerhouse cavern in relatively weak rock, failure of rock mass surrounding the excavation and large deformation of the roof and walls have to be considered. For this, it is important to understand the behaviour of rock masses and the interaction of support with these rock masses during excavation. Rock support such as bolt and shotcrete should be determined based on development of deformation pattern and failure in rock mass surrounding large caverns (Hoek and Moy 1993).

Powerhouse is planned in schistose augen gneiss rock with chlorite schist parting. Rock mass has three predominant joint sets and has cover ranging from 150m to 190m and 178m at centre. As rock mass in Himalaya are generally deeply weathered, existing rock cover may not contribute to in-situ stress as normally expected. In case of deep weathering, low confinement stress might be setup above the roof, which might lead to block or wedge fall during the excavation. However, due to unavailability of information about the depth of weathering above the powerhouse area and time limitation of the thesis, structurally controlled failure analysis has not been carried out.

Rock mass along the Test Tunnel is slightly to moderately weathered, fractured, sheared, heavily jointed and poor to very poor in quality (Q-0.5 to 4) with partings of chlorite schist. With the increasing width or radius of the opening, deformation of an opening increases in general. Also, with the increase in size of the opening, size of the loaded area increases and hence strength of rock mass decreases (Palmström and Stille 2010). In jointed rock mass with clay or deformable properties like chlorite schist, probability of squeezing increases. Plastic deformation analysis has been done to assess potential squeezing and extent of squeezing.

8.1 Empirical and semi analytical methods

Q-system (1993) and Goel et al. (1995) have been used to predict potential squeezing. HM (2000) and PS (2018) have been used to identify extent of potential squeezing. Detail calculation is presented in Table 8-1. As per Q-system and Goel et al. approach, rock mass qualifies for mild squeezing to non-squeezing. Maximum deformation potential as per HM and PS is less than 1%, which represents non-squeezing conditions. Considering total strain of 0.2%

and equivalent diameter of cavern to be around 26m, total deformation is found to be around 52mm.

Table 8-1 Deformation analysis at Powerhouse cavern using different methods

Q system (1993)			Goel et al. (1995)		HM 2000	Panthi and Shrestha (2018)			
σθ max (MPa)	σcm (MPa)	σθ max/σcm	Rock mass number (N)	Limiting overburden (m)	Total strain (%)	Erm (Gpa)	G (Gpa)	K	Total strain (%)
7.73	4.3	1.8	0.5 to 4	32 to 424	0.2	5.1	2.3	0.20	0.1
Mild squeezing			Non to Mild squeezing		Few supports problems/Non squeezing				

These methods are usually developed for circular tunnels. Both Q-system and Goel et al. are based on rock mass classification system. Q-system is independent of size of the opening and can be used for all underground openings. However, deformation is directly dependent to dimension of the opening. Thus Q-system being independent of opening size is both advantage and a limitation. As compared to Q-system, Goel's proposed method considers the dimension of the opening, which is an advantage. However, this method is based on empirical data of circular tunnels. All three methods by Goel, Hoek and Marinos and Panthi and Shrestha are dependent on tunnel dimension. For this, equivalent radius has to be assumed for cavern. This is not realistic and practical. As the ratio of height to width for cavern differs from 1, shape of plastic zone and degree of squeezing will also vary in cavern as compared to tunnels (Vestad 2014). Complex excavation dimension and excavation progress in large cavern as well affect the deformation in addition to stress conditions and rock mass quality and strength. The effects of these are not properly considered in the selected methods. However, these methods give firsthand estimate on degree of squeezing. In this aspect, numerical modeling is the most suitable option for analysis of large-scale caverns, which makes it possible to model the true geometry of the opening with rock mass properties and prevailing in-situ stress situation.

8.2   Numerical modelling

RS2 is used to assess the overall stability of powerhouse cavern. In reality, caverns are excavated in different stages by heading and benching of 3-5m and subsequently support are installed. However, for simplicity and for study purpose, excavation and support installation in this cavern has been carried out at three stages (first-roof, second benching of 3m and third-full excavation) as per discussion with supervisor (24/04/2020). Model set up for cavern is shown in Figure 8-1. Input parameter is set as per Table 5-1 and tectonic stress is kept as 2.5 MPa.
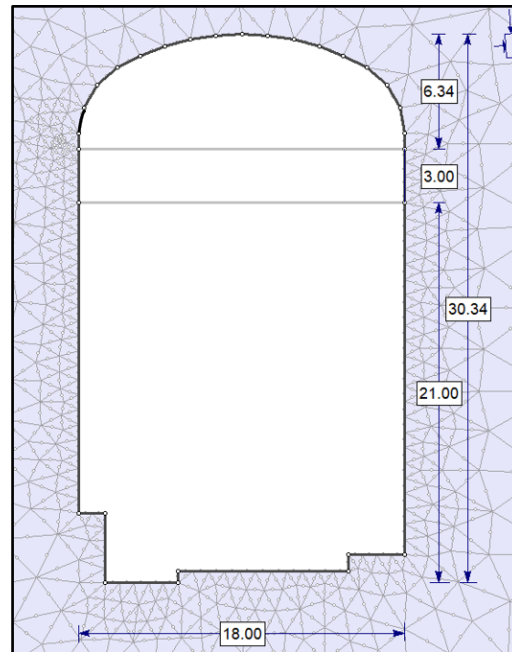
Figure 8-1 Powerhouse cavern profile and excavation stages (Dimensions are in meter)

8.2.1 Elastic analysis

Strength factor has been analyzed for different excavation stages. As seen in final excavation stage (Figure 8-2), there is a zone of overstress surrounding the whole cavern with SF less than 1. Particularly, overstress zone has been extended more (around 10m) in both wall side of
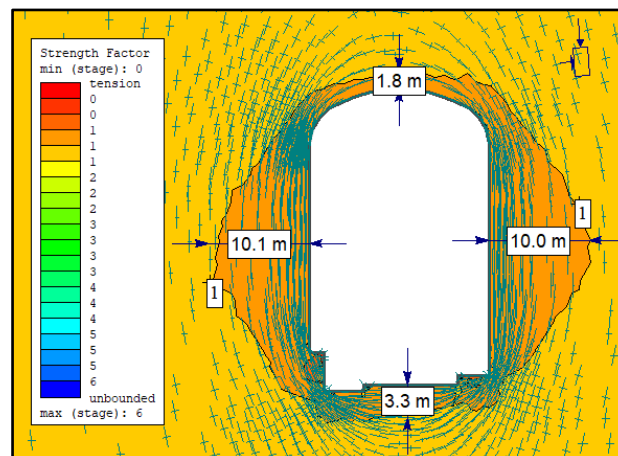
Figure 8-2 Powerhouse cavern strength factor and stress distribution (Elastic anlaysis)

cavern and less in roof and invert. This means rock mass within this zone will fail, if left unsupported. Thus, plastic analysis is required. Similarly, stress trajectories as shown in Figure 8-2 indicates that confining stress along the walls is very less. This leads to concentration of high compressive tangential stress in the high walls. Maximum elastic displacement has been found to be 0.032m.

8.2.2 Plastic analysis

Plastic analysis with and without support has been carried out for Powerhouse cavern. Figure 8-3 shows the total deformation and yielded elements without support. Maximum displacement has taken place in the wall (103mm) and total wall displacement is 194mm, which is high as compared to total deformation of 52mm determined by semi-analytical methods. Potential failure zone indicates a yielded finite element zone, where the tensile and shear strength of the
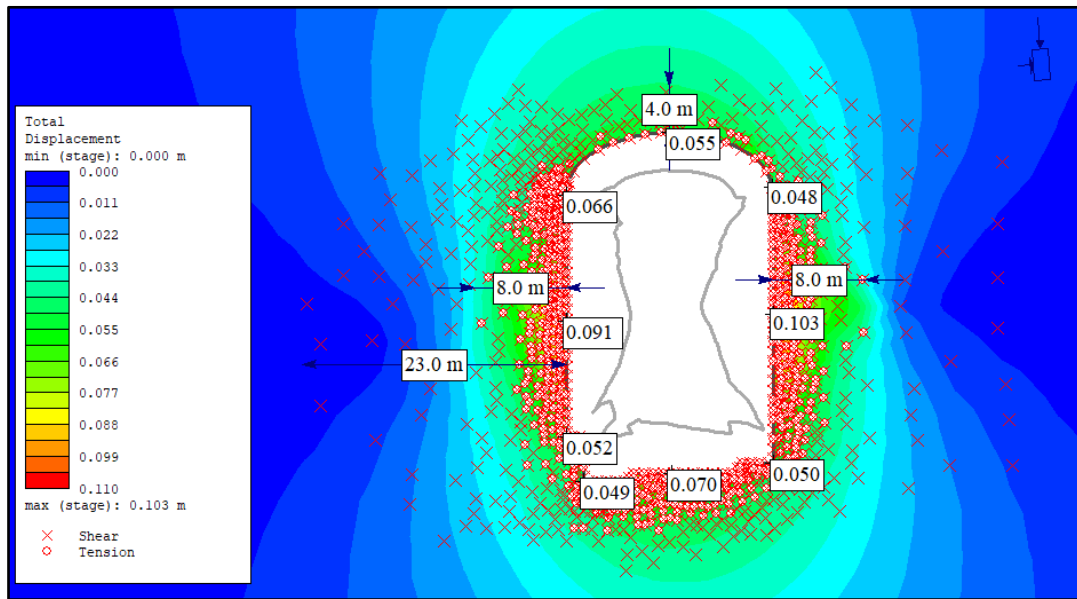

Figure 8-3 Total deformation and yielding elements for unsupported plastic analysis

rock mass has been exceeded. Total number of yielded finite elements is 693. Potentiality of tensile fracture around wall and invert are considerable, where minimum principal stresses are negative. Tension due to negative stresses might cause some problems in stability. The extension of failure zone, where both tensile and shear failure has occurred, is around 8m from wall in both sides. However, apart from this combined failure zone, further failure has extended by shear only (23m). In roof, potential failure zone extends approximately 4m from roof. As per Hoek and Moy (1993), if the progressive failure of rock mass takes place, then at certain extent of failure, formation of continuous open cracks takes place behind the walls. This leads to collapse of a large mass of sidewall rock. Thus, possibility of this failure should be stabilized by extensive support.

Based on Q system-Grimstad and Barton (1993), recommended support system for Powerhouse cavern with Q value in the range of 0.5 to 4 and Excavation Span Ratio (ESR) equal to 1 is presented in Table 8-2. Similarly, bolt lengths for cavern wall and crown are determined based on empirical approach discussed in 2.5.1, and are presented in Table 8-3.

Table 8-2 Preliminary support estimation as per Q system-Grimstad and Barton (1993)

Description	Span/ESR	Support
Wall	30.34	Bolt length of 8m @ 1.6-2.4 c/c, fiber reinforced shotcrete of 10-20 cm thickness
Roof	18	Bolt length of 5m @ 2-2.5 c/c, fiber reinforced shotcrete of 10-13cm thickness

Table 8-3 Predicted support as per Hoek and Moy (1993)

Description	Span (m)	Bolt length (m)	Bolt spacing (m)
Wall	30.34	6.6	1.5
Roof	18	4.7	1.5

One of the ways to determine approximate extent of rock requiring support is the analysis of failure zone. Since, zone of failure has extended all around the cavern, installation of pattern bolting is required in this case, which reinforces the entire rock mass. Based on failure zone, length of bolt required will be more than 8m. Similarly, for cavern roof, bolt length of around 6m is required, which enables bolt to extend beyond failure zone by 2m and get anchored in undamaged rock.

Considering all these discussions above about rock support, following support has been proposed for wall and roof of the cavern and is considered as "Case A" (see Table 8-4). Although potential shear and tension failure has occurred in invert, support for invert has not been considered at this stage as lower part of cavern will be filled with concrete to form turbine foundation and for other service structures.

Table 8-4 Proposed support for Powerhouse cavern (Case A)

Description	Bolt type	Bolt length and spacing	Fiber reinforced Shotcrete
Wall	Fully grouted	8m @ 1.5m x 1.5m c/c	12 cm
Roof	Fully grouted	6m @ 2m x 2m c/c	10 cm

Plastic analysis with support estimated in Table 8-4 has been carried out. Yielding in both rock mass and supports and the total deformation are shown in Figure 8-4. As bolts are installed within the failure zone, extent of shear and tensile failure zone has not been reduced significantly. Thus, most of the bolts installed in both side of walls are fully yielded in tension (indicated by yellow color).
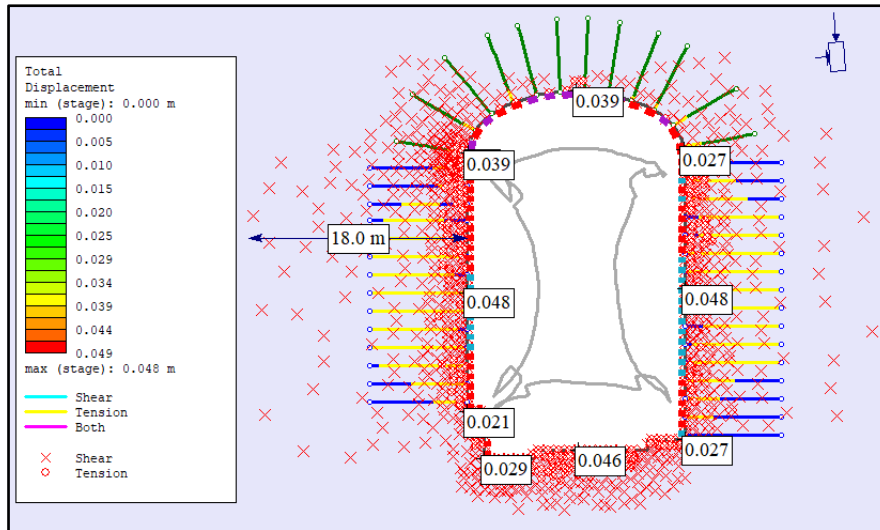

Figure 8-4 Total deformation and yielding elements with supported (Case A) plastic analysis

Likewise, similar failure of certain roof bolt has taken place. Similarly, shotcrete in walls are mostly yielded (indicated by red color). As per Hoek and Moy (1993), extent of failure zone should be kept as small as possible with a priority in reducing extent of potential tensile failure zone. As rock mass in cavern is very poor to poor with large failure zone, Li (2017) suggests the use of long cable bolts along with tightly spaced rock bolts. Also, as height of side walls increases, length of anchorage requirement also increases. Thus, considering these aspects, cable bolts as "Plain strain cable" has been proposed in addition to "case A" support and is estimated using empirical relation from Table 2-6. Table 8-5 shows revised supports along with cable bolts and is represented as "Case B". Although major failure zone has occurred mainly

Table 8-5 Proposed support with cable bolts for powerhouse cavern (Case B)

Description	Bolt type	Bolt length and spacing	Fiber reinforced Shotcrete	Plain strand cable length and spacing
Wall	Fully grouted	8m @ 1.3m x 1.3m c/c	15 cm	12m @ 4m x 4m c/c
Roof	Fully grouted	6m @ 1.8m x 1.8m c/c	15 cm	9m @ 5m x 5m c/c

beyond the wall, cable bolts are also considered for roof due to its large span.

Again, plastic analysis has been carried out using support as described in Case B. Yielding in both rock mass and supports and the total deformation are shown in Figure 8-5. It can be seen
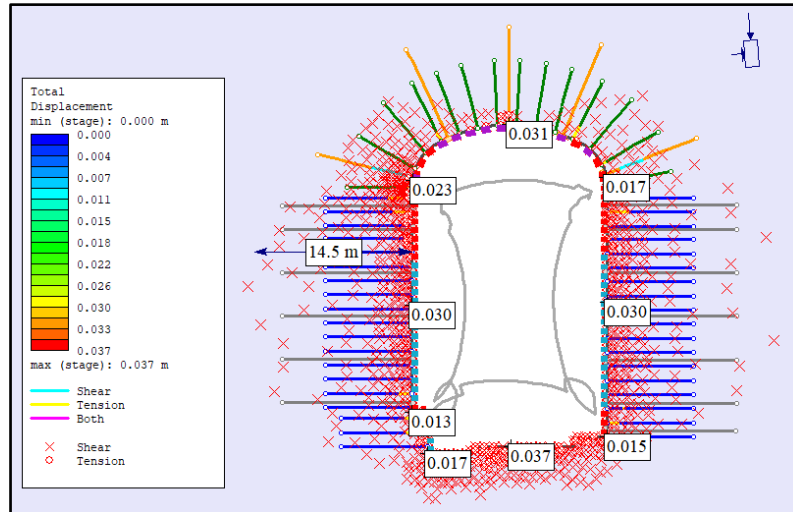

Figure 8-5 Total deformation and yielding elements with supported (Case B) plastic analysis

that rock mass failure zone has been reduced and is almost contained by the envelope of reinforcing bolts. Extent of potential tensile fracture zone has been reduced substantially as compared to cavern without support and Case A. Both maximum and minimum principal stress around the cavern have improved significantly. Tightly spaced bolts in wall have possibly constrained failed rock mass and have formed artificial pressure arch within the failure zone. In addition, cables and shotcrete have provided holding and surface retaining function respectively. Particularly, cable has acted as primary reinforcement system. Details about yielded finite elements, bolts and liners and maximum deformation for cavern without support and support (both cases) are presented in Table 8-6. As per this table, there has been reduction in the number of yielding of all element types with Case B support. However, the reduction in number of yielding of bolt elements is significant as compared to reduction in the yielding of finite elements and liner elements. Majority of support has been loaded within their peak capacity. Out of them, substantial number of bolts are axially loaded up to an average load of 0.18 MN having FoS of 1.4. In general, FoS for bolts ranges from as low as 1.2 to as high as 2.54. However, in reality, as a result of practical constraints, higher factor of safety is not usually possible. Maximum displacement in Case B has improved by small margin of 1cm as compared to case A and total wall closure is reduced to 60mm.

Table 8-6 Comparison of yielding of finite, bolt and liner element in plastic analysis

Description	Yielded finite elements	Yielded bolt elements	Yielded liner elements	Maximum deformation (mm)	Total wall convergence (mm)
Without support	693	-	-	103	194
With support (Case A)	630	203	44	48	96
With support (Case B)	606	44	33	37	60

8.3 Earthquake impact in Powerhouse cavern

In-situ stress situation in rock mass is affected by both tectonic activity and geological environment. This influence is even more in the Himalayan region, where tectonic movement is active resulting in periodic dynamic earthquake. Due to earthquake, permanent reduction in stress state takes place, especially in the areas with weakness and shear zones (Panthi and Basnet 2019a). In contrast, if rock mass is strong, homogeneous and of good quality, risk of stress attenuation during dynamic loading is minimum and in certain occasion, accumulation of stress may take place. Apart from the change in stress state, stability problems like loosening of rocks in poor rock formation, several support failures and increase in deformation from few centimeters to meters may take place during Earthquake (Palmström and Stille 2010). Thus, it is important to carry out dynamic analysis in addition to static analysis to study change in-situ stress state, support failure and change in deformation in a seismically active region like in the Himalaya. For the analysis in RS2, seismic acceleration coefficient of an Earthquake event is required as dynamic input. It represents the (maximum) earthquake acceleration as a fraction of acceleration due to gravity (Rocscience 2020). Around five years ago on 25th April 2015, massive earthquake popularly known as "Gorkha Earthquake" of magnitude 7.8 Richter hit western Nepal. One of the largest aftershocks of it had an epicenter near (around 14 KM) to project area and had a magnitude of 7.3 Richter. As per Panthi and Basnet (2019a), Peak Ground Acceleration (PGA) at surface of Powerhouse area is around 0.6g or 6m/s^2. However, the influence of earthquake in rock mass below surface is relatively low. Based on discussion with

Supervisor (24/04/2020), 10% of PGA is used for dynamic analysis in powerhouse cavern, i.e., 0.06 as horizontal seismic coefficient. Generally, horizontal seismic acceleration coefficient is larger than vertical coefficient, hence, for vertical coefficient, 1/3 of horizontal seismic coefficient is used as per Supervisor's suggestion. With this information, powerhouse cavern with support is analyzed dynamically and comparison between static and dynamic analysis has been made.

Figure 8-6 shows the static and dynamic analysis of cavern with support. Location along the contours are marked with alphabets to compare deformation and in-situ stress state at different
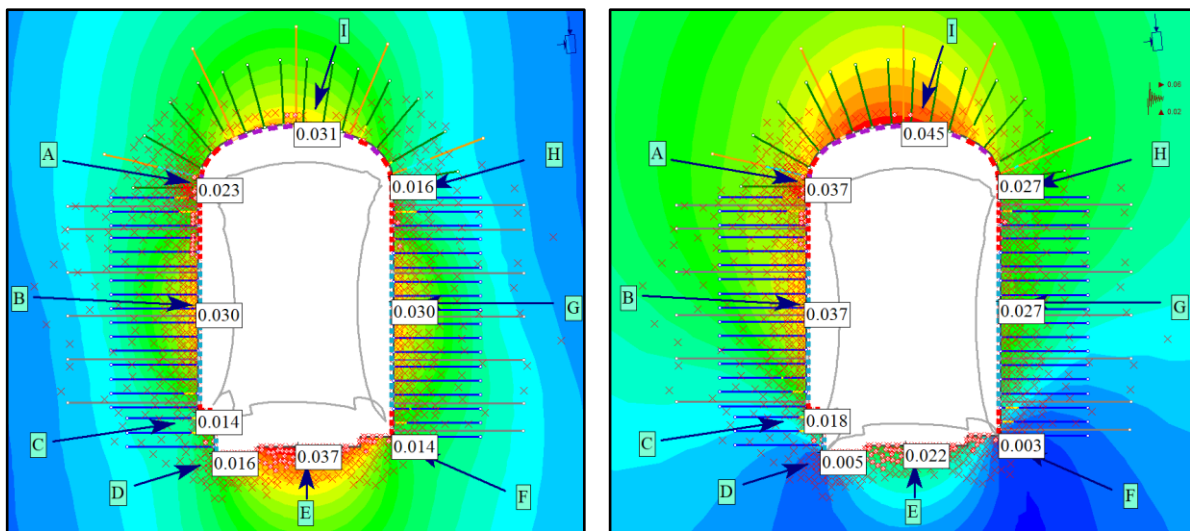
Figure 8-6 Static analysis (left) and dynamic analysis (right) with support showing deformation locations along the cavern perimeter in both analyses. During dynamic analysis, number of yielded finite element has decreased; however, number of yielded bolts has increased as compared to static analysis as shown in Table 8-7. Similarly, yielded number of liners remained almost the same. Slight change in deformation boundary has been occurred due to change in deformation around the perimeter of cavern. As shown in Figure 8-6, maximum displacement

Table 8-7 Comparison of static and dynamic analysis of Powerhouse cavern

Analysis type	Yielded finite element	Yielded bolt element	Yielded liner element	Maximum deformation (mm)	Total wall convergence (mm)
Static	606	44	33	37	60
Dynamic	589	51	34	45	64

in roof (I) has increased to 45mm from 31mm due to dynamic analysis. Except G, deformation in wall and crown has increased in dynamic analysis. This increment might be the reason behind more failure of bolt and liner element during dynamic analysis. In contrast, decrease in deformation has taken place in Invert. Overall, change in deformation has taken place by 3mm to 15mm. In case of in-situ stress state, change in maximum principal stress (σ1) and minimum principal stress (σ3) due to dynamic loading has been presented in Figure 8-7. Minimal increment of around 0.11 MPa has taken place in both stresses in almost all locations. To sum up, it can be said that stress state almost remained the same and is significantly unaffected by dynamic loading. This might be due to rock mass being medium strong and the rock mass itself in this continuum model is assumed as isotropic and homogeneous, without considering any discontinuities. However, discontinuities such as weakness zone and shear zone in rock mass attenuates the stress state during earthquakes.
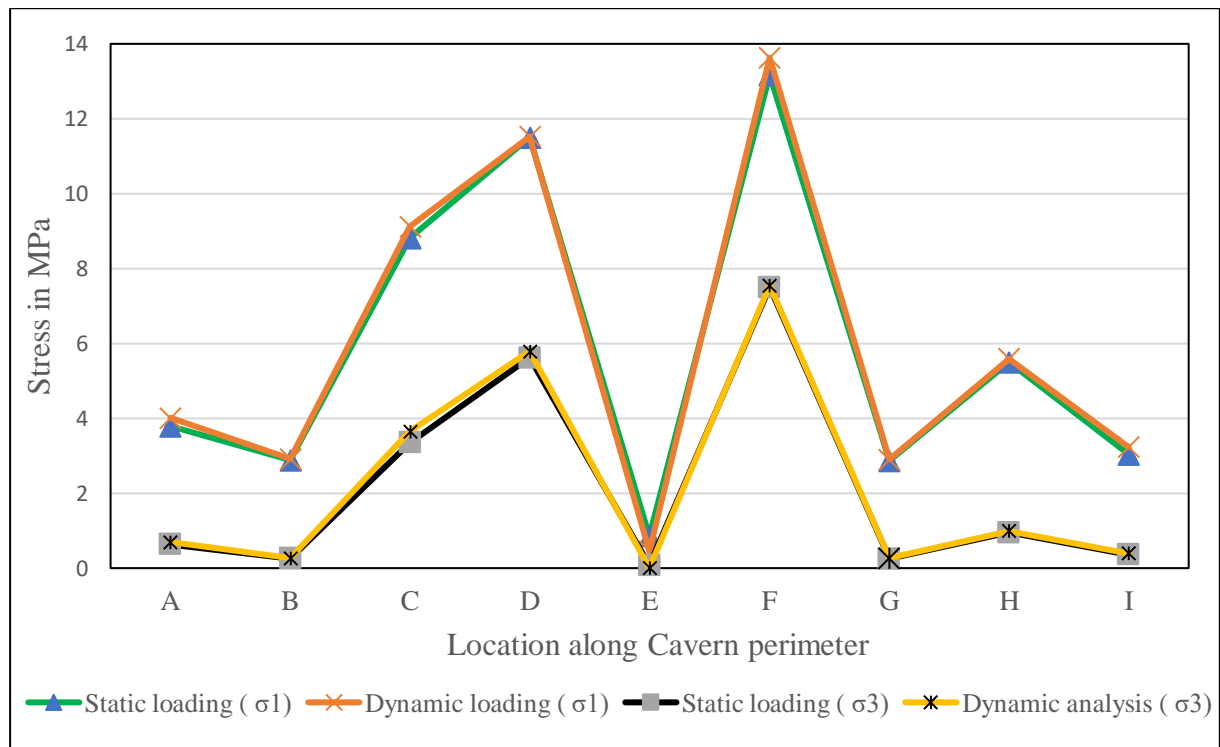

Figure 8-7 Comparison of maximum and minimum principal stress between static and dynamic analysis in Powerhouse cavern

Chapter 9: Findings and Discussion

9.1 Existing layout design

The alignment of HRT and TRT has been found safe with respect to major joint sets. Foliation joints are in favorable direction to tunnel axis. However, one of the discontinuities in Powerhouse cavern is found to be aligned almost parallel to its longitudinal axis and dipping steeply to high walls, which are both undesirable. Taking this into consideration, new alignment for powerhouse cavern is proposed which in addition considers the direction of tectonic stress.

9.2 Applicability of shotcrete lined headrace tunnel at the project

Assessment of shotcrete lined tunnel potentiality has been carried out by Rock Engineering assessment, Norwegian Confinement Criteria (NCC), Modified Norwegian Confinement Criteria, In-situ stress state assessment and Leakage assessment.

Qualitative assessment of rock mass along HRT indicates that majority (55%) of rock mass are fair to poor in quality and remaining are very poor to extremely poor. Tatopani weakness zone at chainage 3+769m might be more vulnerable to hydraulic jacking depending upon in-situ stress state, jointing condition and water pressure. Likewise, rock mass downstream of chainage 5+000m are vulnerable to hydraulic jacking as compared to rock mass u/s of chainage 5+000m due to relative high-water pressure head at these sections, location of tunnel nearby by valley slope and due to the presence of very poor to extremely poor rock mass in downstream stretch of HRT (especially after chainage 5+230m).

Nine different critical sections along the HRT have been assessed based on NCC, Modified NCC and In-situ stress state assessment. The pattern of Factor of Safety calculated by these methods along the HRT is quite similar in nature. Similarly, factor of safety evaluated by Modified NCC and In-situ stress assessment is quite comparable and almost similar, except at chainage 1+050m, 1+590m and 3+769m. Both NCC and In-situ stress assessment evaluates similar factor of safety at chainage 7+205m only. All these three methods of assessment show that tunnel sections u/s of chainage 5+000m are found safe against hydraulic jacking with higher factor of safety. This is due to the availability of higher rock cover (116m-585m) and high lateral cover (103m-425m) even after topographic correction, presence of more fair to poor rock mass quality except weakness zone and more importantly due to low water pressure head of less than 33m. At weakness zone (3+769m), factor of safety calculated by modified NCC (i.e. 12.3) is almost half of what calculated by NCC. These differences in factor of safety are observed in other remaining chainages as well. Similarly, despite setting up RS2 model with

lower tectonic stress of 1.5 MPa at 3+769m, In-situ stress assessment as well shows that weakness zone is safe against hydraulic jacking with factor of safety of 4.4. Water pressure head at this zone is around 28m. However, it should be noted that stress assessment has been carried out with 2D continuum model without representing any discontinuities, which may alter the in-situ stress situation. HRT downstream of chainage 5+000m has been found relatively vulnerable as compared to section u/s of it by all three methods due to low vertical cover, low lateral cover, very poor to extremely poor rock mass and relatively higher water pressure head of maximum 46m. At chainage 7+205m, factor of safety calculated by Modified NCC is lower than 1.3, which indicates the potentiality of hydraulic jacking at this section. This is mainly due to low lateral cover and consideration of Tamakoshi river as weakness zone in Modified NCC, which is quite common in Himalayan river and represents the crushed zone that causes destressing effect. Similarly, NCC, Modified NCC and In-situ assessment method show relatively lower factor of safety along the chainages 5+025m,6+103m and 8+098m, however, is higher than the recommended factor of safety of 1.3.

Leakage assessment has been carried out using Panthi (2006) and Panthi (2010). Leakage assessment shows that specific leakage in most sections downstream from 1+590m has been found to be higher than the recommended limiting value of 1.5 l/min/m. Although chlorite schist and phyllite rock mass d/s of chainage 5+230m is considered relatively impermeable, maximum specific leakage of 14.32 l/min/m has been evaluated at chainage 7+205m. This might be due to closely spaced joints, very low lateral cover, presence of three joint sets and higher water pressure head. Similarly, at chainage 5+025m and 6+103m, specific leakage has been found to be higher than 6 l/min/m. Total leakage of water in these three chainages stretches with only the length of 1200m is around 180 l/sec, which is a considerable loss. Specific leakage estimated in weakness zone (3+769m) is 4.67 l/min/m, which is quite comparable with Lugeon value. To improve permeability and control leakage, pre-injection as a modern ground improvement has been proposed at different vulnerable sections with grout consumption as high as 472 kg/m of Ordinary Portland Cement at chainage 7+205m. This not only controls leakage but also improves rock mass quality by preventing washing out of fine materials and gluing cracks and fissures of the discontinuities along the alignment and save time and cost in implementing concrete lined tunnel.

9.3   Stability challenges along the waterway system

Due to variation in stresses and rock types along the HRT and TRT, different types of rock stress problems or instabilities are expected. HRT at chainage 5+025m is found vulnerable for

block fall due to shallow depth of 49.5m in strongly jointed and strong augen gneiss rock mass. To identify other potential stability problems, following stability analysis has been carried out in detail.

9.3.1 Brittle failure

Rock mass along the HRT up to chainage 1+769m is strong to very strong competent rock mass and has relatively high overburden up to 690m. Qualitative assessment using prevailing methods for prediction of potential rock burst/rock spalling shows that there is potential of having spalling problem with higher probability in Banded gneiss (1+050m). However, Uniaxial compressive and Tensile strength approach indicates spalling does not occur, but it should be noted that it does not consider in-situ stress condition of the rock mass. Quantitative assessment carried out by using Maximum tangential stress and Rock spalling strength approach shows higher depth impact of 0.8m to 1.6m at chainage 1+050m and almost similar failure depth is found by Numerical modelling as well. Based on this analysis, rock support of fiber reinforced shotcrete and bolt has been proposed.

9.3.2 Plastic failure

In Himalayan region, squeezing phenomenon is commonly evident in hydropower tunnel passing through weak, highly schistose, fractured and sheared rock mass (Panthi 2006). HRT and TRT mostly pass through poor to extremely poor in quality, strongly foliated, jointed and anisotropic rock mass. Rock mass are usually with alternate band of chlorite schist, biotite schist and graphite schist and have low rock mass strength. These types of rock mass when subjected to high overburden may suffer from severe squeezing problems. Average rock cover along the HRT is approximately 280m, with more than 70% of rock mass having more than 200m rock cover. As per three empirical methods, out of thirteen selected sections along HRT and TRT, three sections along HRT at chainages 3+026m, 3+769m and 7+846m qualify for severe squeezing, which come in close agreement with extent of squeezing predicted by Hoek and Marinos (2000) and Panthi and Shrestha (2018) method. Both methods have estimated extreme squeezing at chainages 3+026m and 3+769m, among which, 3+769m as Tatopani weakness zone is found to be more critical with total tunnel strain as high as 26.6%. This may result in collapse of tunnel at chainage 3+769m, if constructed without any special consideration to excavation method and the applied support. To limit deformation to 2%, support pressure calculated by both HM and PS is found to be 3.1 MPa and 2.1 MPa, respectively. Numerical modelling has shown that support pressure of 3.17 MPa consisting of bolts, RRS of 35cm and invert concrete limits maximum deformation at 2.1%. However, in reality, it is difficult to install

required support pressure safely in an advancing tunnel. Also, when strain level exceeds 5% and σ_{cm}/P_o <0.2, face stability problems may occur and may require face pre-reinforcement (Hoek 2001). Ability to provide early confinement on tunnel periphery and near the face is considered to be the most important factor in controlling deformation (Barla 2005). In this extreme squeezing at 3+769m, tunnel can be fully excavated after improving rock mass around tunnel by grout injection and using grouted pipe fore poles or grouted fiberglass dowels as pre-reinforcement to rock core ahead of advancing face. Likewise, invert concrete has to be constructed at short distance from tunnel face (4 to 6m) as in Tartaiguille tunnel in France (Barla 2002). This support approach as resistance principle prevents large deformation that would otherwise take place instantly behind the working face with high magnitude as indicated by instantaneous strain (12%) by PS method. After carrying out excavation along with these suggested measures, support pressure can be applied as per plan. For the remaining sections, support combination of fiber reinforced shotcrete of varying thickness (5cm to 30cm), bolts and invert concrete maintain the deformation within 5%.

9.4 Stability challenge in Powerhouse cavern

While designing Powerhouse cavern in relatively weak to moderate rock mass, rock mass failure surrounding the excavation and deformation at walls and roofs should be considered. As per empirical and semi-analytical approach, non to mild squeezing can be expected. But these methods are basically based on the experience from tunnels and dependent on tunnel dimension/radius, which is not realistic in large cavern. Numerical modelling makes it possible to represent true geometry of cross-section. Due to large span, high walls and overburden of 178m, extent of rock mass failure around wall has been found very high with total wall convergence of 194mm. As support like lining, shotcrete and mesh provides very limited effective support and responds passively to deformation in this scenario (Li 2017), cable bolts along with tightly spaced rock bolts and shotcrete has been applied, which confined failure zone within envelope of bolts and cables, reduced tension failure zone substantially and wall convergence to 60mm. In seismically active region like Himalaya, dynamic analysis in addition to static analysis is mandatory. Setting up 0.06 and 0.02 as horizontal and vertical seismic coefficient in model, analysis shows that there has been insignificant impact in stress state with slight increase in deformation (1cm) and few additional support failures. This shows that Powerhouse cavern is safe against earthquake, however, there might be impact in tunnels nearby portal areas during earthquake events.

Chapter 10: Conclusion and Recommendations

10.1 Conclusion

Shotcrete lined pressure tunnel is a cost effective and an innovative solution if existing rock mass condition permits. However, presence of complex topography and geological condition and unstable geo-tectonic environment in Himalaya imposes a challenge in implementing it (Panthi 2014). Thus, it is always important to carry out assessment in terms of topographical situation, in-situ stress state and overall rock engineering aspects. Potentiality of exploiting Headrace tunnel (HRT) of Tamakoshi V HP is assessed based on Rock engineering assessment, Norwegian Confinement Criteria (NCC), Modified NCC, In-situ stress state assessment and Leakage assessment. It is found that HRT can be implemented as shotcrete lined tunnel with the implementation of pre-injection grouting at certain section downstream of chainage 5+000m and at Tatopani weakness zone. Since design approach of this solution does not consider instabilities of tunnel, it is a prerequisite to ascertain stability of tunnel before implementing shotcrete lined tunnel.

From stability analysis of waterway system, it has been found that different factors such as rock mass strength, deformability and rock stress condition, influence the stability. Based on these factors, potentiality of having brittle failure at Banded gneiss section as well as plastic failure with maximum deformation as high as 26.6% at Tatopani weakness zone have been assessed in the HRT. As per system behavior or the combined effect of ground behavior and installed rock support, it has been found that stability challenges along the tunnel can be confined within acceptable limit with the proposed support system. This indicates that HRT of Tamakoshi V HP can be designed as Shotcrete lined pressure tunnel along with the use of fiber reinforced shotcrete (Sfr), bolt (B) and invert concrete in majority portion of HRT and some additional support of Reinforced Ribs of Shotcrete (RRS) and pre-injection at Tatopani weakness zone. Likewise, stability of Powerhouse cavern with support combination of cable bolt, bolt and fiber reinforced shotcrete is found safe in both static and dynamic analysis. However, it is emphasized that reliability and quality of proposed support in all the underground elements, particularly shotcrete, should be maintained to its design level with better quality control.

Based on analysis carried out in this master thesis, following conclusions can be made.

> ➢ Planning and design of underground structure is very risky and challenging in the Himalaya due to its presence of young and fragile geology and unstable geo-tectonic

environment. Thus, it is of utmost important to carry out detailed engineering geological investigation prior to the design of any underground structures.

➢ The most important element in any kind of analysis is the determination of most representative and appropriate rock mass parameters. Quality of the result from different methods ultimately depend on the quality of input parameter. Hence, while obtaining parameter from different sources, it must be verified with experienced engineering geologist.

➢ For the preliminary design of unlined/shotcrete lined pressure tunnel in the Himalaya, Modified NCC by Panthi and Basnet (2018b) is more relevant to determine safe location because of its consideration of the topography complexity, tectonic environment and weakness or fault zone as that of Himalaya in the proposed equation.

➢ Correct estimation of the magnitude of minimum principal stress is always crucial for the design of unlined/shotcrete lined pressure tunnels and shafts.

➢ In shotcrete lined tunnel assessment, leakage assessment should be carried out in order to ensure that leakage is within acceptable limit. Preliminary assessment can be done using semi-empirical approach by Panthi (2006) and Panthi (2010) but one should be careful while selecting input parameter of joint sets.

➢ The severity and the type of overstressing induced instabilities along any tunnel are mainly governed by rock type and its mineralogical composition, strength and quality, geometry of the underground opening and the in-situ stress state.

➢ It is important to know the assumptions and limitations of different methods and the results obtained from different methods should always be compared and discussed with an experienced engineering geologist. Right selection of appropriate empirical and semi-analytical methods along with numerical modelling always provide reliable and fruitful analysis. However, lack of good understanding about the rock mass of project area may not result in trustworthy results.

➢ It is useful to determine preliminary support from classification system like Q-system, Hoek and Marinos (2000) and Panthi and Shrestha (2018) and should be compared and revised using Numerical modelling to determine final optimum support.

10.2   Recommendations

Considering that the thesis has different limitations, further works are suggested below to improve the assessment carried out and implement the project successfully.

> ➢ During the analysis, it is experienced that the most uncertain parameter has been found to be Tectonic stress. Thus, measurement of in-situ stress is crucial at Powerhouse cavern from stability viewpoint and at chainages 5+025m, 7+205m and 3+769m (weakness zone) to verify minimum principal stress.

> ➢ 2D and 3D numerical modelling of tunnels should be carried out with actual discontinuities and with water pressure that prevails during operation that may affect long term stability. In addition, dynamic analysis should be carried out to assess impact of seismic loading on in-situ minimum principal state.

> ➢ Monitoring of the deformation on Test Tunnel near powerhouse should be done and numerical modelling should be adopted in powerhouse cavern as a part of design as you go philosophy, in which the assumed parameters and predictions are improvised together with the availability of information and actual rock conditions, that are revealed as construction progresses. Based on this and consultation with experienced engineering geologist, necessary changes in construction procedure and supports should be made accordingly.

> ➢ Numerical modelling of powerhouse cavern along with adjacent transformer cavern should also be analyzed to analyze its impact on deformation, pillar stability and stress distribution.

> ➢ Water leakage test should be carried out at potential areas by pumping water through exploratory drill holes or probe holes drilled ahead of the advancing face at a pressure equal to anticipated maximum static water pressure during operation. Based on it, decision related to pre-injection requirement should be made. Likewise, at Tatopani weakness zone, probe holes help to identify condition of rock mass ahead.

> ➢ Water filling test should be carried out after completion of complete excavation and pre-injection grouting to determine any possible leakage sections. If found, planning should be done for either post-grouting or full concrete lining as per site condition.

> ➢ Monitoring of tunnel behavior like deformation, inflow/leakage, block fall, failure in support during construction and operational period should always be prioritized so that effectiveness of support can be determined.

References

BARLA G (2002) Tunneling under squeezing rock conditions. Tunneling Mechanics-Advances in Geotechnical Engineering and Tunneling

BARLA G (2005) Design analyses for tunnels in squeezing rock. Overview lecture, Department of Structural and Geotechnical Engineering, Politecnico di Torino, Italy

BARTON N (2002) Some new Q value correlations to assist in site characterisation and tunnel design. International journal of rock mechanics and mining sciences

BASNET CB (2018) Applicability of Unlined/Shotcrete Lined Pressure Tunnels for Hydropower Projects in the Himalaya. PhD thesis, Norwegian University of Science and Technology, Trondheim, Norway

BASNET CB, PANTHI KK (2017) 3D insitu stress model of Upper Tamakoshi Hydroelectric Project Area. Hydro Nepal (21):34-41

BASNET CB, PANTHI KK (2018) Analysis of unlined pressure shafts and tunnels of selected Norwegian hydropower projects. Journal of Rock Mechanics and Geotechnical Engineering 10:486-512

BASNET CB, PANTHI KK (2019a) Detailed engineering geological assessment of a shotcrete lined pressure tunnel in the Himalayan rock mass conditions: a case study from Nepal. Bulletin of Engineering Geology and the Environment

BASNET CB, PANTHI KK (2019b) Evaluation on the Minimum Principal Stress State and Potential Hydraulic Jacking from the Shotcrete-Lined Pressure Tunnel: A Case from Nepal. Rock Mechanics and Rock Engineering 52(7):2377-2399

BENSON RP (1989) Design of Unlined and Lined Pressure Tunnels. Tunneling and Underground Space Technology 4(2):155-170

BROCH E (1983) Estimation of strength anisotropy using the point load test. International journal of rock mechanics and mining sciences and geomechanics abstracts 20:181-187

CARRANZA-TORRES C, FAIRHURST C (2000) Application of the Convergence-Confinement Method of Tunnel Design to Rock Masses That Satisfy the Hoek-Brown Failure Criterion. Tunneling and Underground Space Technology 15(2):187-213

CROWDER JJ, BAWDEN WF (2004) Review of Post-Peak Parameters and Behaviour of Rock Masses: Current Trends and Research

DEOJA B, DHITAL M, WAGNER A (1991) Risk engineering in the Hindu Kush Himalaya. International centre for integrated mountain development (ICIMOD), Nepal

DHITAL, MR (2015) Higher Himalaya of Koshi Region. Geology of the Nepal Himalaya. Springer International

EDVARDSSON S, BROCH E (2002) Underground Powerhouses and High Pressure Tunnels. Norwegian University of Science and Technology, Department of Hydraulic and Environmental Engineering Vol. 14

GOODMAN RE (1993) Engineering Geology. Rock in Engineering Construction, John Wiley & Sons, Inc.

GORKHAPATRA (2020) Policy and program of fiscal year 2077/2078 (Full text). Gorkhapatra Online, Kathmandu, Nepal

References

GRIMSTAD E, BARTON N (1993) Updating of Q system. Proceedings of the International Symposium on sprayed concrete-Modern use of wet mix sprayed ocncrete for underground support, Oslo, Norway

HENCHER S (2016) Practical Rock Mechanics, Taylor and Francis Group

HOEK E (1998) Tunnel support in weak rock. Symposium of Sedimentary Rock Engineering. Taipei, Taiwan

HOEK E (2001) Big Tunnels in Bad Rock: 2000 Terzaghi Lecture. ASCE Journal of Geotechnical and Geoenvironmental Engineering 127(9):726-740

HOEK E (2007) Practical Rock Engineering. https://www.rocscience.com/learning/hoeks-corner

HOEK E, BROWN ET (1997) Practical estimates of rock mass strength. International journal of rock mechanics and mining sciences 34(8):1165-1186

HOEK E, CARRANZA-TORRES C, CORKUM B (2002) Hoek-Brown failure criterion - 2002 Edition. Proceedings North American Rock Mechanics Society Meeting, Toronto, pp.263-273

HOEK E, MARINOS P (2000) Predicting tunnel squeezing in weak heterogenous rock masses Tunnels and tunnelling international, 32

HOEK E, MOY D (1993) Design of large powerhouse caverns in weak rock. Comprehensive Rock Engineering, pp. 85-110

LI, CC (2017) Principles of rockbolting design. Journal of Rock Mechanics and Geotechnical Engineering, pp. 396-414

MARTIN C, CHRISTIANSSON R (2009) Estimating the potential for spalling around a deep nuclear waste repository in crystalline rock. International Journal of Rock Mechanics and Mining Sciences 46:219-228

NASSERI MHB, RAO KS, RAMAMURTHY T (2003) Anisotropic strength and deformational behavior of Himalayan schists. International Journal of Rock Mechanics and Mining Sciences 40:3-23

NEA (2019) Detailed Design Report of Tamakoshi V Hydroelectric Project. Part F3-Geological, Geotechnical and Construction Material Investigation report, Nepal Electricty Authority, Kathmandu, Nepal

NFF (2010) Rock Support in Norwegian Tunnelling. Norsk Forening For Fjellsprengningsteknikk (NFF) Helli Grafisk AS, Oslo, Norway

NFF (2016) Norwegian Rock Caverns. Norsk Forening For Fjellsprengningsteknikk (NFF) HELLI - Visuell kommunikasjon AS,Oslo, Norway

NILSEN B, PALMSTRÖM A (2000) Engineering Geology and Rock Engineering. Norwegian Group for Rock Mechanics (NBG) Vol. 2

NILSEN B, THIDEMANN A (1993) Rock Engineering. Norwegian Institute of Technology, Division of Hydraulic Engineering Vol. 9

PALMSTRÖM A, SINGH R (2001) The deformation modulus of rock masses — comparisons between in-situ tests and indirect estimates. Tunnelling and Underground Space Technology 16(2):115-131

PALMSTRÖM A, STILLE H (2010) Rock engineering. Thomas Telford Limited, London

References

PANTHI KK (2006) Analysis of engineering geological uncertainties related to tunnelling in Himalayan rock mass conditions. PhD thesis, Norwegian University of Science and Technology, Trondheim, Norway

PANTHI KK (2010) Note on estimating specific leakage using Panthi's approach. Norwegian University of Science and Technology, Trondheim, Norway

PANTHI KK (2012) Evaluation of rock bursting phenomena in a tunnel in the Himalayas. Bulletin of Engineering Geology and the Environment 71(4):781-769

PANTHI KK (2013a) Predicting Tunnel Squeezing: A Discussion based on Two Tunnel Projects. Hydro Nepal: Journal of Water Energy and Environment (12):20-25

PANTHI KK (2013b) Pre-injection versus post-injection grouting - a review of a case from the Himalaya. Presentation at the 47th US Rock Mechanics/Geomechanics Symposium, San Francisco, CA, USA, pp.1-7

PANTHI KK (2014) Norwegian Design Principles for High Pressure Tunnels and Shafts: Its Applicabilty in the Himalaya. Hydro Nepal: Journal of Water Energy and Environment (14)

PANTHI KK (2015) Himalayan rock mass and possiblity of limiting concrete lined pressure tunnel length in hydropower projects in the Himalaya. Geosystem Engineering 18(1): 45-50

PANTHI KK (2017) Review on the prevailing methods for the prediction of potential rock burst/rock spalling in tunnels. Fjellsprengningsdagen - Bergmekanikkdagen - Geoteknikkdagen 2017. Ed. by K. K. Dunham et al. Oslo: Norsk Forening for Fjellsprengningsteknikk, Norsk Bergmekanikkgruppe and Norsk Geoteknisk Forening

PANTHI KK (2018a) Lecture notes on TGB5110 ENGINEERING GEOLOGY AND TUNNELING (Autumn)

PANTHI KK (2018b) Methods Applied in the Prediction of Brittle Failure in Tunnels and Underground Caverns. Hydro Nepal: Journal of Water Energy and Environment (22):5-9.

PANTHI KK (2019) Lecture notes on TGB4190 ENGINEERING GEOLOGY OF ROCKS AC (Spring)

PANTHI KK, BASNET CB (2016) Review on the Major Failure Cases of Unlined Pressure Shafts/Tunnels of Norwegian Hydropower Projects. Hydro Nepal: Journal of Water Energy and Environment (18):6-15

PANTHI KK, BASNET CB (2017) Design review of headrace system for the Upper Tamakoshi project, Nepal. Hydropower and Dams 24(1):60-67

PANTHI KK, BASNET CB (2018a) A dynamic analysis of in-situ stress state at the Upper Tamakoshi Hydroelectric Project area, Nepal. Hydro Nepal: Journal of Water Energy and Environment (23):42-47

PANTHI KK, BASNET CB (2018b) State-of-the-art design guidelines in the use of unlined pressure tunnels/shafts for hydropower scheme. 10th Asian Rock Mechanics Symposium (ARMS10),Singapore

PANTHI KK, BASNET CB (2019a) Evaluation of earthquake impact on magnitude of the minimum principal stress along a shotcrete lined pressure tunnel in Nepal. Journal of Rock Mechanics and Geotechnical Engineering 11:920-934

References

PANTHI KK, BASNET CB (2019b) Leakage potential through a shotcrete lined high-pressure headrace tunnel - an analysis on a case from Nepal. Rock Mechanics for Natural Resources and Infrastructure Development - Fontoura, Rocca & Pavón Mendoza (Eds), pp.722-728

PANTHI KK, NILSEN B (2005) Significance of grouting for controlling leakage in water tunnels - a case from Nepal. Proceedings: ITA-AITES 2005 World Tunneling Congress and 31st ITA general assembly, Istanbul, Turkey, pp.931-937

PANTHI KK, SHRESTHA PK (2018) Estimating Tunnel Strain in the Weak and Schistose Rock Mass Influenced by Stress Anisotropy: An Evaluation Based on Three Tunnel Cases from Nepal. Rock Mechanics and Rock Engineering

Rocscience (2020) RS2. https://www.rocscience.com/help/rs2

SCHELLING D (1992) The Tectonostratigraphy and Structure of Eastern Nepal Himalaya. Tectonics 11(5):925-943

SELMER-OLSEN R, BROCH E (1977) General design procedure for underground openings in Norway. Int. Symp. ROCKSTORE 77 2:11-18

SHRESTHA PK (2014) Stability of tunnels subject to plastic deformation - a contribution based on the cases from the Nepal Himalaya. PhD thesis, Norwegian University of Science and Technology, Trondheim, Norway

SINGH B, GOEL RK (2012a) Tunneling Hazards. Engineering Rock Mass Classification: Tunneling, Foundations and Landslides, pp.63-84

SINGH B, GOEL RK (2012b) Rock Mass Quality Q system. Engineering Rock Mass Classification: Tunneling, Foundations and Landslides, pp.85-118

STEFANUSSEN W (2017) Engineering geological experience from International Projects. Compendium of TGB4190 Engineering geology of rocks, Department of Geoscience and Petroleum, Norwegian University of Science and Technology, Trondheim, Norway

SUNUWAR SC (2016) Geological mapping in the Nepal Himalaya: importance and challenges for underground structures. Journal of Nepal Geological Society 51:89-95

VESTAD, ML (2014) Analysis of deformation behavoir at the underground caverns of Neelum Jhelum HPP, Pakistan. Master thesis, Norwegian University of Science and Technology, Trondheim, Norway

Appendices

A. Standard Charts and Figures

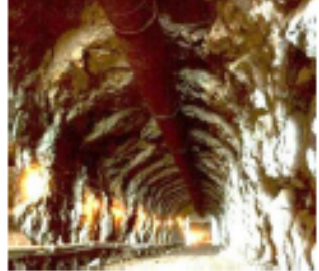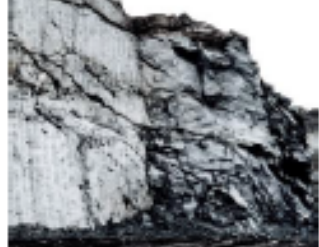### A1 Weathering classification according to ISRM (1978) (Panthi 2006)

Term	Description of rock mass conditions	Weathering grade
Fresh rock	No visible sign of rock material weathering; perhaps slight discolouration on major discontinuity surfaces.	I
Slightly weathered	Discolouration indicates weathering of rock material and discontinuity surfaces. All the rock material may be discoloured by weathering and may be some what weaker externally than in its fresh condition.	II
Moderately weathered	Less than half of the material is decomposed and/or disintegrated to a soil. Fresh or discoloured rock is present either as a continuous framework or as corestones.	III
Highly weathered	More than half of the rock material is decomposed and/or disintegrated to a soil. Fresh or discoloured rock is present either as a discontinuous framework or as corestones.	IV
Completely weathered	All rock material is decomposed and/or disintegrated to soil. The original mass structure is still largely intact.	V
Residual soil	All rock material is converted to soil. The mass structure and material fabric are destroyed. There is a large change in volume, but the soil has not been significantly transported.	VI

A2 Classification of squeezing by Singh and Goel (2012a)

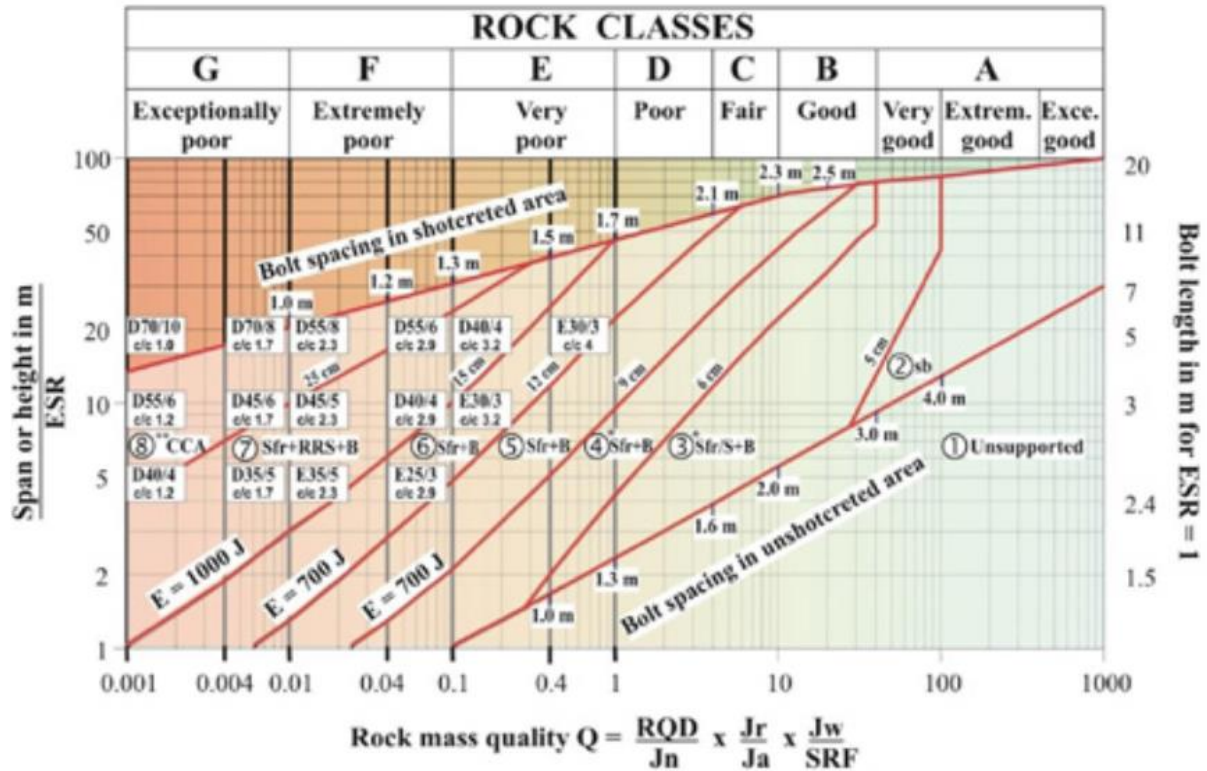| S. No.	Ground conditions	Correlations for predicting ground condition
1	Self-supporting	$H < 23.4 \, N^{0.88} \cdot B^{-0.1}$ and $1000 \, B^{-0.1}$ and $B < 2 \, Q^{0.4}$ m
2	Non-squeezing	$23.4 \, N^{0.88} \cdot B^{-0.1} < H < 275 N^{0.33} \cdot B^{-0.1}$
3	Mild squeezing	$275 \, N^{0.33} \cdot B^{-0.1} < H < 450 N^{0.33} \cdot B^{-0.1}$ and $J_r/J_a < 0.5$
4	Moderate squeezing	$450 \, N^{0.33} \cdot B^{-0.1} < H < 630 N^{0.33} \cdot B^{-0.1}$ and $J_r/J_a < 0.5$
5	High squeezing	$H > 630 N^{0.33} \cdot B^{-0.1}$ and $J_r/J_a < 0.25$
6	Mild rock burst	$H \cdot B^{0.1} > 1000$ m and $J_r/J_a > 0.5$ and $N > 1.0$

A3 Disturbance factor D (Hoek 2007)

Appearance of rock mass	Description of rock mass	Suggested value of D
	Excellent quality controlled blasting or excavation by Tunnel Boring Machine results in minimal disturbance to the confined rock mass surrounding a tunnel.	D = 0
	Mechanical or hand excavation in poor quality rock masses (no blasting) results in minimal disturbance to the surrounding rock mass. Where squeezing problems result in significant floor heave, disturbance can be severe unless a temporary invert, as shown in the photograph, is placed.	D = 0 D = 0.5 No invert
	Very poor quality blasting in a hard rock tunnel results in severe local damage, extending 2 or 3 m, in the surrounding rock mass.	D = 0.8
	Small scale blasting in civil engineering slopes results in modest rock mass damage, particularly if controlled blasting is used as shown on the left hand side of the photograph. However, stress relief results in some disturbance.	D = 0.7 Good blasting D = 1.0 Poor blasting
	Very large open pit mine slopes suffer significant disturbance due to heavy production blasting and also due to stress relief from overburden removal. In some softer rocks excavation can be carried out by ripping and dozing and the degree of damage to the slopes is less.	D = 1.0 Production blasting D = 0.7 Mechanical excavation

A4 Hoek and Brown constant m_i (Hoek and Marinos 2000)

Rock type	Class	Group	Texture			
			Coarse	Medium	Fine	Very fine
SEDIMENTARY	Clastic		Conglomerates (21 ± 3) Breccias (19 ± 5)	Sandstones 17 ± 4	Siltstones 7 ± 2 Greywackes (18 ± 3)	Claystones 4 ± 2 Shales (6 ± 2) Marls (7 ± 2)
	Non-Clastic	Carbonates	Crystalline Limestone (12 ± 3)	Sparitic Limestones (10 ± 2)	Micritic Limestones (9 ± 2)	Dolomites (9 ± 3)
		Evaporites		Gypsum 8 ± 2	Anhydrite 12 ± 2	
		Organic				Chalk 7 ± 2
METAMORPHIC	Non Foliated		Marble 9 ± 3	Hornfels (19 ± 4) Metasandstone (19 ± 3)	Quartzites 20 ± 3	
	Slightly foliated		Migmatite (29 ± 3)	Amphibolites 26 ± 6	Gneiss 28 ± 5	
	Foliated*			Schists 12 ± 3	Phyllites (7 ± 3)	Slates 7 ± 4
IGNEOUS	Plutonic	Light	Granite 32 ± 3 Granodiorite (29 ± 3)	Diorite 25 ± 5		
		Dark	Gabbro 27 ± 3 Norite 20 ± 5	Dolerite (16 ± 5)		
	Hypabyssal		Porphyries (20 ± 5)		Diabase (15 ± 5)	Peridotite (25 ± 5)
	Volcanic	Lava		Rhyolite (25 ± 5) Andesite 25 ± 5	Dacite (25 ± 3) Basalt (25 ± 5)	
		Pyroclastic	Agglomerate (19 ± 3)	Breccia (19 ± 5)	Tuff (13 ± 5)	

A5 Q-system chart and various excavation support ratio categories (Grimstad and Barton 1993)

ROCK CLASSES

G	F	E	D	C	B	A
Exceptionally poor	Extremely poor	Very poor	Poor	Fair	Good	Very good / Extrem. good / Exce. good

Span or height in m / ESR

Bolt spacing in shotcreted area

D70/10 c/c 1.0 | D70/8 c/c 1.7 | D55/8 c/c 2.3 | D55/6 c/c 2.9 | D40/4 c/c 3.2 | E30/3 c/c 4

D55/6 c/c 1.2 | D45/6 c/c 1.7 | D45/5 c/c 2.3 | D40/4 c/c 2.9 | E30/3 c/c 3.2

⑧ CCA | ⑦ Sfr+RRS+B | ⑥ Sfr+B | ⑤ Sfr+B | ④ Sfr+B | ③ Sfr/S+B | ② sb | ① Unsupported

D40/4 c/c 1.2 | D35/5 c/c 1.7 | E35/5 c/c 2.3 | E25/3 c/c 2.9

E = 1000 J | E = 700 J | E = 700 J

Bolt length in m for ESR = 1

Bolt spacing in unshotcreted area

Rock mass quality $Q = \dfrac{RQD}{Jn} \times \dfrac{Jr}{Ja} \times \dfrac{Jw}{SRF}$

REINFORCEMENT CATEGORIES

1) Unsupported
2) Spot bolting, **sb**
3) Systematic bolting, and unreinforced or fibre reinforced shotcrete, 5-6 cm), **Sfr/B+S**
4) Fibre reinforced shotcrete and bolting, 6-9 cm, **Sfr+B**
5) Fibre reinforced shotcrete and bolting, 9-12 cm, **Sfr (E700) +B**
6) Fibre reinforced shotcrete and bolting, 12-15 cm, **Sfr (E700) +B**
7) Fibre reinforced shotcrete > 15 cm + reinforced ribs of shotcrete and bolting, **Sfr (E1000) +RRS+B**
8) Cast concrete lining, **CCA** or **Sfr (E1000) +RRS+B**

The bolts are 20 or 25 mm in diameter

E) Energy absorbtion in fibre reinforced shotcrete at 25 mm bending during plate testing

D45/6 c/c 1.7 = RRS with totally 6 reinforcement bars in double layer in 45 cm thick ribs with centre to centre (c/c) spacing 1.7 m. Each box corresponds to Q-values on the left hand side of the box

*) Up to 10 cm in large spans
) Or **Sfr+RRS+B

Temporary mine openings	*ESR* = 3–5
Permanent mine openings, water tunnels for hydro power (excluding high pressure penstocks), pilot tunnels, drifts and headings for large excavations	1.6
Storage rooms, water treatment plants, minor road and railway tunnels, surge chambers, access tunnels	1.3
Power stations, major road and railway tunnels, civil defence chambers, portal intersections	1
Underground nuclear power stations, railway stations, sports and public facilities, factories	0.8

B. Detailed calculations and results

B1 Support properties and pressure calculation at chainge 3+026m

Rock bolts		
Bolt daimeter (mm)	0.025	mm
length of bolt (m)	3	m
Ultimated load (pull out test)	0.254	MN
Deformation load constant	0.143	m/MN
Young's modulus	210000	MPa
Circumferential bolt spacing	1	
Longitudinal bolt spacing	1	
Max support pressure	0.25	MPa
Elastic stiffness	5.81	MPa/m
Max displacement	0.044	m
Shotcrete		
Unconfined compressive strength	25	MPa
Youngs modulus	30000	MPa
Radius of tunnel	3.2	m
Thickness of shotcrete	0.3	m
Poisson's ratio	0.25	
Max support pressure	2.23	MPa
Elastic stiffness	1690.7	MPa/m
Max displacement	0.0013	m
Minimum of maximum displacement	0.00132	m
Combined stiffness	1696.5	MPa/m
Combined maximum support pressure	2.24	MPa
Reduction	30	%
Reduced combined maximum support pressure	1.57	MPa
Reinforced Concrete		
Unconfined compressive strength	35	MPa
Youngs modulus	35000	MPa
Radius of tunnel	3.2	m
Thickness of concrete	0.4	m
Poisson's ratio	0.25	
Max support pressure	4.10	MPa
Elastic stiffness	2700.6	MPa/m
Max displacement	0.0015	m
Reduction	30	%
Reduced maximum pressure	3.80	
Average support pressure	2.7	MPa

B2 Support properties and pressure calculation at chainge 3+769m

Rock bolts		
Bolt daimeter (mm)	0.025	mm
length of bolt (m)	3	m
Ultimated load (pull out test)	0.254	MN
Deformation load constant	0.143	m/MN
Young's modulus	210000	MPa
Circumferential bolt spacing	1	
Longitudinal bolt spacing	1	
Max support pressure	0.25	MPa
Elastic stiffness	5.81	MPa/m
Max displacement	0.044	m
Reinforced ribs of Shotcrete		
Unconfined compressive strength	35	MPa
Youngs modulus	30000	MPa
Radius of tunnel	3.2	M
Thickness of shotcrete	0.35	M
Poisson's ratio	0.25	
Max support pressure	3.62	MPa
Elastic stiffness	1998.8	MPa/m
Max displacement	0.0018	m
Minimum of maximum displacement	0.0018	m
Combined stiffness	2004.6	MPa/m
Combined maximum support pressure	3.63	MPa
Reduction	30	%
Reduced combined maximum support pressure	2.54	MPa
Reinforced Concrete		
Unconfined compressive strength	35	MPa
Youngs modulus	35000	MPa
Radius of tunnel	3.2	M
Thickness of concrete	0.4	M
Poisson's ratio	0.25	
Max support pressure	4.10	MPa
Elastic stiffness	2700.6	MPa/m
Max displacement	0.0015	M
Reduction	30	%
Reduced maximum pressure	3.80	
Average support pressure	3.17	MPa

Reinforcement details				
	Dia (mm)	Spacing (m)	Poisson ratio	Youngs mod
RRS	20	0.2	0.3	200Gpa
Reinforced concrete (for all section)	25	0.3	0.3	200Gpa

B3 Support properties and pressure calculation at chainge 7+846m

| Rock bolts		
Bolt diameter (mm)	0.025	Mm
length of bolt (m)	3	M
Ultimate load (pull out test)	0.254	MN
Deformation load constant	0.143	m/MN
Young's modulus	210000	MPa
Circumferential bolt spacing	1	
Longitudinal bolt spacing	1	
Max support pressure	0.25	MPa
Elastic stiffness	5.81	MPa/m
Max displacement	0.044	M
Shotcrete		
Unconfined compressive strength	25	MPa
Youngs modulus	30000	MPa
Radius of tunnel	3.2	m
Thickness of shotcrete	0.25	m
Poisson's ratio	0.25	
Max support pressure	1.88	MPa
Elastic stiffness	1390.4	MPa/m
Max displacement	0.0013	m
Minimum of maximum displacement	0.0013	m
Combined stiffness	1396.21	MPa/m
Combined maximum support pressure	1.88	MPa
Reduction	30	%
Reduced combined maximum support pressure	1.32	MPa
Reinforced Concrete		
Unconfined compressive strength	35	MPa
Youngs modulus	35000	MPa
Radius of tunnel	3.2	m
Thickness of concrete	0.4	m
Poisson's ratio	0.25	
Max support pressure	4.10	MPa
Elastic stiffness	2700.6	MPa/m
Max displacement	0.0015	m
Reduction	30	%
Reduced maximum pressure	3.80	
Average support pressure	2.6	MPa

C. RS2 modelling results

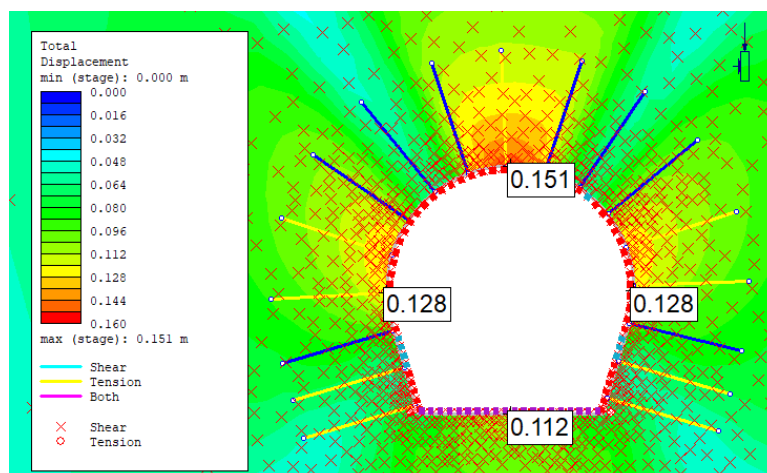## C1 Numerical modelling at chainage 3+026m

1. Strength factor by elastic analysis
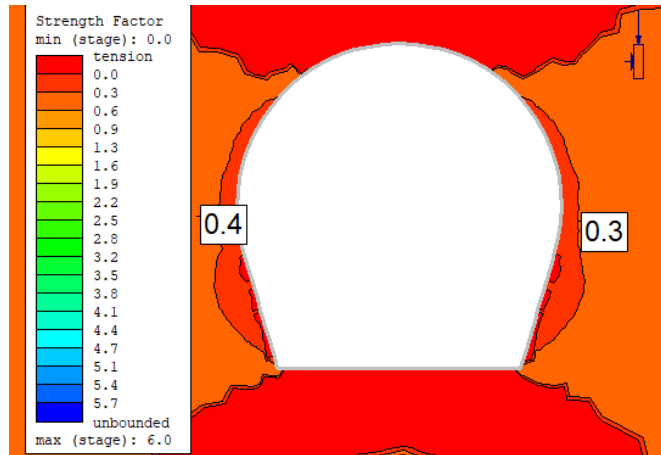
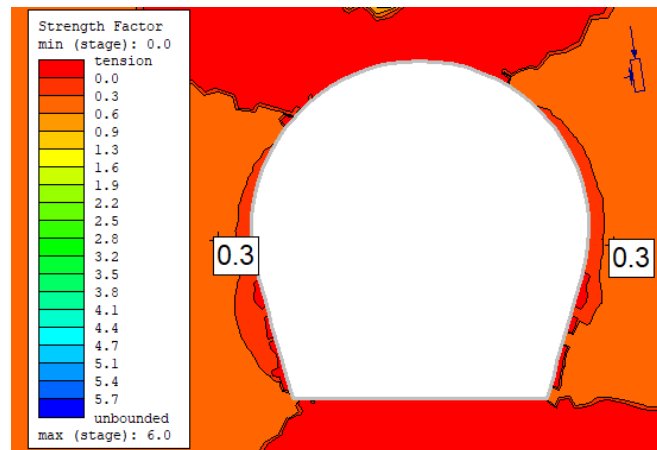2. Total displacement without support by plastic analysis
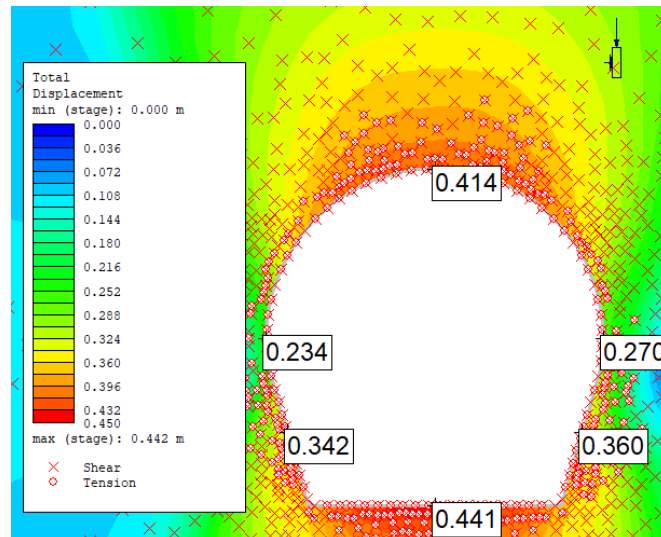
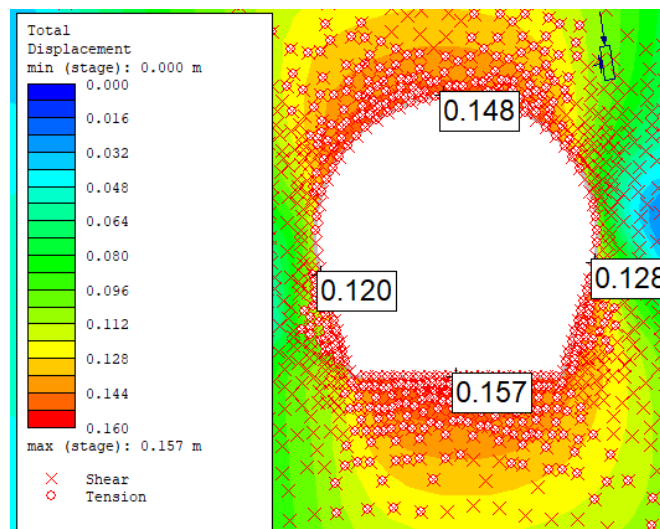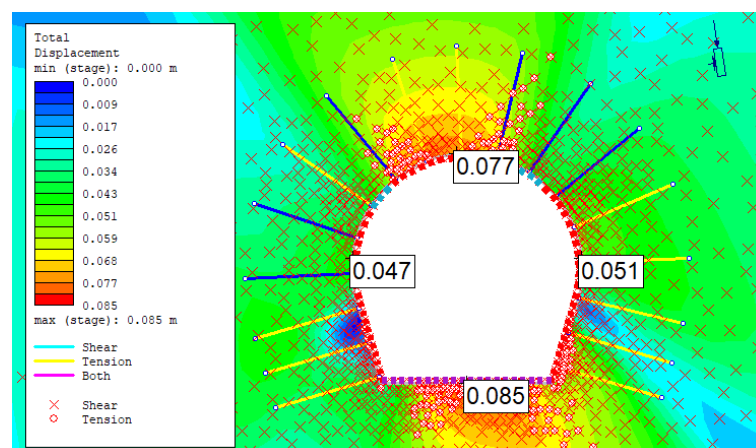3. Total displacement with support by plastic analysis

C2 Numerical modelling at chainage 7+846m

1. Strength factor by elastic analysis

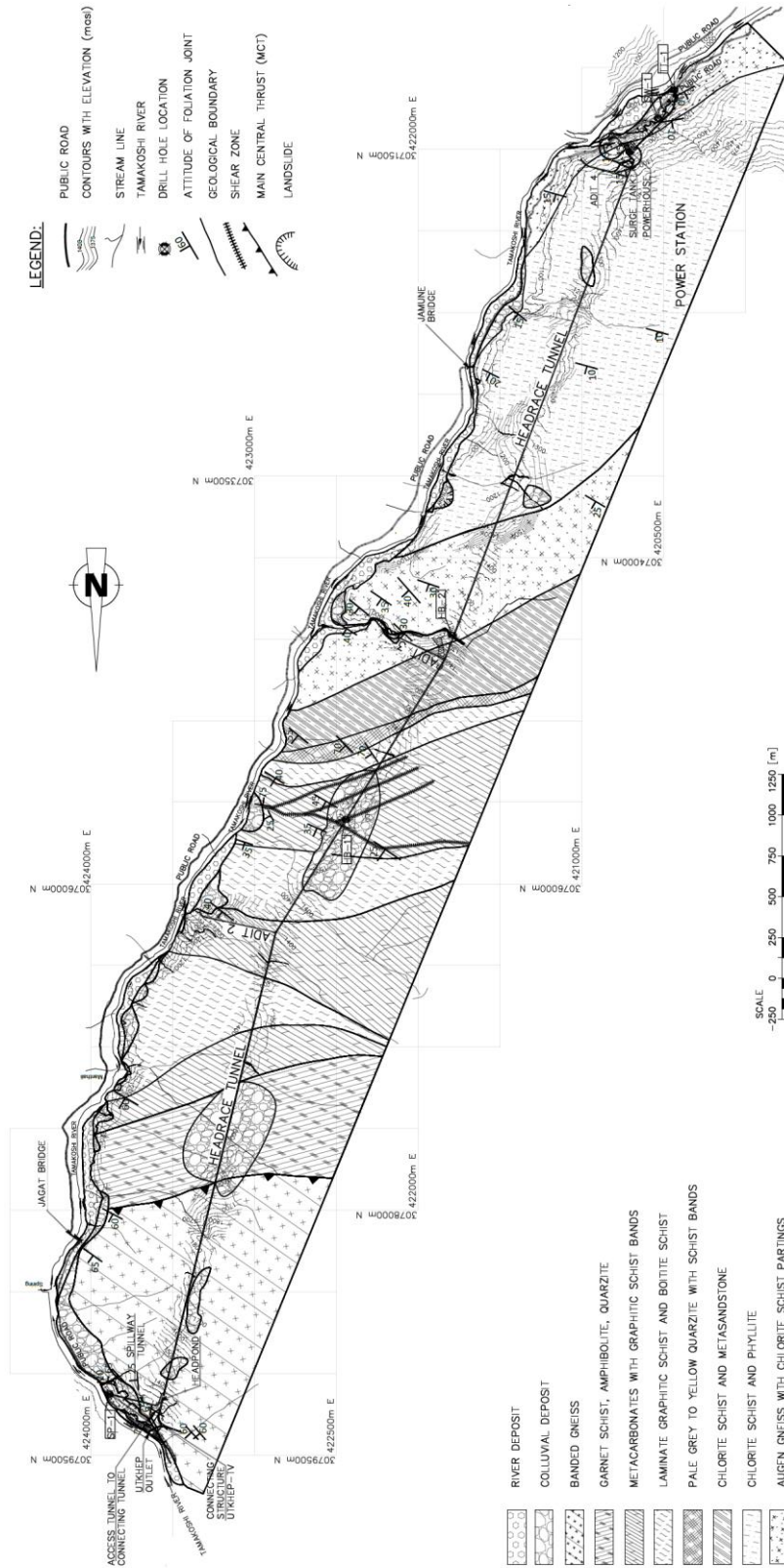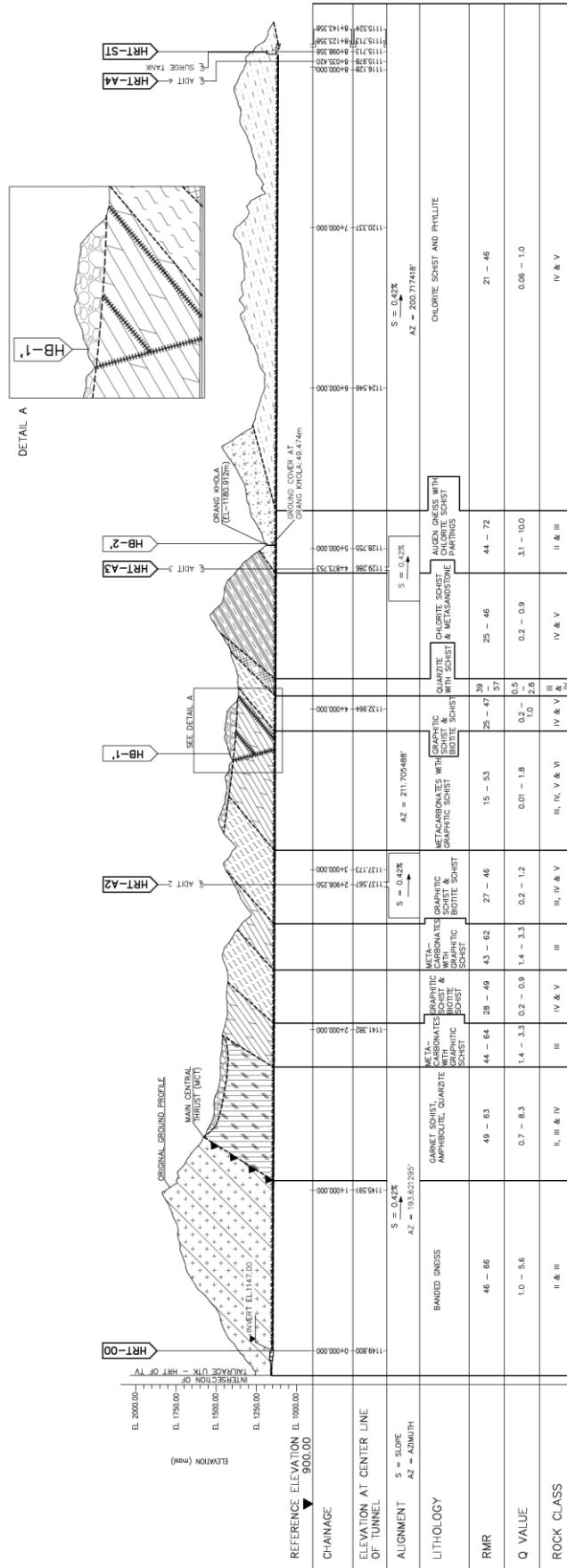2. Total displacement without support by plastic analysis

3. Total displacement with support by plastic analysis

Appendices

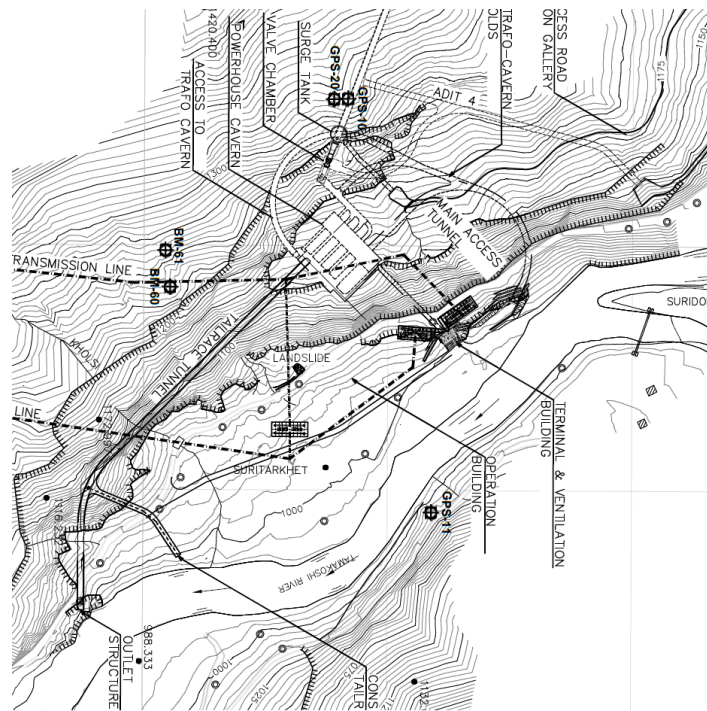# D. Project related documents and drawings

D1 Project plan (NEA 2019)

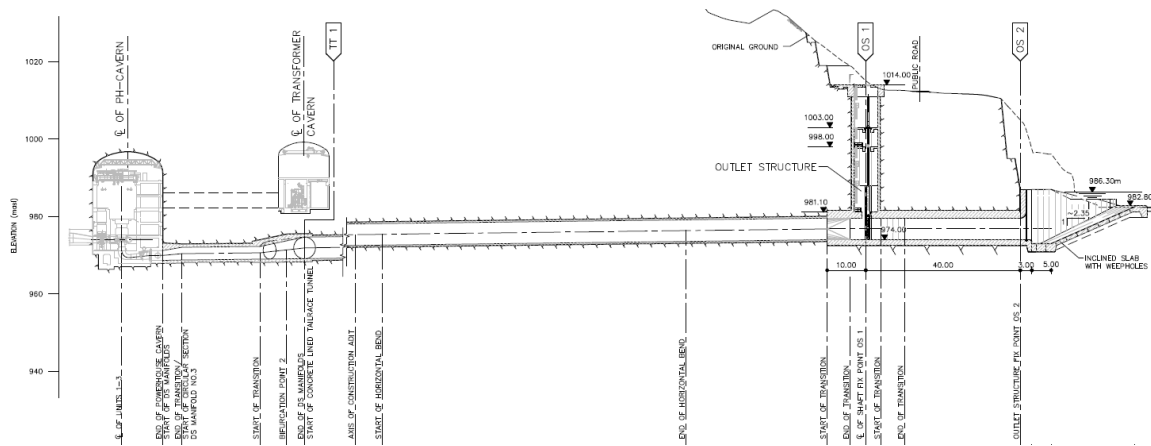**D2 Longitudinal profile of the Headrace Tunnel alignment (NEA 2019)**

Appendices

D3 Plan of Powerhouse area and Tailrace Tunnel (NEA 2019)

D4 Longitudinal profile of the Powerhouse area and Tailrace Tunnel alignment (NEA 2019)

Appendices

E. Formal Letter

Regd. No. 164865/073/074

Tamakoshi Jal Vidhyut Company Ltd.

Ref. No.: 076/77 Cha No.: 159

Date: 1st December, 2019

To,
Dr. Krishna Kanta Panthi,
Faculty of Engineering (IV),
Department of Geoscience and Petroleum,
Norwegian University of Science and Technology,
Trondheim, Norway.

Subject: Data for MSc Thesis Work.

With reference to your letter dated 20th November, 2019, Ref: no. R-1, we hereby provide you with the following requested data and information of the project, Tamakoshi V Hydroelectric Project;

1. Executive Summary of the Project.
2. Geological and engineering geological investigation report.
3. Topographic, geological and other civil engineering drawings.

These data and information shall be used for educational purpose only and is strictly forbidden to use for the commercial purposes.

We wish Mr. Kundan Chauhan a good luck for completion of his MSc thesis work.

Best Regards,

Nasib Man Pradhan.
Chief Executive Officer.

CC: Norwegian University of Science and Technology